TEXAS STATE UNIVERSITY
SAN MARCOS
The rising STAR of Texas

Evaluation, Presentation and Repair of Microbial Acid-Produced Attack of Concrete

Technical Report 0-6137-1

Cooperative Research Program

TEXAS STATE UNIVERSITY—SAN MARCOS
DEPARTMENT OF ENGINEERING TECHNOLOGY
SAN MARCOS, TEXAS

TEXAS DEPARTMENT OF TRANSPORTATION

in cooperation with the
Federal Highway Administration and the
Texas Department of Transportation
http://tti.tamu.edu/documents/0-6137-1.pdf

Technical Report Documentation Page

1. Report No.	2. Government Accession No.	3. Recipient's Catalog No.
FHWA/TX-11/0-6137-1		

4. Title and Subtitle	5. Report Date
EVALUATION, PRESENTATION AND REPAIR OF MICROBIAL ACID-PRODUCED ATTACK OF CONCRETE	Published: October 2011
	6. Performing Organization Code
7. Author(s)	8. Performing Organization Report No.
Jiong Hu, Dittmar Hahn, Walter Rudzinski, Zhuo Wang, and Luzelva Estrada	Report 0-6137-1
9. Performing Organization Name and Address	10. Work Unit No. (TRAIS)
Texas State University-San Marcos The Texas State University System San Marcos, Texas 78666	11. Contract or Grant No. Project 0-6137
12. Sponsoring Agency Name and Address	13. Type of Report and Period Covered
Texas Department of Transportation Research and Technology Implementation Office P.O. Box 5080 Austin, Texas 78763-5080	Technical Report: September 2009-August 2011
	14. Sponsoring Agency Code

15. Supplementary Notes

Project performed in cooperation with the Texas Department of Transportation and the Federal Highway Administration
Project Title: Evaluation, Presentation and Repair of Microbial Acid-Produced Attack of Concrete
URL:http://tti.tamu.edu/documents/0-6137-1.pdf

16. Abstract

The Texas Department of Transportation (TxDOT) has approximately 50,000 bridges in its inventory and the deterioration of concrete under these bridges, most of which are reinforced, has been a critical issue affecting the service condition. Recent research on deteriorated concrete columns on bridges in Texas indicated that microbial colonization might be a factor promoting the surface deterioration of bridge columns continuously exposed to water. Although microbial activities may be involved in the surface deterioration, it is however not clear how severe the deterioration is and whether it is a significant contributor to the deterioration. Field and laboratory investigations are needed to identify the impact of microbial induced deterioration (MID) on TxDOT bridges.

To evaluate the severity of the deterioration and determine whether MID is a significant contributor to the deterioration, visual inspection and a number of *in situ* tests were performed on columns of twelve selected TxDOT bridges. Laboratory tests including microbial, chemical composition, mineralogy and petrographic analyses were performed to investigate the potential cause and extent of the deterioration. Results from this comprehensive study were used to provide evidence of concrete degradation and ascertain the degree of deterioration caused by microbial attack. The study also evaluated the effectiveness and consistency of various measurements used in this study and provided a suggested test procedure to identify microbial attack on concrete and evaluate the integrity of deteriorated concrete due to the attack. In addition, a preliminary evaluation of the microbial attack resistance of commonly used TxDOT mixes was performed through evaluation of resistance of a series of mixes subjected to field and/or sulfuric acid solution exposure.

17. Key Words	18. Distribution Statement
Bridges, concrete, column *in situ* tests, microbial, chemical, mineralogy, petrographic, deterioration, inspection	No restrictions. This document is available to the public through NTIS: National Technical Information Service Alexandria, Virginia 22161 http://www.ntis.gov

19. Security Classif.(of this report)	20. Security Classif.(of this page)	21. No. of Pages	22. Price
Unclassified	Unclassified	226	

Form DOT F 1700.7 (8-72) Reproduction of completed page authorized

EVALUATION, PRESENTATION AND REPAIR OF MICROBIAL ACID-PRODUCED ATTACK OF CONCRETE

by

Jiong Hu, Ph.D.
Assistant Professor
Texas State University-San Marcos

Dittmar Hahn, Ph.D.
Professor
Texas State University-San Marcos

Walter Rudzinski, Ph.D.
Professor
Texas State University-San Marcos

Zhuo Wang
Graduate Research Assistant
Texas State University-San Marcos

and

Luzelva Estrada
Graduate Research Assistant
Texas State University-San Marcos

Report 0-6137-1
Project 0-6137
Project Title: Evaluation, Presentation and Repair of Microbial Acid-Produced Attack of Concrete

Performed in cooperation with the
Texas Department of Transportation
and the
Federal Highway Administration

Published: October 2011

TEXAS STATE UNIVERSITY-SAN MARCOS
The Texas State University System
San Marcos, Texas 78666

DISCLAIMER

This research was performed in cooperation with the Texas Department of Transportation (TxDOT) and the Federal Highway Administration (FHWA). The contents of this report reflect the views of the authors, who are responsible for the facts and the accuracy of the data presented herein. The contents do not necessarily reflect the official view or policies of the FHWA or TxDOT. This report does not constitute a standard, specification, or regulation. The researcher in charge of the project was Jiong Hu.

ACKNOWLEDGMENTS

This project was conducted in cooperation with TxDOT and FHWA. The authors wish to express their appreciation to the TxDOT personnel for their support throughout this study. Special thanks are extended to Kevin Pruski as the project director, Duncan Stewart as Research Engineer, Project Monitoring Committee (PMC) members Ryan Barbork, Doug Marino, Victoria McCammon, Andy Naranjo, and Lloyd Wolf, and Sandra Kaderka as contract specialist. William Pecht, Mickey Estlack, Edward Morgan, and the assistance of the TxDOT district engineers and all the personnel that helped in conducting the laboratory and field studies is also acknowledged. The authors would also like to thank Dr. Yoo-Jae Kim, Dr. Fatih Bektas, Dr. Soon-Jae Lee, Dr. Clois Powell, Dr. Necip Guven, Dr. Gary Beall, Shane Arabie and Ted Cera for their assists in this project, thanks also goes to all research assistants that involved in this study.

TABLE OF CONTENTS

Page

LIST OF FIGURES

Page

LIST OF TABLES

Page

CHAPTER 1:
INTRODUCTION

RESEARCH BACKGROUND

The Texas Department of Transportation (TxDOT) has approximately 50,000 bridges in its inventory. The deterioration of concrete under bridge structures, most of which is reinforced, has been a critical issue affecting the service condition of these bridges. In additional to well-known concrete durability problems associated with alkali-silica reactions (ASR), sulfate attack, delayed ettringite formation (DEF), carbonation, and freeze-thaw damage, another surface deterioration phenomenon, microbial induced deterioration (MID) has recently been identified on concrete of Texas bridges and generated strong concern at the Texas Department of Transportation (TxDOT). Figure 1 shows examples of typical TxDOT bridge columns with suspected MID issues.

(a) **(b)**

Figure 1. Examples of Deteriorated Concrete Bridge Columns with Suspected MID.
(a) FM 276 @ Patroon Bayou (Sabine County),
(b) SH 31 WB @ Kickapoo Creek (Henderson County).

A research study performed by the Texas Transportation Institute (TTI) and Texas A&M University on deteriorated concrete columns on bridges in Texas indicated that microbial colonization was a significant factor promoting the surface deterioration of bridge columns

continuously exposed to water and identified many of the microbes involved in the attack (Trejo et al. 2008). The microbes present were found to be acid-producing and directly correlated with the degree of damage. Although microbial activities may be involved in the surface deterioration of bridge columns, it is not clear how severe the deterioration is and whether it is a significant contributor to the deterioration. Field and laboratory investigations are needed to identify the impact of MID on TxDOT bridges. Research also indicates that the mechanism of MID is still yet to be fully understood, and further information is needed in order to determine the environmental factors that initiate the process, sustain microbial growth, and lead to an increase in acidity.

RESEARCH OBJECTIVES

The goal of this project was to identify the microbes degrading concrete, understand the mechanism of attack, evaluate methods for in situ and laboratory evaluation of MID and evaluate commonly used TxDOT concrete materials in MID resistance and provide recommendations for possible remedial actions. Specific technical objectives of this project are:

1. To identify microbes associated with the degradation of concrete, and understand their mechanism of attack.
2. To evaluate the significance of MID issues in TxDOT structures from field and laboratory investigations and provide guidelines in predicting the service life of structures under different microbial deterioration conditions.
3. To develop in situ test procedures to identify microbial attack on concrete and effective procedures to evaluate microbial induced deterioration; and
4. To evaluate the resistance of typical TxDOT concrete mixtures against MID, and provide recommendations for possible remedial actions.

The results will also provide TxDOT with a better understanding of how significant is the issue of MID in TxDOT structures and the mechanism of microbial attack, together with insights into the factors that contribute to microbial degradation. Effective methods (procedures) will be available identifying markers associated with microbial attack. This early warning approach would be helpful in determining concrete structures that would be susceptible to failure and appropriate for remediation. The study of microbial attack resistance of concrete with different

materials and mix design will also point toward improved methods to prevent and remediate microbial attack.

SCOPE OF RESEARCH AND ORGANIZATION OF THE REPORT

The report represents the project summary report for TxDOT project 0-6137. The following describes the report's organization by chapter.

Chapter 1 presents general background, research objectives and scope of research of the project.

Chapter 2 gives background information based on a literature review of previous studies on microbial induced attack on concrete. The review focuses on the mechanism of MID, test methods, and factors that affect the corrosion generated by MID. In addition, state-of-the-practice MID remediation is summarized.

Chapter 3 describes site locations included in this project and in situ tests performed to evaluate concrete deterioration caused by microbial attack. Procedures of field concrete, water, and mud sample collection are also described. Results of visual inspections and *in situ* measurements from site visits are summarized in this chapter.

Chapter 4 describes procedures and results from microbial, chemical, mineralogy and petrographic analyses performed in the laboratory in order to determine the mechanism and level of deterioration from microbial attack. Results include types of microbes and their relative abundance, the elemental composition of the exterior of deteriorated concrete, pH, sulfate and chloride concentration, and the microstructure of deteriorated concrete.

Chapter 5 evaluates effectiveness and consistency of various measurements used in this study. The chapter also describes a suggested *in situ* and laboratory test procedure to identify microbial attack on concrete and evaluate the integrity of deteriorated concrete due to the attack.

Chapter 6 summarizes results from a preliminary evaluation of the microbial attack resistance of concrete containing different types of cement, supplemental cementitious materials (SCMs) and coating agents. A series of typical TxDOT concrete mixes were prepared and subjected to field, sulfuric solution and combination of field and sulfuric acid solution exposure. Resistance against microbial attack from selected TxDOT mixes was evaluated.

Chapter 7 summarizes conclusions and recommendations based on the findings of this project. It also suggests directions for further research.

CHAPTER 2:
LITERATURE REVIEW

MECHANISM OF MICROBIAL INDUCED DETERIORATION (MID)

Microbial induced deterioration (MID), also known as microbial induced corrosion (MIC) is a process of deterioration induced through the microbial production of acids, usually sulfuric acid, produced by sulfate-reducing bacteria and sulfur-oxidizing bacteria. This deterioration involves a chemical reaction between hydration products in the hardened concrete and biologically produced sulfuric acid, which alter the concrete chemical composition leading to early deterioration and loss of mass and strength. The resulting deterioration can cause leakage and structural failure (Sand and Bock 1991).

While a very limited amount of information is available on microbial communities potentially being involved in the deterioration of concrete bridge structures, damage from microbial colonization on sewer systems, water treatment plants, agricultural construction, and concrete cooling towers has been extensively documented (Park 1945, Vincke et al. 2001, Jensen et al. 2008, Maeda et al. 1999, Yamanaka et al. 2002, Okabe et al. 2007, Zhang and Zhang 2006). In environments with a high concentration of anaerobic bacteria, such as in a sewage system, the anaerobic respiration process produces hydrogen sulfide gas. Turbulence from force mains, drop manholes, and pump stations allow the hydrogen sulfide gas to release into the atmosphere in pipes and manholes. As shown below in Equation (1), sulfide gas is then converted into sulfuric acid by the aerobic *Thiobacillus* bacteria that grow on the concrete surfaces above the wastewater flow.

$$H_2S+2O_2 \rightarrow H_2SO_4 \quad (1)$$

Once *Tithiaoxidans* becomes established, the rate of sulfuric acid production increases causing a higher rate of concrete deterioration. When the sulfuric acid attack occurs, the surface pH drops and sulfuric acid permeates and will react with calcium hydroxide and Calcium Silicate Hydrate (C-S-H) to form gypsum ($CaSO_4 \cdot 2H_2O$) (Shook and Bell 1998, Vincke et al. 2002, Vincke et al. 2001; Parande et al. 2006; Yang and Nonaka 1998) as shown in the following equations (2) and (3):

$$Ca(OH)_2 + H_2SO_4 \rightarrow CaSO_4 \bullet 2H_2O \quad (2)$$

$$3CaO \bullet 2SiO_2 \bullet 3H_2O + 3H_2SO_4 + 4H_2O \rightarrow 3CaSO_4 \bullet 2H_2O + 6Si(OH)_2 + 4H_2O \quad (3)$$

The formation of gypsum causes expansion with an increase in volume by a factor of 1.2 to 2 and softening which under severe and continuous exposure may result in complete deterioration of the hardened concrete. Furthermore, the reaction between gypsum and calcium aluminate hydrate (C_3A) with the formation of a tricalcium aluminate forming calcium sulphoaluminate, known as ettringite ($CaO{\cdot}Al_2O_3{\cdot}3CaSO_4{\cdot}32H_2O$) causes an even larger volume expansion. The chemical reaction is shown in the following equation (4):

$$3CaSO_4{\bullet}2H2O + 3CaO{\bullet}Al_2O_3 + 30H_2O \rightarrow 3CaO{\bullet}Al_2O_3{\bullet}3CaSO_4{\bullet}32H_2O \quad (4)$$

This secondary ettringite is in an unstable state under the condition of strong acidity, and it will be decomposed into $CaSO_4{\bullet}2H_2O$ and $Al_2(SO_4){\bullet}nH_2O$ by sulfuric acid. While gypsum does not provide structural support, especially under high moisture conditions which dissolve the gypsum, the delayed formation of ettringite inside hardened concrete can generate internal stress and further result in concrete deterioration (Bock and San 1986, Lauer 1990, Berndt 2001, Roberts 2002, Zhang and Zhang 2006).

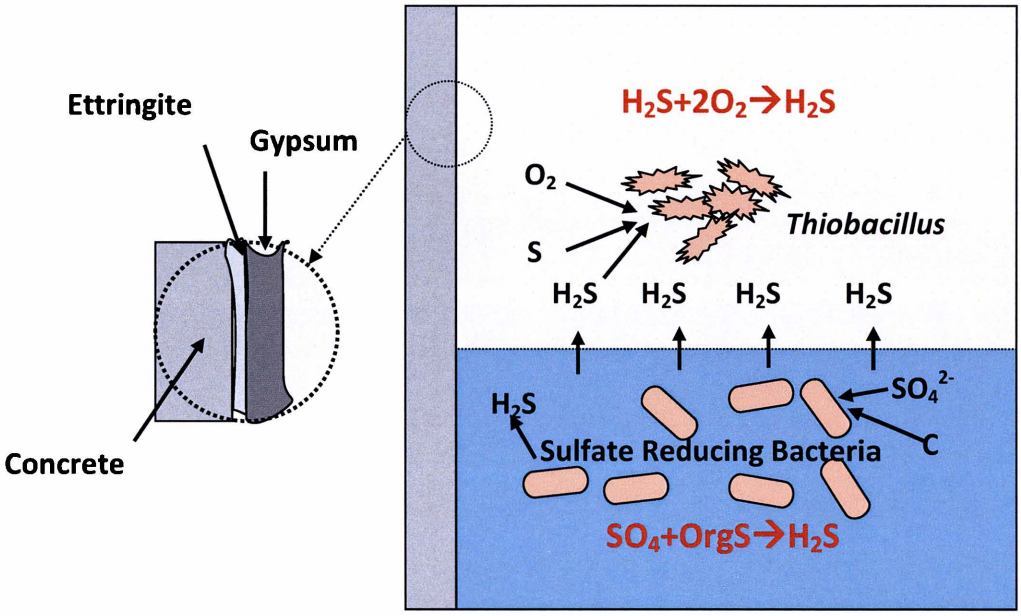

Figure 2. Mechanism of Microbial Induced Deterioration (MID).

In summary, as schematically shown in the diagram above in Figure 2, the MID process involves anaerobic bacteria that produce hydrogen sulfide (H_2S), which eventually forms sulfuric acid which reacts with calcium hydroxide ($Ca(OH)_2$) to form gypsum ($CaSO_4{\cdot}2H_2O$). The formation of gypsum is associated with an increase in concrete volume by a factor of 1.2 to 2. A further reaction between gypsum and calcium aluminate hydrate with the formation of ettringite

($CaO \cdot Al_2O_3 \cdot 3CaSO_4 \cdot 32H_2O$) can cause an even larger volume of expansion. While gypsum does not provide structural support, especially under high moisture conditions, the delayed formation of ettringite inside hardened concrete can generate internal stress and further result in concrete deterioration.

TEST METHODS IN MICROBIAL ATTACK IDENTIFICATION

A considerable number of test methods and procedures have been developed and used to identify MID of concrete. Microbial analyses include total microbial cell counts, *in situ* fluorescence, and DNA extraction (Mori et al. 1991, Davis et al. 1998, Bell et al. 1999, Welton et al. 2005, Okabe et al. 2007) while chemical analyses including hydrogen ion and sulfate concentration (Mori et al. 1991, Monteny et al. 2001, De Belie 2004. Okabe et al. 2007) were successfully used to identify microbial attack. On the other hand, another major approach for assessing the extent of deterioration of concrete uses mechanical testing methods such as the rebound hammer test, ultrasonic pulse velocity (UPV) and pin penetration depth tests to reflect concrete deterioration indirectly (Akman and Guner 1984, Yang and Nonaka 1998). Microbial attack simulation can also be used to evaluate the effects of different mixes on the resistance of concrete against MID and to quantify concrete degradation due to MID (Mori et al. 1991, Davis et al. 1998, Yang and Nonaka 1998, Vincke et al. 2002, De Belie 2004, Welton et al. 2005, Bassuoni and Nehdi 2007, De Muynck et al. 2008).

Data is currently available on some of the types of microbes implicated in concrete deterioration. Recent work by several groups, mainly in Japan, Belgium, and Denmark, has provided significant baseline data on the importance of sulfur (and iron) oxidizing bacteria in deteriorated concrete in sewage treatment plants or sewer systems (Maeda et al. 1999, Yamanaka et al. 2002, Okabe et al. 2007, Jensen et al. 2008), or on their abundance in constructed environments with low pH (Nicomrat et al. 2006). These studies have linked several phyla to concrete corrosion in sewage treatment plants with major populations (i.e., up to 80% of all bacteria) represented by *Acidithiobacillus thiooxidans*, *A. ferrooxidans* and other *Acidithiobacillus* species, and to a lesser extent by members of *Leptospirillum* groups I, II and III, *Thiomonas intermedia, Thiobacillus plumbophilus* or *Halothiobacillus neapolitanus* (Okabe et al. 2007). Many of these bacteria are difficult to obtain in pure culture or have not been isolated successfully, yet data on their presence, abundance, and diversity may be obtained by

using molecular biology tools such as *in situ* hybridization and polymerase-chain-reaction (PCR) analyses. These analyses are unaffected by the limitations of culturability. The abundance of organisms has been related to large declines in pH, i.e., from pH 12 in unaffected concrete to pH 2, and with a concomitant increase in sulfate concentration (Okabe et al. 2007).

Due to a lack of complete understanding of the mechanism of concrete degradation due to MID, methods for field site identification of microbial induced degradation are still very limited. Besides visual inspection of concrete deterioration, physical and chemical tests are commonly used to evaluate overall concrete quality and deterioration. The very limited information that has been provided from field tests with regard to MID, includes poroscope for field permeability, and aquameter for concrete surface moisture content, surface pH and carbonation depth (Ismail et al. 1993, McPolin et al., 2007, Giannantonio 2008). Other approaches for assessing the extent of chemical reaction between sulfuric acid and concrete employed mechanical testing methods such as the rebound hammer test, ultrasonic pulse velocity and pin penetration depth tests (Akman and Guner 1984, Yang and Nonaka 1998). However, all of the above mentioned measures can only reflect concrete deterioration indirectly, rather than identify markers associated with microbial attack or key environmental parameters that promote microbe activity and growth.

In addition, a variety of methods have been applied in laboratory analyses of the degree of concrete deterioration due to MID, and the effect of different mixes on the resistance of concrete against microbial attack. Parameters such as the visual observation of deterioration (Yang and Nonaka 1998, Okabe et al. 2007), mechanical properties including surface roughness, mass and volume loss, and strength loss were used to quantify concrete degradation (Mori et al. 1991, De Belie 1996, Davis et al. 1998, Yang and Nonaka 1998, Bell et al. 1999, Monteny et al. 2001, Vincke et al. 2002, De Belie 2004, De Belie 2005, Bassuoni and Nehdi 2007, Okabe et al. 2007, De Muynck et al. 2008). Mineralogical and petrographic analysis including Scanning Electron Microscopy (SEM), X-ray Diffraction (XRD), and X-Ray Fluorescence (XRF) were also used to quantify degradation of concrete under microbial attack (or simulation) (Mori et al. 1991, Davis et al. 1998, Yang and Nonaka 1998, Vincke et al. 2002, De Belie 2004, Welton et al. 2005, Bassuoni and Nehdi 2007, De Muynck et al. 2008). Research has also successfully related the number of microbes present in deteriorated concrete to the degree of damage and the acid conditions produced from microbes (Milde et al., 1983; Trejo et al. 2008). Although all of the above mentioned analyses indicate the involvement of sulfur oxidizers in the latter stages of the

corrosion process, information is still missing on microorganisms or chemicals in the environment (e.g., sulfide) that might initiate the corrosion process, i.e., decrease the pH from pH 12 to values of about pH 8 (or lower depending on the organism). In summary, current practice in microbial induced deterioration identification is still mainly based on laboratory biological tests of specimens collected by scraping, coring, or adhesive tape from suspected locations; the procedures are either time consuming or not practical to effectively evaluate suspected structures.

INFLUENCE OF MID ON CORROSION OF REINFORCEMENT

Reinforced concrete such as that used for bridge columns deteriorates not only due to natural degradation, but the deterioration can also be aggravated by the corrosion of the reinforcement inside concrete. Generally, reinforcing steel in concrete is protected against corrosion as the solid concrete serves as an ideal barrier and prevents moisture and oxygen from contacting steel. In addition, because of the high alkalinity of the concrete, a passive film forms on the steel and prevents the anodic dissolution of the iron, which in turn reduces the rate of corrosion to a very low and harmless value. Thus, concrete cover provides chemical as well as physical protection to the steel.

One major mechanism of MID influencing reinforcement corrosion is the deterioration of concrete cover. Due to MID, the level of protection can be significantly reduced because of the loss of surface concrete. In addition, due to the deterioration of concrete, an excess amount of cracks might serve as a means for moisture and oxygen to react with steel. When surface concrete deteriorates, the depth of cover over the reinforcement is reduced, and the reinforcement underneath the concrete surface will be more susceptible to corrosion. Related research shows that the tendency of steel corrosion in reinforcement concrete is sensitive to the depth of concrete cover, as small changes in the cover depth can lead to early corrosion while the depth and integrity of the concrete cover is critical for the long-term service life of reinforced concrete bridge elements (Trejo and Reinschmidt 2007).

It is a well-known fact that the natural high alkalinity of concrete serves as a natural protection of reinforcement from corrosion, in addition to a loss of covering thickness from concrete deterioration, a decrease in pH can also cause the dissolution of the protective layer around the steel. The steel reinforcement will therefore be more liable to corrosion which in turn

causes cracking and spalling of concrete. A potential-time behavior study indicated that the steel rebar will be in an active corrosion condition when the pH value of concrete drops under a citrate level (Parande and Palaniswamy 2005).

An additional chemical factor associated with MID which also affects concrete surfaces is carbonation. This phenomenon is expedited by the microbial production of CO_2, which in turn leads to surface acidification and colonization by additional organisms (Ismail et al. 1993; Sand 1997). The carbonic acid from CO_2, together with the sulfuric acid produced from H_2S, reduces the pH at the concrete surface, which makes the structure more susceptible to corrosion of the reinforcement and the resulting deterioration can cause leakage and structural failure. In addition, as the surface of concrete at bridge columns generally is subject to long-term wetting, the water will diffuse through the porous structure of concrete or by traveling along cracks and react with steel, which might also lead to corrosion of reinforcement.

In summary, the microbial growth over a concrete surface can significantly reduce the alkalinity of concrete, from pH 11 to 13 in unaffected concrete to a pH as low as 2. In addition, as concrete serves as a natural protection of reinforcement from corrosion, MID can endanger reinforcement due to the loss of concrete covering. The natural protection of reinforcing steel in concrete may be subjected to a significant reduction due to microbial attack. Despite the importance of this issue, likely due to the complexity of reaction and difficulty in simulating the attack, data on the deterioration of reinforcement due to microbial attack is very limited. It should be noted that much of the research citing microbial induced corrosion refers to the deterioration of concrete, polymers, glass, ceramics and metals caused by microbial attack, instead of corrosion of reinforcement itself. In order to distinguish this, the term of corrosion in this report refers solely to corrosion of concrete reinforcement due to the oxidation process of steel.

STATE-OF-THE-PRACTICE REPAIR AND REMEDIATION METHODS

Efforts to minimize or prevent microbial attack in concrete have been extensive. Traditionally, efforts to control deterioration due to microbial attack have been focused on coating the concrete or using plastic liners. Several other techniques currently in use around the world include spraying with magnesium hydroxide to raise the concrete surface pH and using antibacterial admixtures inside concrete (Sydney et al. 1996, Shook and Bell 1998, Ramsburg

2004). In general, there are three major preventative measures for the deterioration due to microbial attack: (1) coatings; (2) sewer treatment; and (3) modification of concrete materials.

The principle of coating is to treat surfaces with water repellents such as epoxy coatings, solid polyurethane, silanes or siloxanes, pore blockers, and acid resistant coatings (Redner et al. 1991, Parande et al. 2006; Shiwei, 2006). Materials for surface protection (coatings) to resist chemical attack are described in detail in the report of ACI Committee 515, "Guide for Protection of Concrete against Chemical Attack by Means of Coatings and Other corrosion Resistant Materials." Generally speaking, coating materials with low permeability can reduce the direct interaction of harmful chemicals with concrete, hence reduce potential damage. A related approach is to apply antimicrobial chemicals or bio-toxic materials (metal oxide) to the concrete surface to inhibit the growth of bacteria (William et al. 1998; Hewayde et al. 2005). The practice is typically applied by mixing the bacterial inhibitors with concrete and spraying as shotcrete. Other application modes include mixing the inhibitors with an epoxy, with the mixture applied to the concrete surface using spraying equipment. Results show that although surface treatment may prevent further deterioration, most of the treatments are costly and do not provide adequate, long-term protection or control. Vaidya et al. (2007) developed an innovative method for mitigating MID in concrete sewer pipes by driving nanoparticles (electrokinetics) containing an antimicrobial agent into the hardened concrete via its pore structure. This electrokinetic coating is an electrical deposition method, which involves the application of a weak electric field between the pipe reinforcement and a solution of nanoparticles. It should be noted that the concrete coating produced in this way is not 100% effective, as acid can penetrate the coatings through pinholes and react with the concrete; thus destroying the bond of coating to the concrete. In addition, the difference in coefficient of thermal expansion of the different layers may compromise the integrity of the surface coating, which generally results in degradation with age and a constant need for maintenance (De Belie et al. 2006). The number of bridge columns and cost of these materials also do not allow the technique to be used on a regular basis as a remediation option.

Another common method used to prevent microbial deterioration of concrete in sewer lines is to continuously or regularly inject chemicals such as potassium permanganate, chloride, and oxygen into raw sewage.(Padival et al. 1995, Ramsburg 2004). The crown spray process uses a similar approach (Esfandi 1986, James 2003, Sydney et al. 1996). The principle behind

the crown spray process involves spraying the crown region of a pipe with a high pH material (magnesium hydroxide), thus elevating the region's alkalinity. The previous methods are expensive and only temporary fixes that need to be repeated on a regular basis (time between application approximately 6-9 months) due to depletion and washout of the magnesium hydroxide (Vaidya 2007). Also, the process is not applicable to structures such as bridge columns exposed to open water.

One other major effort to control deterioration from microbial induced distress is to carefully design concrete. Based on the "Guide to Durable Concrete" developed by the American Concrete Institute (ACI 2008), it is essential to design high quality concrete and provide enough cover to prevent the steel reinforcement from corrosion. An effective way of decreasing the chemical attack on Portland cement concrete is to decrease the C_3A content (Mather 1968). Accordingly, the use of Type V sulfate-resistant cement and Type II moderately sulfate-resistant cement (with a maximum C_3A content of 5% and 8% respectively according to ASTM C150) should increase the microbial attack resistance of concrete. Results also show that high alumina cement concrete or Calcium Aluminate concrete generally performs better than portland cement concrete, because of the absence of free hydrated lime (De Belie, 1997; Saucier and Lamberet 2009). Studies have shown that the application of SCMs, such as slag, fly ash, and silica fume can increase considerably the sulfate attack resistance of concrete. Cementitious materials significantly reduce the permeability of concrete (Bakker 1980, Metha 1981, Hyman 2005). Other than reduce the amount of C_3A inside concrete, cementitious materials also combine with the alkalis and calcium hydroxide released during the hydration of cement (Vander Bosch 1980, Roy and Idorn 1982, Idorn and Roy 1986), and reduce the potential for gypsum formation (Lea 1971, Biczok 1972, Kalousek et al. 1972, Metha 1976).

Based on a similar mechanism as from sulfate attack, preliminary research has been performed in studying the effectiveness of cement type (Saricimen et al. 2003, Davies 2005, De Belie 2005), addition of polymer (Beenldns et al. 2001, Monteny et al. 2001, Xiong et al. 2001, Vincke et al. 2002, De Belie 2005, De Belie et al. 2006, Parande et al. 2006), and cementitious materials (De Belie 1996, Liskowitz et al. 1998, Berndt et al. 2001, De Belie 2004, De Belie 2005; Berndt, 2011) against microbial attack. Results indicate that the above mentioned materials may be able to provide concrete with better resistance against microbial attack, in different degrees. Other minerals such as montmorillonite were also found to potentially improve MID

resistance. Due to the plate morphology of montmorillonite, the expectation for barrier performance against microbial attack is also expected. Calcium exchanged montmorillonite has been reported to play a role in reducing the alkali-silica reaction (Shimatani 1987), presumably, reducing the potential damage from microbial attack. The substitution of montmorillonite for cement or fine aggregate to prepare a concrete nanocomposite therefore is expected to enhance the microbial attack resistance of concrete. However, a systematic study of the effect of different materials on MID resistance of concrete is needed to mitigate microbial attack on concrete (Berndt et al. 2001).

It should be noted that after appropriate removal of deteriorated surface layers, repairs and rehabilitation can be achieved through many of the above-mentioned measures. Research shows that by applying high-density polyethylene (HDPE) sheets with fresh mortar containing bacterium inhibitors, sulphur-oxidising bacterial deterioration can be effectively repaired (Atsunori and Maeda 1999). The repair method is advantageous because it can be applied to large sheets without making wrinkles, there are less holes to support the concrete panels and fewer welding spots. However, if sulphate were not appropriately removed and remained in the concrete, the sulphate would react with the fresh mortar in the cement and produce ettringite that would peel the mortar from the concrete, with the consequence of an acceleration of deterioration.

Another common practice is to apply antibacterial remediation in concrete. Additives including antibacterial hydrotalcite (Nonaka and Sato 2001), poly(hexamethyleneguanidin) phosphate (Tsudome et al. 2004), sodium fluoride (Utrobin et al. 2009), Dopamelanin (Solis 2010), Katain (2667-22-3) inhibitor Kl-1 (65988-15-0) (Goncharov 1984), and organomontmorillonite prepared by the exchange with benzyl-C10-18-alkyldimethyl quaternary ammonium chlorides (Beklimyshev et al. 2008) have proven to be effective in MID remediation. Some other commercially available technologies for MID remediation are summarized in Appendix A.

In summary, the attack of concrete by bacteria is a worldwide problem associated with the degradation of concrete and the transmission of diseases associated with human contact with the infected concrete surface. Technologies associated with the remediation of this problem cover a wide range of chemistry. It should be noted that although these techniques have shown some promise in reducing MID, it is still necessary to further characterize the deterioration

process to allow the development of new control technologies (Davis et al. 1998, Bell et al. 1999).

CHAPTER 3:
FIELD SAMPLE COLLECTION AND IN SITU TESTING

SITE LOCATIONS

In this project, twelve bridges identified by TxDOT with suspected MID were selected according to advice provided by project director and Project Monitoring Committee (PMC) on the project. All bridges were in the eastern half of Texas, i.e., east of Interstate-35. Of the twelve bridges, two were from Liberty county, one was from Robertson County, three were from Hunt county, one was from Jefferson county, three were from Sabine county, and two were from Henderson county. It should be noted that all the selected twelve bridges are under fresh water body conditions. The locations of the twelve bridges are shown in Figure 3 below.

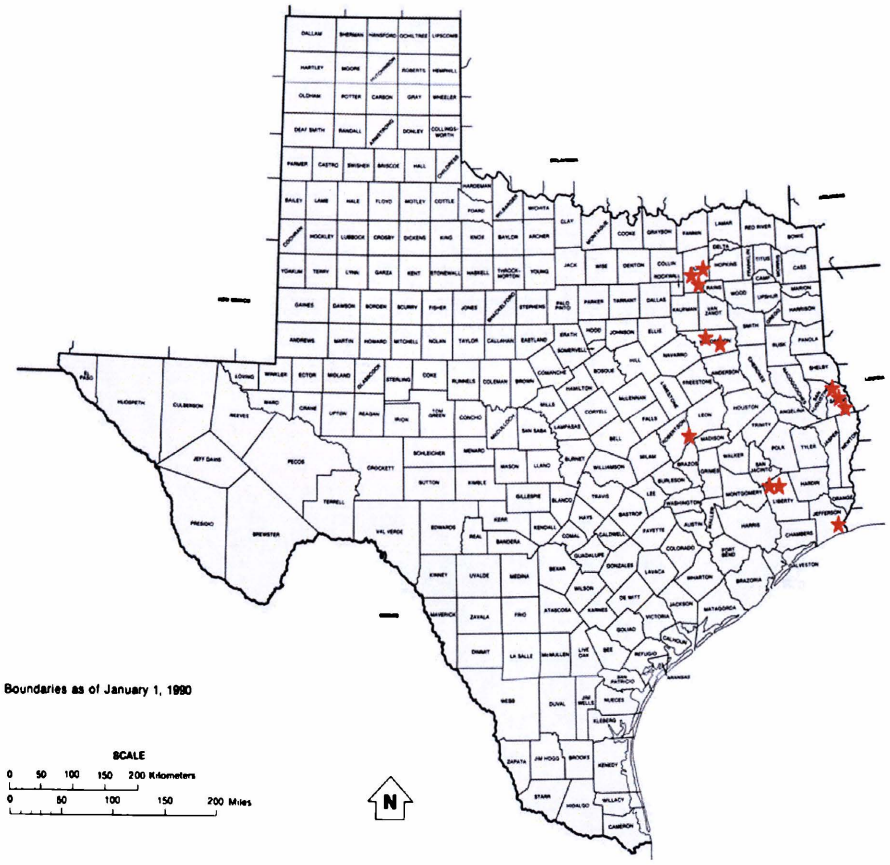

Figure 3. Site Visit Locations.

Detailed information of site visit locations, county, GPS latitudes and longitudes and year built for each bridge visited are summarized in Table 1.

Table 1. Information on the Locations of the Site Visits.

	Site Location	County	GPS Lat.	GPS Long.	Year Built
1	FM 787 @ Tarkington Bayou	Liberty	30.35467624	-95.05299129	1930*
2	SH 21 @ Navasota River	Roberston	30.86970776	-96.19254394	1959
3	SH 276 @ Lake Tawakoni	Hunt	32.90405349	-95.99853246	1959
4	SH 82 @ Alligator Bayou	Jefferson	29.87770685	-93.97911691	1952
5	FM 276 @ Patroon Bayou	Sabine	31.52276283	-93.79931811	1967
6	SH 21 @ Carrice Creek	Sabine	31.45585875	-93.76156541	1967
7	FM 3121 @ Palo Gaucho Bayou	Sabine	31.41320518	-93.78129968	1968
8	SH 31 WB @ Kickapoo Creek	Henderson	32.30112370	-95.50136160	1930s
9	SH 31 EB @ Kickapoo Creek	Henderson	32.29986000	-95.50582000	1970s
10	FM 787 @ Tarkington Bayou	Liberty	30.35529000	-95.05120000	1930
11	FM 751 @ Duck Creek	Hunt	32.85147471	- 96.05812551	1959
12	FM 751 @ S. Fork Sabine River	Hunt	32.86086642	-96.06713390	1959

* Bridge was originally built in 1930 and widened in 1973

Visual inspection and *in situ* evaluations were performed on all twelve bridges. Water, mud and concrete samples from columns were collected for further laboratory investigation through microbial, chemical, mineralogy and petrographic analysis. Information on the date and weather conditions for each visit is summarized in Table 2.

Table 2. Date and Weather Conditions for Each Visit.

	Site Location	Date of Visit	Temperature	Humidity
1	FM 787 @ Tarkington Bayou	11/05/09	74°F	55%
2	SH 21 @ Navasota River	11/19/09	74°F	49%
3	SH 276 @ Lake Tawakoni	12/10/09	36°F	41%
4	SH 82 @ Alligator Bayou	4/30/10	75°F	81%
5	FM 276 @ Patroon Bayou	12/3/10	52°F	76%
6	SH 21 @ Carrice Creek	12/3/10	71°F	59%
7	FM 3121 @ Palo Gaucho Bayou	12/3/10	78°F	54%
8	SH 31 WB @ Kickapoo Creek	4/14/11	80°F	63%
9	SH 31 EB @ Kickapoo Creek	4/14/11	75°F	81%
10	FM 787 @ Tarkington Bayou	7/21/11	89°F	54%
11	FM 751 @ Duck Creek	7/22/11	75°F	81%
12	FM 751 @ S. Fork Sabine River	7/22/11	90°F	63%

VISUAL INSPECTIONS

Before field sampling and *in situ* testing, visual inspections were performed to examine bridge column appearance. A hammer test as shown in Figure 4 was also used to evaluate the

soundness of the surface and near-surface concrete; the test involved striking areas of surface delamination. Information such as visual evidence of concrete cracking, spalling, delamination, efflorescence, softening of concrete and corrosion of steel were recorded. Based on the visual inspections, locations for *in situ* testing and specimen extraction were determined, and generally three to four representative columns from each bridge were selected.

Figure 4. Hammer Test of Concrete Condition.

IN SITU TESTS

In order to evaluate the level of deterioration under a variety of conditions, a number of *in situ* tests were performed on selected bridge columns. Most tests including Schmidt rebound hammer, half-cell corrosion potential, and covering thickness were generally performed at twelve inch intervals, starting at six inches above water or ground level and up to seven feet above (depending upon accessibility). At each measured height, five to seven measurements (with intervals of at least six inches) were taken, outliers (results with differences equal to or greater than 20% of the average value) were removed, and the average reading from each nominal height were reported. The ultrasonic pulse velocity (UPV) and in situ phenolphthalein pH tests were performed only at selected locations. An abrasive stone was used to remove the loss (soft) mortar on concrete columns prior to testing on an as-needed basis, in order to expose the underlying concrete.

Figure 5. Schmidt Rebound Hammer Test.

The Schmidt rebound hammer test as shown in Figure 5 was used to measure the hardness of the concrete surface. Tests were performed according to ASTM C805 "*Standard Test Method for Rebound Number for Hardened Concrete*" and the results can be converted to estimated compressive strengths.

Figure 6 Ultrasonic Pulse Velocity (UPV) Test.

The Ultrasonic Pulse Velocity (UPV) test as shown in Figure 6 was performed on bridge columns to measure the velocity of an ultrasonic wave passing through the concrete, so as to

estimate the degree of internal concrete deterioration. UPV tests were performed according to ASTM C 597 "*Standard Test Method for Pulse Velocity through Concrete*", with direct transmission, i.e., two transducers lined up directly opposite each other on the column. 50K Hz frequency P-wave was applied in the measurement. It should be noted that the test was not performed on cylindrical columns or columns with high levels of surface deterioration (i.e. greater than ½ inch of penetration) due to the lack of full contact between the concrete surface and the transducers.

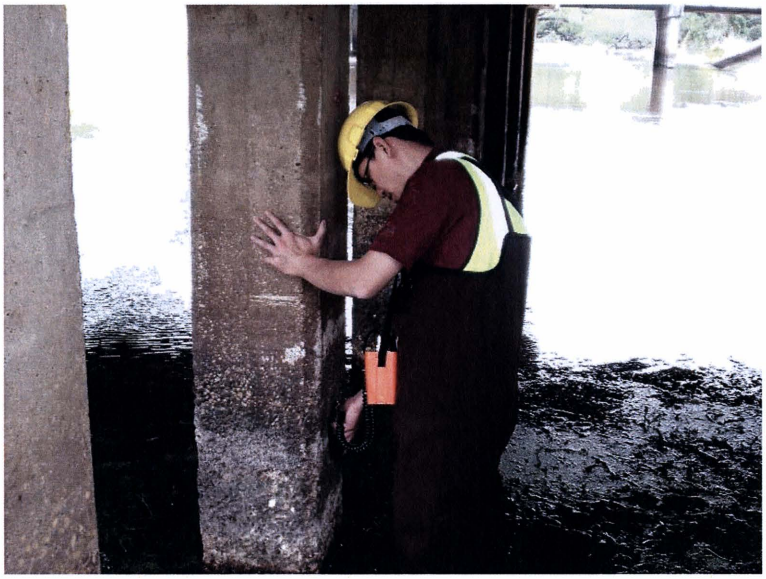

Figure 7. Covermeter (Rebar Locator) Test.

A covermeter (rebar locator) as shown in Figure 7 was used to locate rebar underneath concrete. The covering thickness of the concrete encircling the rebar was estimated through the measurement based upon an electromagnetic pulse-induction method. It should be noted that the measurements were only performed in the direction parallel to the main reinforcement direction (i.e., vertical direction) in this study.

Figure 8. Half-Cell Corrosion Potential Test.

Corrosion activity was measured with a half-cell corrosion potential measuring device as shown in Figure 8. The device is the same one as shown in Figure 7, with an exchangeable gauge that can also accept a half cell attachment. The measurement is associated with the steel corrosion rate, which can signal the severity of rebar corrosion. The corrosion potential of reinforcement was a qualitative measure through the evaluation of the potential difference between a standard portable half-cell, normally a Copper/ Copper Sulphate ($Cu/CuSO_4$) or Silver/Silver Chloride (Ag/AgCl) standard reference electrode placed on the surface of the concrete with the steel reinforcement underneath. The half-cell potential method measures the current flow (in the form of ion migration) through the concrete between anodic and cathodic sites accompanied by an electric potential field surrounding the corroding bar when there is active corrosion that exists. Procedures as described in ASTM C876 "*Standard Test Method for Half-Cell Potentials of Uncoated Reinforcing Steel in Concrete*" were used, and the (corrosion) potential was measured against a silver/silver chloride reference half cell in this study. The corrosion potential usually is presented as the voltage of current flow. With the silver/silver chloride half cell used in the present study, a voltage higher than -120mV indicates a 90% chance of no active corrosion, a voltage lower than -270 mV indicates a 90% chance of active corrosion, while voltages between -120mV and -270mV indicate a uncertainty of active corrosion. It should be noted that since the measurement requires direct contact with rebar, half

cell corrosion potential tests were only performed at selected columns, and that depended on accessibility and level of deterioration.

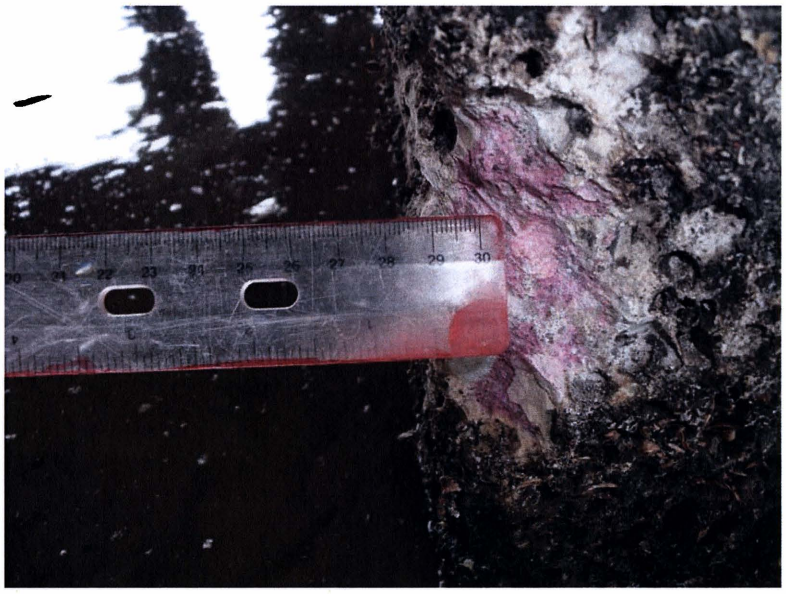

Figure 9. *In Situ* Phenolphthalein pH Test.

In addition to the nondestructive tests as mentioned above, as MID generally is associated with reduction of pH, an *in situ* phenolphthalein pH measurement was performed as shown in Figure 9. Prior to each test, fresh fracture concrete surfaces with depths of up to 10mm were exposed with a sterilized metal chisel. Upon application of a phenolphthalein solution to the surface of the concrete, areas with low or no deterioration turned pink because of high alkalinity, while other areas remained colorless indicating a reduced pH value (lower than 8), likely due to either chemical or microbial attack or carbonation. MID generally is associated with colorless phenolphthalein (or low pH).

Sample Collection

Several water and mud samples underneath each bridge were taken at various locations within the general area of each concrete column in order to determine the pH, microbe type and quantity. As shown in Figure 10, surface concrete samples with adherent microbial organisms were removed by a sterilized metal chisel and/or steel brush and collected at locations with different levels of deterioration. In order to estimate a difference in the chemical composition, and type and population of microbial organisms within each location, deteriorated, semi-

deteriorated and non-deteriorated organic surface scrapings were obtained from selected bridge columns supporting the bridge span. Generally, deteriorated specimens were taken at approximately 6 inches to 12 inches above water level, non-deteriorated specimens were taken at approximately 4 feet to 6 feet above the water level (depending on the accessibility) and semi-deteriorated specimens were taken approximately at a midpoint between the other two heights.

Figure 10. Chemical and Microbial Specimen Collection.

As shown in Figure 11, core specimens, one and a half inches in diameter and two to three inches deep were extracted from various columns. It should be noted that nearly all core specimens were in good condition with no sign of crumbling after they were removed from the drill pit. This observation is consistent with the visual observation and hammer tests which demonstrated that most bridge columns appeared to be in fairly good condition with different levels of deterioration on the concrete surface but no sign of internal deterioration or cracking.

Figure 11. Core Specimen Collection.

Surface and core concrete specimens were used to analyze microbe type and quality, sulfate and chloride concentration, minerals and the microstructure of the concrete. In addition, core specimens were also used to determine the degree of MID by examining the change of pH over the depth of concrete using a phenolphthalein color test.

VISUAL INSPECTION AND IN SITU TEST RESULTS

Examples of overview and close up looks for deterioration are shown in Table 3. It should be noted that due to seasonal changes at the time of visit, water levels varied significantly, which may result in a lack of accessibility to selected sections of bridge columns (i.e. Bridge 3) or full exposure of sections of bridge columns that are under water most of the time (i.e. Bridge 5, Bridge 6 and Bridge 7).

(a) (b)

(c) (d)

Table 3. Examples of Visual Inspection. (a) Bridge 5 (overview), (b) Bridge 5 (close up view), (c) Bridge 9 (overview), (d) Bridge 9 (close up view).

Observations during visual inspection are summarized in Table 4. Visual inspections indicated that all twelve bridges have different levels of deterioration, mostly with softening of the surface and near surface concrete and light to medium levels of scaling (indicated by penetration depths of less than half an inch). Generally, the higher above water level, the less

degree of deterioration is observed, which is consistent with the hypothesis of MID since microbes are more active in a high moisture environment. In most cases, deterioration was found to reach several feet above the water level at the time of site visit. Details of results from visual inspection can be found in Appendix B.

Table 4. Summary of Visual Inspection.

Bridge	Scaling (Penetration Depth)	Observation of Deterioration
1	No (original columns) Light (< ¼") (expansions)	Original columns - no obvious deterioration. 1973 columns - loss of surface mortar.
2	Light (< ¼")	Loss of surface mortar in central wall span. Bottom part appeared to be repaired.
3	Medium (1/4"-1/2")	Loss of surface mortar and exposure of coarse aggregate.
4	Medium(1/4"-1/2")	Severe vertical cracks in main rebar direction. Visual rebar exposure and corrosion.
5	Medium (1/4"-1/2")	Loss of surface mortar and exposure and pop out of coarse aggregate.
6	Medium (1/4"-1/2")	Loss of surface mortar. Exposure of coarse aggregate. Suspected construction defects.
7	Medium (1/4"-1/2")	Loss of surface mortar and exposure and pop out of coarse aggregate.
8	Severe (½" to 1")	Loss of surface mortar. Exposure of coarse aggregate. Visual rebar exposure and corrosion and very severe scaling (up to 3" penetration) on selected columns.
9	Severe (½" to 1")	Loss of surface mortar. Exposure of coarse aggregate.
10	Light (< ¼")	Loss of surface mortar
11	Medium (1/4"-1/2")	Loss of surface mortar. Exposure of coarse aggregate.
12	Medium (1/4"-1/2")	Loss of surface mortar. Exposure of coarse aggregate.

Among the twelve bridges visited, Bridge 8 and Bridge 9 show the highest level of scaling, with a significant loss of concrete cover and approximately half an inch to one inch of overall penetration. For Bridge 8, up to three inches of penetration and visual reinforcing steel exposure was observed in a few columns (two out of the 28 total columns). Bridge 4 also showed a high level of deterioration; with severe vertical cracks observed parallel to the main rebar direction, as well as visual rebar exposure and corrosion. It is worthwhile to point out that the deterioration observed in Bridge 4 is different from all other eleven bridges as the deterioration reaches well above ground level and the level of reinforcement corrosion and cracking are significant. As Bridge 4 is located within an area with significant traffic from oil refinery plants,

the difference is likely due to two major factors: 1) possible chemical deterioration due to the contamination of the water under the bridge from nearby oil refineries and possible coupled bio/chemical deterioration; and 2) corrosion product or the reinforcing steel as a result of chloride exposure. These observations are consistent with results from *in situ* measurements, which are to be presented later in this chapter. In general, for Bridge 4 although the deterioration appears to be severe, the deterioration stays only on the surface of the concrete. Hammer tests performed on the surface of the concrete showed that even with a loss of surface mortar and surface scaling, the remaining concrete was still in relatively sound condition. Further evidence from *in situ* tests, confirming the integrity of the columns, comes from core samples that showed no evidence of crumbling or collapsing. Visual inspection indicates that most bridge columns appear to be in fairly good condition.

Another observation worth mentioning is the role of aggregate and mix design , which may affect the resistance of the columns against microbial attack, i.e., concrete with limestone as aggregate might be more susceptible to MID than gravel as aggregate. To support this argument, columns from Bridge 1 built in 1973 that used limestone as aggregate have a higher level of deterioration than the original columns built in 1930 which used gravel. The new section is more than 40 years younger than the original section, yet has more deterioration. Similar evidence that supports this hypothesis comes from a comparison of columns from Bridge 6 (which used gravel as aggregate) with columns from Bridge 5 and Bridge 7 (both of which used limestone as aggregate). Although all the bridge columns were built in the same time period and exposed to the same body of water, Bridge 6 has a much lower loss of surface mortar on the concrete surface. Although no definitive conclusions can be drawn at this point, the above mentioned evidence indicates that aggregate and mix design may play a role in exacerbating MID.

Results from rebound hammer, UPV, half-cell and covering thickness tests at different column testing heights and bridges are summarized in Figure 12 to Figure 16. In these figures, the first digits of specimen label refers to bridge number, and the digits following "C" refer to column number, and test location. It should be noted that selected measurements were performed over wall sections and a label of "Wall" was used to correspond to test locations.

As expected, rebound hammer tests as summarized in Figure 12 indicate, in general, an increase of strength or surface hardness with an increase in the height of the column, which is consistent with the observation that deterioration is less severe when it is away from water level.

In spite of this, the rebound results are highly scattered, and generally standard deviations increase at lower elevation, with up to a 50% variation observed in some locations, which is reasonable as the estimation of strength of concrete is related to surface hardness, and the direct exposure of aggregate apparently increases the variation in test results.

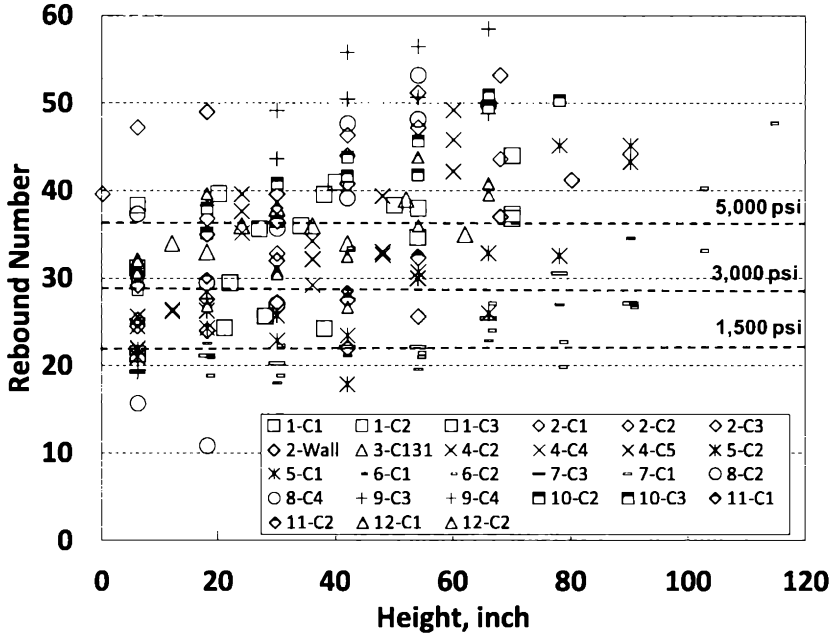

Figure 12. Summary of Rebound Hammer Test Results.

The UPV results as shown in Figure 13 indicate that most of the wave velocity falls between 12,000 to 14,000 ft/s, yielding an estimated strength of 3,000 to 5,000 psi (Malhotra and Carino 2004). The UPV readings indicate a good quality of concrete underneath the deteriorated surfaces. It should be noted that due to the high level of surface deterioration in Bridge 8 and Bridge 9, UPV readings were not reliable because of insufficient contact between the transducers and concrete and therefore were disregarded. Comparing the surface hardness measurements with the rebound hammer test, a lower degree of variation was observed from the UPV test, which is probably due to the UPV test measuring overall concrete quality instead of surface concrete condition. However, no clear relationship between UPV and height of testing location was observed.

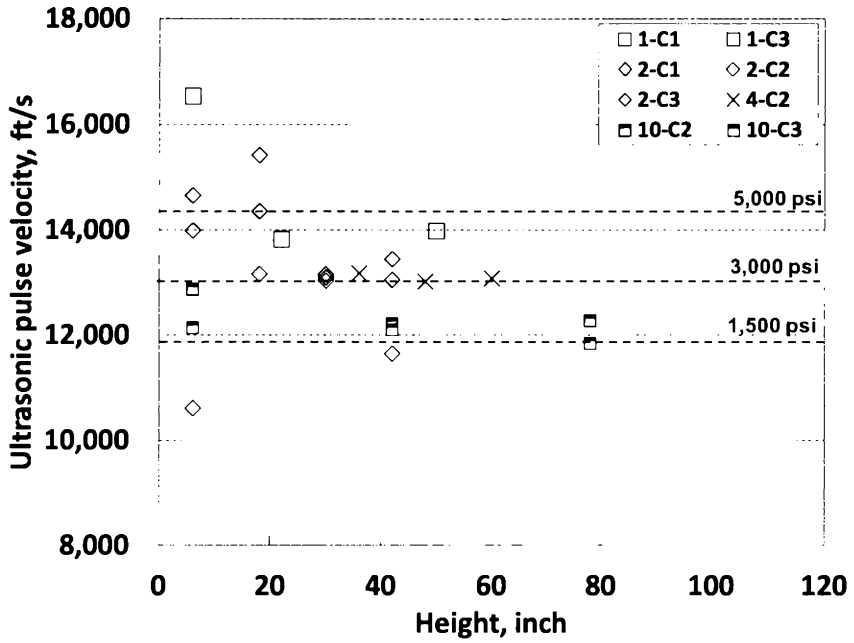

Figure 13. Summary of UPV test results.

Results from half-cell corrosion potential tests as shown in Figure 14 demonstrate a clear trend of decreasing corrosion potential with an increase in the height of the column. It should be noted that the trend of decreasing corrosion potential is not unexpected as changes in moisture content, dissolved oxygen and changes in the concentration of chloride, sulfate or other ions in the concrete as one progresses upward from the waterline will result in an increase in the corrosion potential readings (i.e., less potential of corrosion), regardless of the present of MID. However, despite the above mentioned parameters that can influence corrosion, most of the bridge columns show only a low to medium level of corrosion potential and only one site (Bridge 4), has a high level of corrosion potential which may have been caused by a significant amount of vertical cracking.

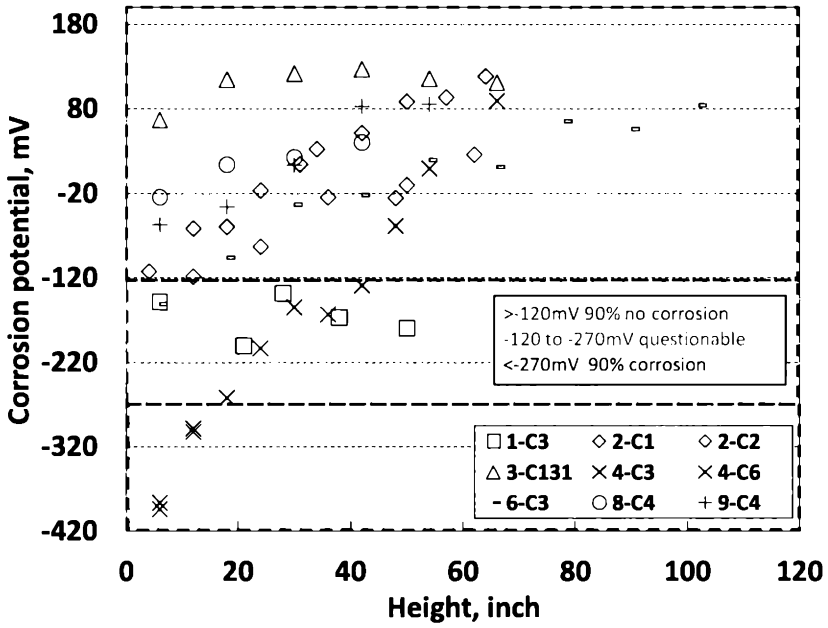

Figure 14. Summary of Half Cell Test Results.

Results from the cover meter test as shown in Figure 15 indicate that most of the bridge columns still have more than one and a half inches of concrete covering, with standard deviations mostly less than half an inch, which indicates that the reinforcement is still well protected.

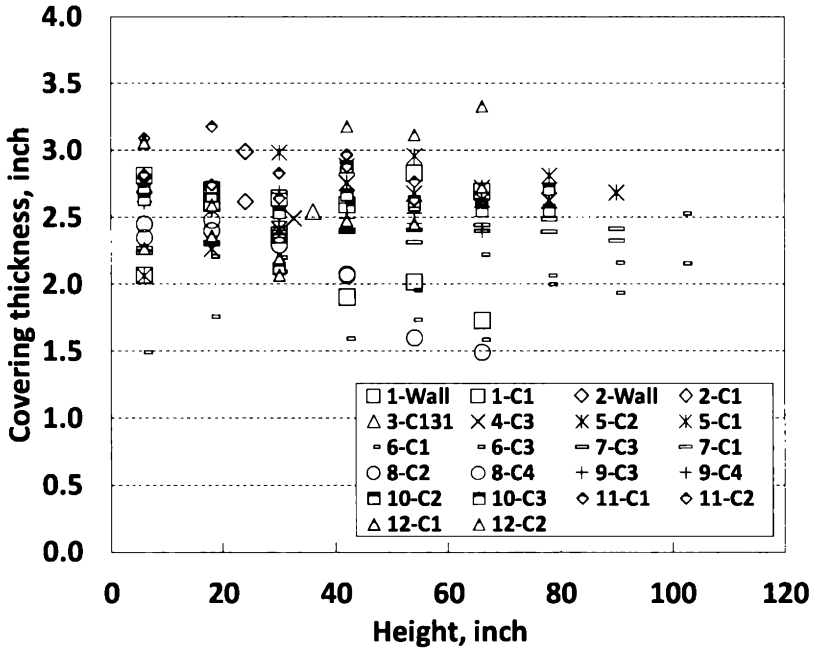

Figure 15. Summary of Covering Thickness Test Results.

Phenolphthalein pH indicator showed acidification of surface concrete in most tested bridge columns. However, results as shown in Figure 16 indicate that for all the columns tested, there was generally less than 5 millimeters of neutralized surface concrete. It should be noted that Figure 16 is presented differently than Figure 12 to Figure 15, as only a couple of measurements were taken at each of the bridges.

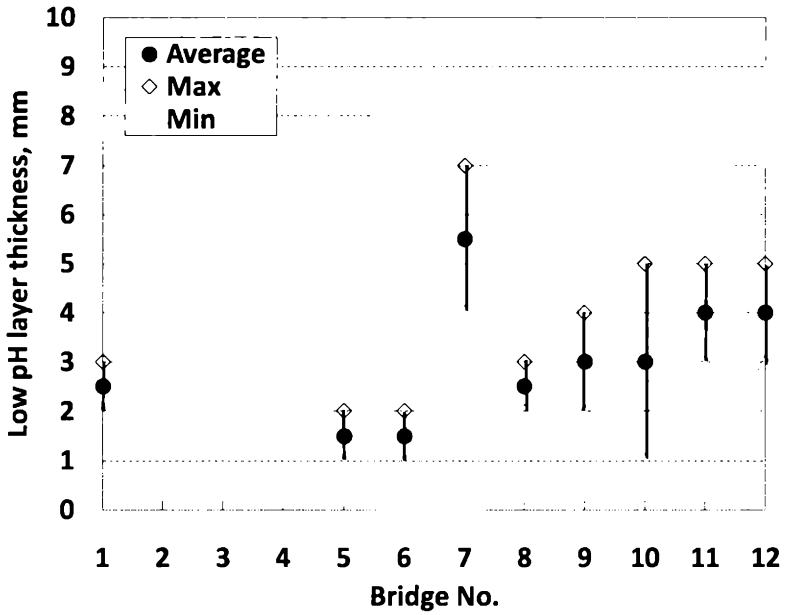

Figure 16. Summary of *In Situ* Phenolphthalein pH Test Results.

In summary, although visual inspection shows various levels of deterioration with a light to medium level of scaling, the hammer test and *in situ* test results clearly indicate that the concrete columns have maintained their integrity, with deterioration only on the surface. Results from chemical, biological and petrographic analysis from specimens collected from the field are to be discussed in the following section. As summarized in Table 4, as most of the bridges visited were more than 40 years old, the deterioration rates are slow and the extant of deterioration is not likely to pose an urgent risk to the safety of these bridges.

CHAPTER 4:
MICROBES IDENTIFICATION AND MECHANISM ANALYSIS

LABORATORY TEST METHODS

Water, mud and concrete specimens collected from the field site were analyzed in the laboratory in order to determine the mechanism and severity of microbial attack. Types of microbes and their relative abundance were identified. The relative abundance of sulfate and chloride in water, mud and concrete, together with a measurement of pH at different depths from the concrete surface was determined. Concrete mineral compositions and microstructures were analyzed using X-ray diffraction (XRD), scanning electron microscopy (SEM) and petrographic analysis.

Microbial Analysis

The aim of the microbial analysis was to identify major groups of microbes found in deteriorating concrete on bridges in Texas, and relate their abundance to potential declines in pH, i.e., from pH 12 in unaffected concrete to pH as low as 2, and with a concomitant increase in sulfate concentration (Okabe et al. 2007). Since many of these bacteria are difficult to obtain in pure culture or have not been isolated successfully yet, data on their presence, abundance, and diversity were obtained by using molecular tools such as *in situ* hybridization analyses which is unaffected by the limitations of culturability.

In this study, subsamples of microbial organisms from surface concrete collected in the field were fixed with paraformaldehyde (PFA) in phosphate buffered saline (PBS), then dispersed in 50% ethanol in PBS to a final volume of 1.5 ml and stored at -20°C until further use (Hahn et al, 1992, Amann et al. 1990). Quantitative analyses of microbial populations were then performed by *in situ* hybridization and epifluorescence microscopy. *In situ* hybridization was performed to provide information on the abundance and diversity of the microbial community in a top-down approach using a set of probes that target microbial populations with increasing specificity. Analyses started with the analysis of DAPI (4'-6-Diamidino-2-phenylindole , a DNA-intercalating dye) stained cells that should represent all organisms. Since the amount of sample analyzed could not be quantified with respect to accurate weight or volume, only percentages are presented. Detectability was determined as the percentage of organisms detected by specific

probes (e.g. all Bacteria and all Eukarya) compared to those detected by the DNA-intercalating dye DAPI.

In situ hybridization with fluorescent (i.e. Cy3-labeled) probes targeting ribosomal RNA (rRNA) sequences and concomitant staining with the DNA-intercalating fluorescent dye DAPI was used to analyze the microbial communities in deteriorated and non-deteriorated concrete samples by epifluorescence microscopy. In contrast to molecular tools targeting DNA sequences that are generally used for qualitative analyses (i.e. presence-absence assessments), this techniques allowed to visualize and quantify organisms on different taxonomic levels. DAPI-staining allows visualizing all organisms (i.e. all DNA-containing cells of the three Domains, the Bacteria, the Archaea and the Eukarya). Cy3-labeled probe EUB338 only detects a subset of the DAPI-stained cells because it binds to a signature sequence on the 16S rRNA that is only present in members of the Domain Bacteria. In addition to probe EUB338, probes specifically targeting signature sequences on rRNA of the remaining two Domains, of subgroups within the Domain Bacteria, and of bacteria shown to inhabit deteriorating concrete in sewer systems were used for an increasingly more specific analysis of microorganisms in concrete samples. In contrast to molecular tools targeting DNA sequences that are generally used for qualitative analyses (i.e., presence absence assessments), this techniques allowed to visualize and quantify organisms on different taxonomic levels. Details of microbial analysis procedures can be found in Appendix C.

Chemical Analysis

The pH of the water samples, mud and concrete scrapings was determined using a pH meter. For the water, the pH was measured directly. For the mud and concrete scrapings, approximately 0.5 grams of dried mud or crushed concrete was weighed and placed in solution with 10mL of DI water. The pH of various core samples was first measured on the surface using phenolphthalein indicator in an approach similar to the procedure performed on site. The degree of penetration for each sample was measured around the perimeter of the core specimen by measuring the depth of the colorless solution. For the analysis of sulfate and chloride, the water and mud samples were prepared in the same way as for pH analysis. Because the most relevant ion previously found to be related to microbial degradation was sulfate produced from the oxidation of sulfide, the sulfate content, together with chloride concentrations, was measured in

surface concrete and mud specimen collected from the visited sites. Chloride was included in the analyses because of the potential influence of salt on concrete column degradation.

Concrete scrapings were ground into a fine powder using a mortar and pestle, then weighed and extracted with DI water at a weight ratio of 2:1 water: scrapings. After extraction, samples were analyzed using a Lachet ion chromatograph. The analysis protocol was EPA method 300.0 (Determination of inorganic anions by ion chromatography). The percent sulfate and chloride were then calculated based on the level of dilution during sample preparation. Details of chemical analysis procedures can be found in Appendix D.

Mineralogy and Petrographic Analysis

A previous study indicated that a major phenomenon associated with MID is the production of ettringite and gypsum. Mineralogy and petrographic analyses therefore focused on changes in hydration products, essentially the formation of ettringite and gypsum, which could be attributed to possible microbial attack (De Belie 2006). A semi-quantitative XRD measurement was performed identifying the fraction of minerals such as ettringite and gypsum in surface concrete by comparing the integrated intensities of the diffraction peaks with each of the known phases. A petrographic and SEM study was also used to evaluate the microstructure of surface and subsurface concrete, and to identify minerals from selected concrete surface sample and core samples. The information was used to evaluate the extent of concrete deterioration. Details of mineralogy and petrographic analysis procedures can be found in Appendix E.

MICROBIAL ANALYSIS RESULTS

In situ detection of bacteria in biofilm samples obtained from visibly deteriorated (a) and non-deteriorated (b) concrete sections retrieved from Bridge 3 is shown in Figure 17. Samples from both sections clearly show the presence of different communities of bacteria as indicated by differences in size and morphology both after DAPI-staining (left panel) and hybridization with Cy3-labeled probe EUB338 detecting most members of the Domain Bacteria (right panel).

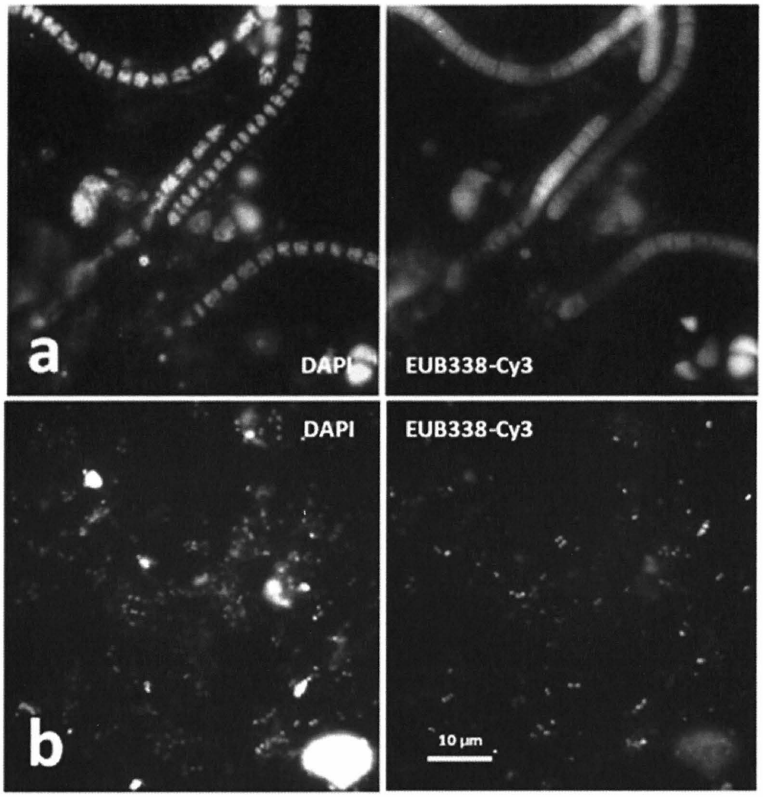

Figure 17.Example of Bacteria Communities of Deteriorated and Non-Deteriorated Concrete Surfaces.

Basic community structures for concrete samples collected from bridge 1 to 12 are summarized in Table 5. As shown in the table, the detectability of organisms was very high with most organisms detectable by *in situ* hybridization. Results as shown in Figure 18 indicated that except for bridge 1 (with DAPI-stained cells present in the range between 15 to 25 x 10^8 cells per sample), most bridges had DAPI-stained cells in the range between 1 to 5 x 10^8 cells per sample. However, there was no trend of effect of specimen height on relative counts of organism observed. As shown in Table 5, in all cases, Eukarya were detected only occasionally, and generally in percentages less than 1% of the entire community (i.e. the DAPI-stained cells). Bacteria were detected in variable percentages of the DAPI stained cells, while Archaea were not detected at all. More detailed analyses of members of the Domain Bacteria resulted in the detection of few phylogenetic groups. However, none of the respective probes resulted in the detection of significant numbers of cells, which means that most of the bacterial cells remained unidentified. These results do not support the original hypothesis that members of the β- and γ-subdivision of Proteobacteria should be dominant in deteriorated concrete samples, comparable

to results obtained for sewage plants where members of the β- and γ-subdivision of Proteobacteria have been shown to play a major role in the deterioration of concrete (Okabe et al. 2007). Thus, even concrete samples from bridges with more significant deterioration do not reflect similar conditions and microbial communities known to be responsible for concrete deterioration in sewage plants. The observation was anticipated due to the different nature of the two environments. Although individual sites differed from each other with respect to basic composition of microbial community structure, and the detectability of microbes, similar results were obtained for all bridges. Details of microbial analysis results from each individual bridge can be found in Appendix C.

Table 5. Basic Community Structures for Concrete Samples for Visited Bridges.

Bridge		1	2	3	4	5	6	7	9	10	11	12
All organisms	DAPI (x 10^8 per sample)	14.8	1.1	1.1	1.3	4.6	3.3	3.1	2.1	2.1	1.6	1.9
Domain-level analyses (in percent of DAPI counts)*	Eukarya	59	0	43	19	0	0	0	14.7	15.9	21.7	20.8
	Archaea	0	0	0	0	0	0	0	0	0	0	0
	Bacteria	41	100	57	81	77.0	35.2	51.2	17.8	19.3	19.5	13.7
Within domain Bacteria	α-subdivision of Proteobacteria	0	22	26	0	0	0	0	0	0	0	0
	β-subdivision of Proteobacteria	0	14	0	0	0	0	0	0	0	0	0
	γ-subdivision of Proteobacteria	0	13	0	0	6.5	5.1	4.8	18.0	21.2	17.6	20.5
	δ-subdivision of Proteobacteria	0	0	0	0	0	0	0	0	0	0	0
	Gram-positive bacteria with high DNA G+C content	0	18	0	0	0	0	0	0	0	0	0
	Gram-positive bacteria with low DNA G+C content	0	0	0	0	0	0	0	0	0	0	0
	Cytophaga-Flavobacterium cluster of the CFB phylum	0	0	0	0	0	0	0	0	0	0	0
	Planctomycetes	0	0	0	0	0	0	0	0	0	0	0
Bacteria shown to inhabit deteriorating concrete in sewer systems	Leptospirillum groups I, II and III	0	0	0	0	5.7	3.0	0	0	0	0	0
	Acidithiobacillus thiooxidans, A. ferrooxidans	0	0	0	0	0	0	0	0	0	0	0
	Thiomonas intermedia	0	0	0	0	0	0	0	0	0	0	0
	Halothiobacillus neapolitanus	0	0	0	0	0	0	0	0	0	0	0

*Except for DAPI, all data are expressed as % of all organisms

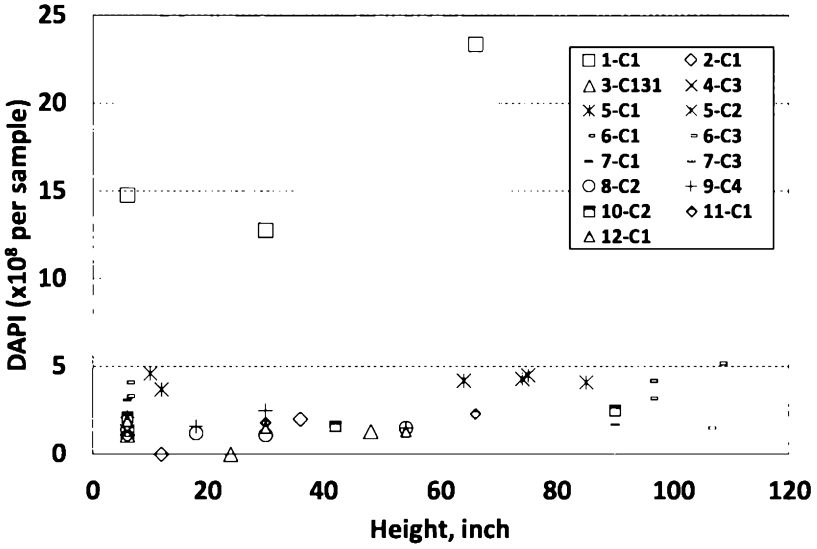

(a)

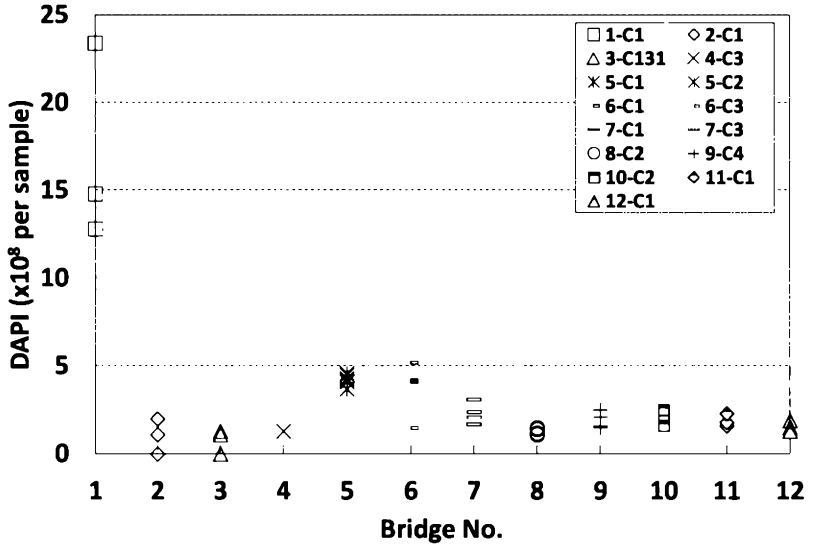

(b)

Figure 18. DAPI Counts of All Organisms. (a) DAPI Counts with Different Specimen Heights, (b) DAPI Counts in Different Bridges.

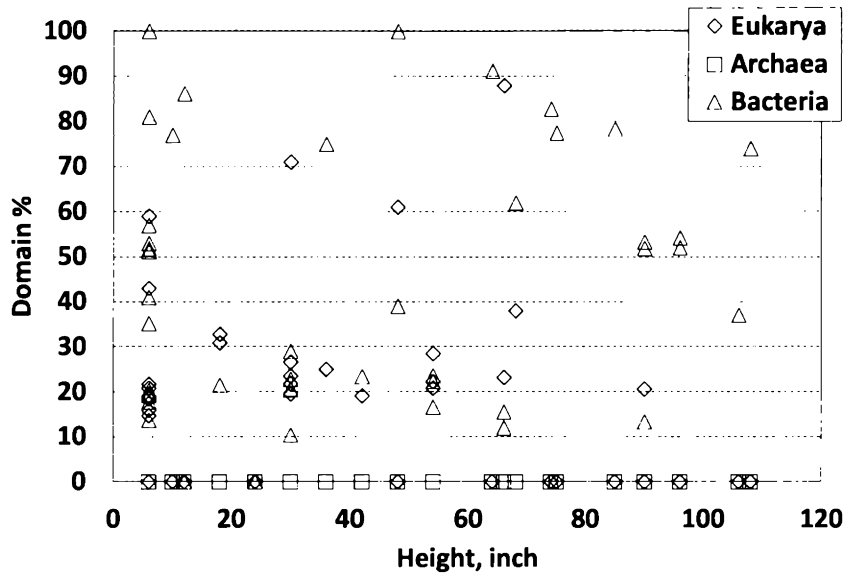

(a)

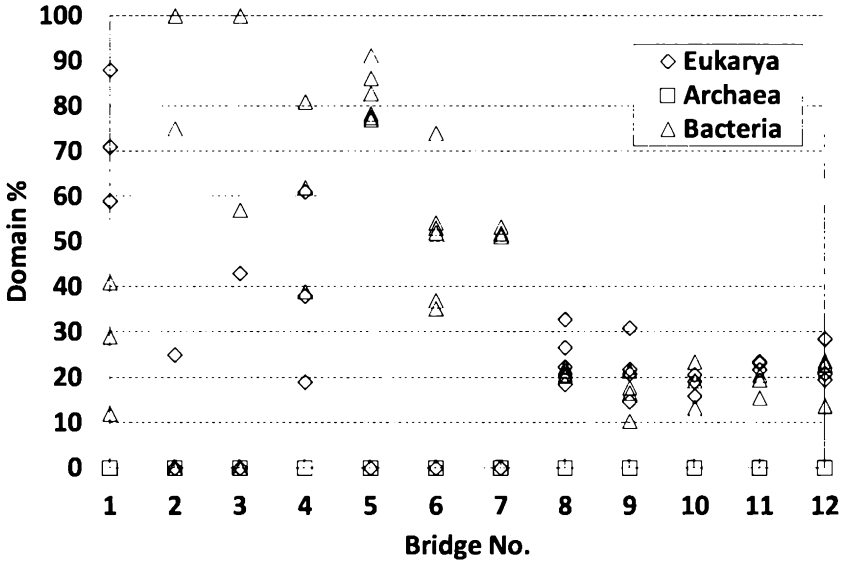

(b)

Figure 19 Domain Analyses Results (in Percent of DAPI Counts). (a) Domain% with Different Specimen Heights, (b) Domain% in Different Bridges.

CHEMICAL ANALYSIS RESULTS

Results of pH measurements of water, mud and surface concrete as shown in Figure 20 indicates that most of the bridge columns that are in contact with water having a pH of approximately 6. For all samples, the pH of the water and the mud correspond to each other, while the pH of the surface concrete scraping samples is higher and slightly basic ranging from about 7 to 9, which is lower than what is found in the interior of the concrete. However, the pH

of concrete is not as low as 2 to 3 as found in sewage plants as reported in the literature (Zhang and Zhang 2006; Parande et al. 2006). Results of sulfate concentration measurements from bridges 1 to 12 are summarized in Figure 21; the results indicate traces of sulfate on the concrete surface, which could indicate potential transformations by sulfur-oxidizing bacteria. Similarly, results of chloride concentration from bridge 1 to 12 are summarized in Figure 22. With respect to elevation along a concrete column, no clear trend emerges with respect to the concentration of sulfate or chloride. Details of pH, sulfate and chloride test results can be found in Appendix D.

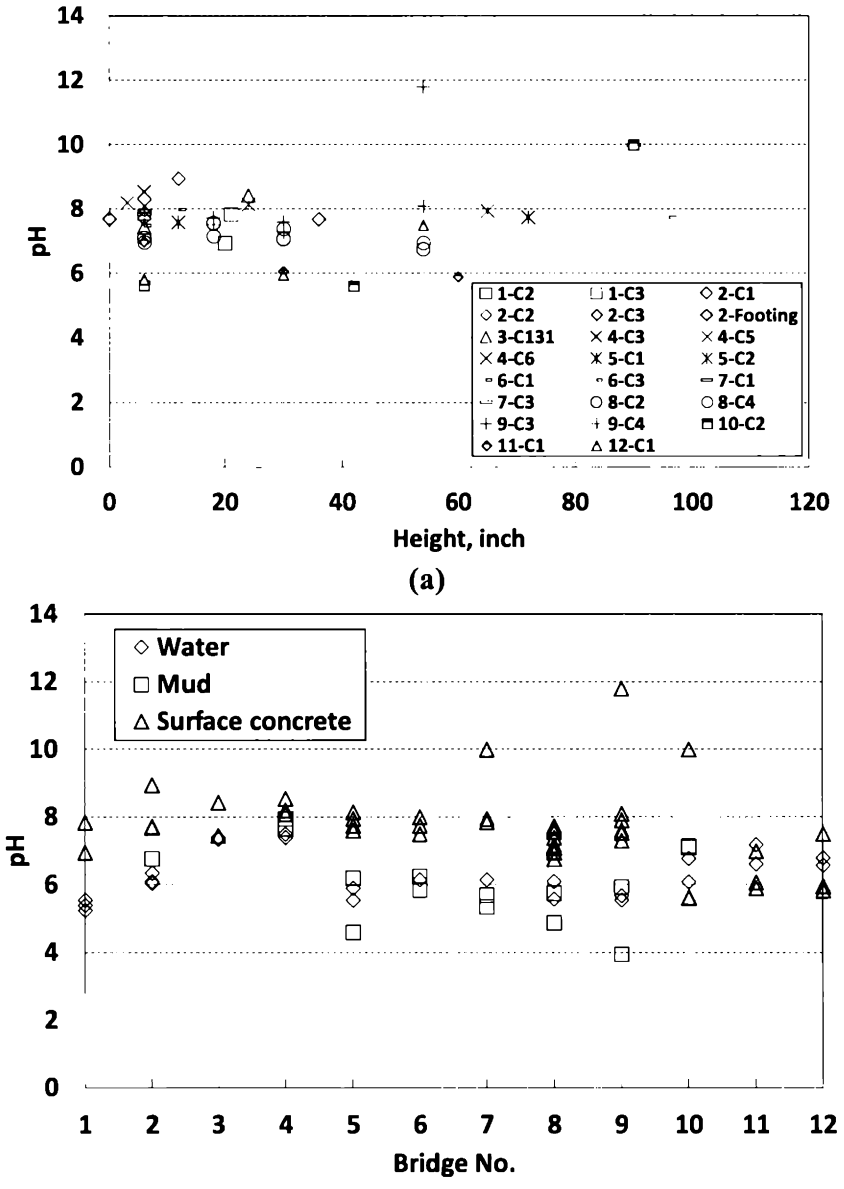

Figure 20. pH of Water, Mud and Surface Concrete Samples. (a) pH at Different Specimen Heights, (b) pH in Different Bridges.

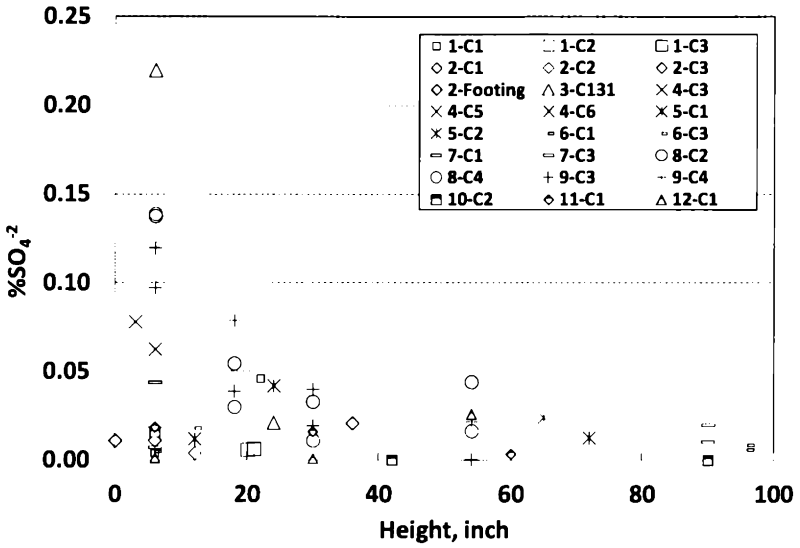

(a)

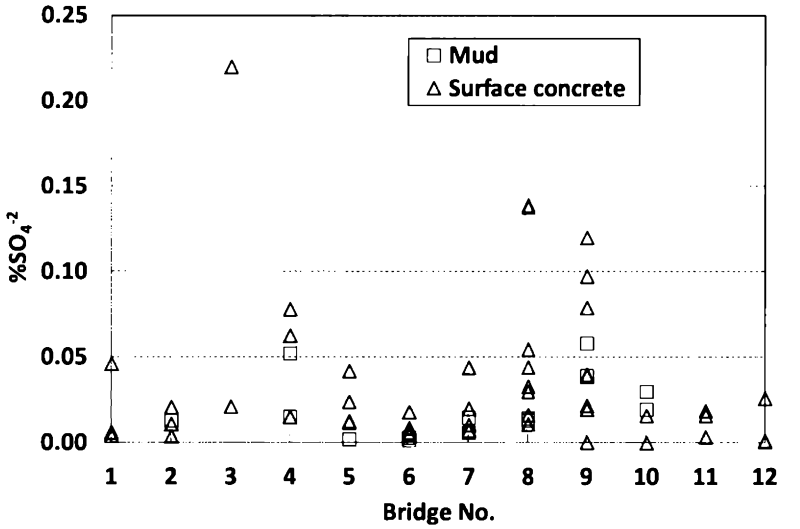

(b)

Figure 21. Sulfate Content of Mud and Surface Concrete Samples. (a) Sulfate Content at Different Specimen Heights, (b) Sulfate Content in Different Bridges.

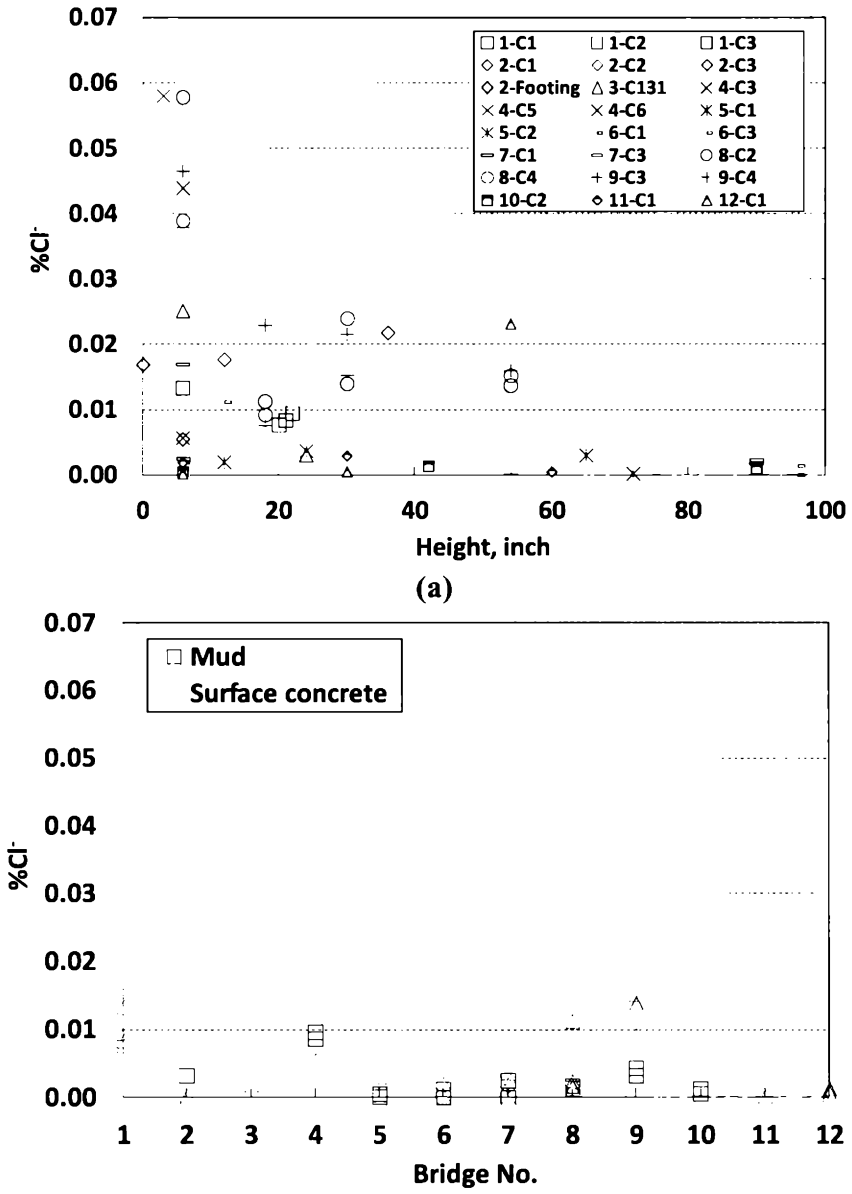

Figure 22. Chloride Content of Mud and Surface Concrete Samples. (a) Chloride Content at Different Specimen Heights, (b) Chloride Content in Different Bridges.

According to the phenolphthalein test results with concrete core samples, the pH at or near the surface is less than a pH of 8 as determined from a lack of color in the phenolphthalein, but within a few millimeters of the surface the concrete becomes very basic as indicated by the pink color of the phenolphthalein indicator. The results are consistent with *in situ* phenolphthalein tests. The interior appears to be unaffected by exposure to the elements except in some cases where aggregates are formed near the surface providing a conduit for diffusion of

water into the interior and a subsequent lowering of the pH. Details of phenolphthalein tests results from core specimens can be found in Appendix D.

MINERALOGY AND PETROGRAPHIC ANALYSIS RESULTS

Petrographic analysis was performed on samples collected from selected bridges. Examples of petrographic images are shown in Figure 23. It should be noted that both polarized light source (Figure 23a and Figure 23b) and fluorescent light source (Figure 23c and Figure 23d) are used in the petrographic analysis, with fluorescent light was mainly used to identify microcrackings. As shown in Figure 23c and Figure 23d, there are no obvious signs of micro or parallel surface cracks, which basically eliminates a mechanism based on freeze/thaw and chemical attack as causes of deterioration (Walker et al. 2006). In most cases, loss of surface mortar was observed, which results in exposure of coarse aggregate (Figure 23a and Figure 23b). In selected concrete specimen (Figure 23a), there are signs of carbonation as indicated by the clear color difference to the concrete surface. In some cases, eroded aggregate (generally limestone) was found. In addition, there was no clear evidence of ettringite or gypsum on the concrete surface, which is probably due to the fact that most of these materials were dissolved or washed away during a long exposure process. However, both paste and aggregate are generally in good shape below the surface layer. The observations are consistent with a mechanism that suggests that the cause of deterioration in bridge columns is likely due to erosion from the slight acidity of the water bodies that surround these concrete columns.

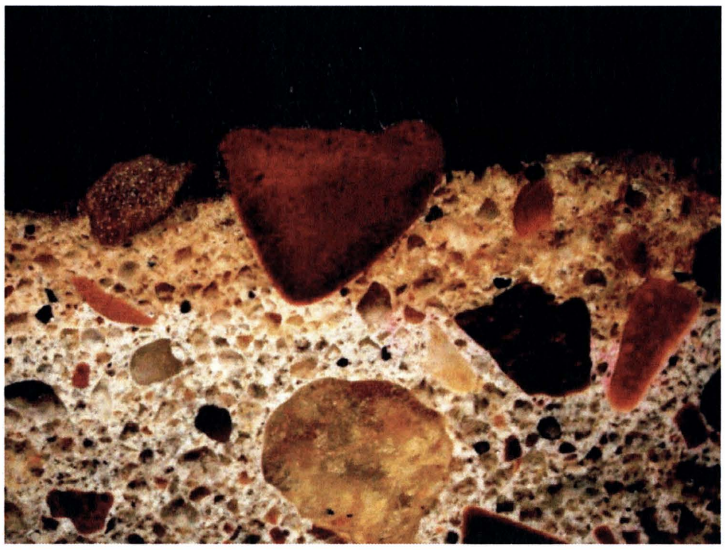

(a)

(b)

Figure 23. Petrographic Analysis Images of Selected Specimen. (a) Bridge 1 (Polarized Light), (b) Bridge 10 (Polarized Light).

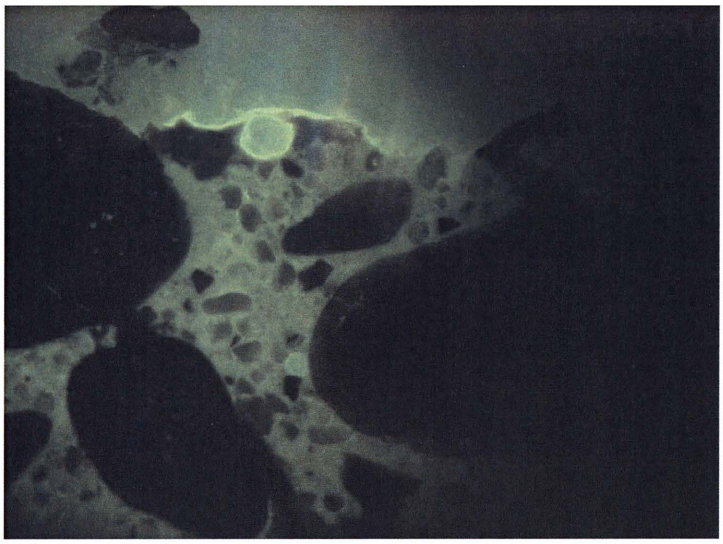

(c)

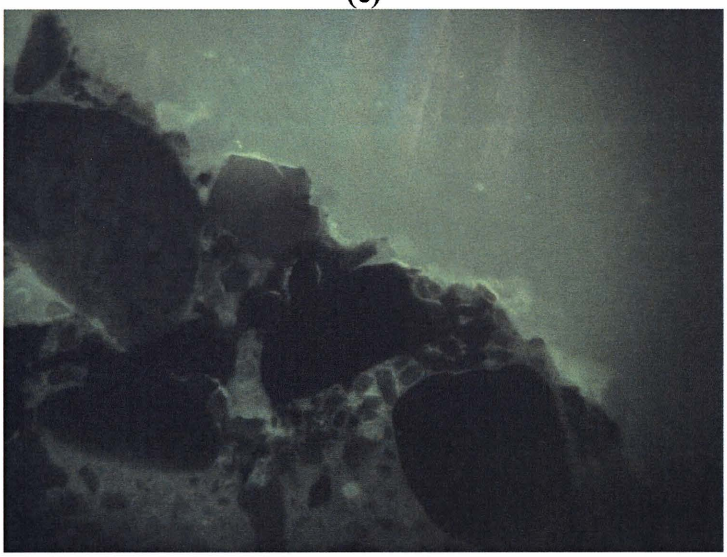

(d)

Figure 23. Petrographic Analysis Images of Selected Specimen.
(c) Bridge 2 (Fluorescent Light), (b) Bridge 8 (Fluorescent Light).

Results from semi-quantitative XRD analysis show that the results are highly dependent on the type of aggregate used in the mix. Quartz and calcite were found in all the specimens. Feldspar and gypsum were found in minor quantities. Portlandite, $Ca(OH)_2$, and ettringite ($6CaO{\cdot}Al_2O_3{\cdot}3SO_3{\cdot}31H_2$) were found as the main hydration products of the cement and no XRD data could be obtained showing C-S-H (calcium silicate hydrate); the latter must be amorphous if it is present.

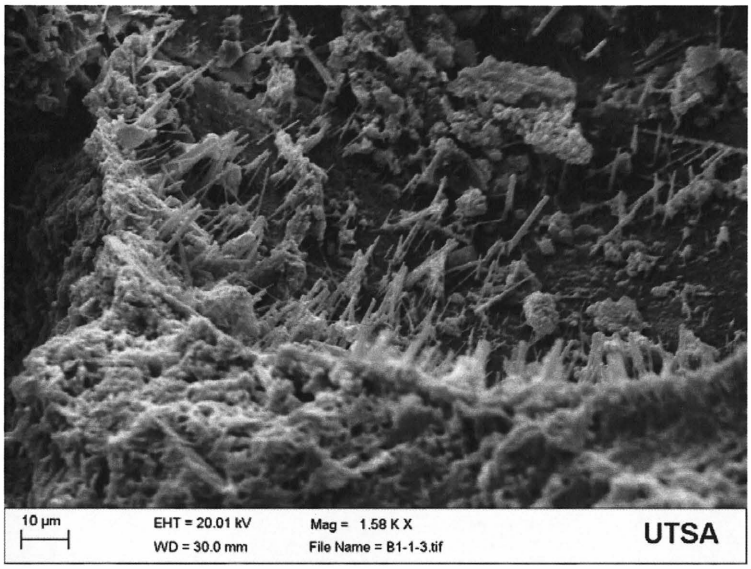

(a)

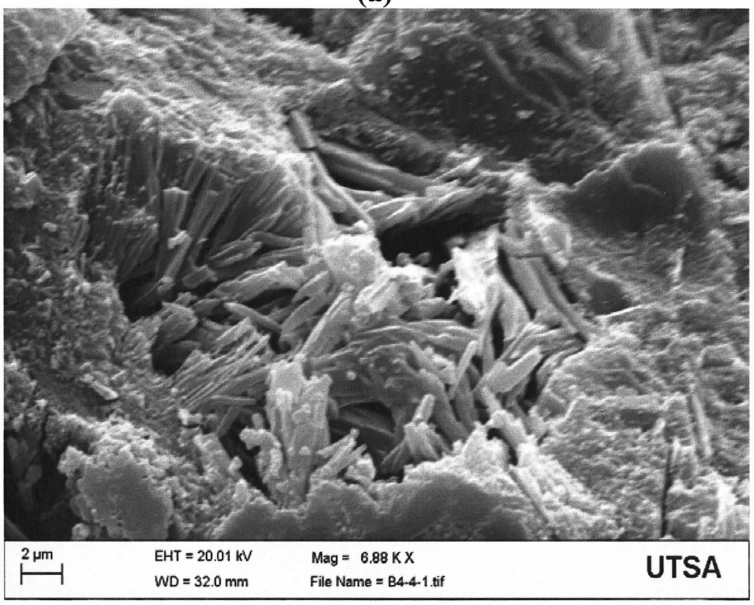

(b)

Figure 24. Scanning Electron Microscopy (SEM) Images of Selected Specimens. (a) Bridge 1, (b) Bridge 4.

Examples of SEM images are shown in Figure 24. It should be noted that near surface specimen were intentionally chosen to examine the microstructure and mineralogy of concrete. The analysis was used to study the changes of concrete microstructure due to MID. While Figure 24a shows collections of ill-defined particles of amorphous C-S-H and ettringite fibers, Figure 24b shows collections of thin crumbled films of amorphous C-S-H and large crystals of portlandite, and provides a close view of C-S-H flakes and portlandite crystals (calcium hydroxide ($Ca(OH)_2$). The results show that hydration reactions of cementation in the cores

mostly involve: crystallization of ettringite, possible precipitation of amorphous C-S-H, and minor quantities of gypsum. However, the amount of ettringite and gypsum found was not as significant as expected, which is probably due to the fact that most of these materials were dissolved or washed away during a long exposure process. Details of SEM, XRD and petrographic analysis can be found in Appendix E.

Mineralogy and petrographic analyses show that besides the different types of aggregates used in the mix, the remaining substances found in the cores mainly are a result of the crystallization of ettringite, possible precipitation of amorphous C-S-H, and minor production of gypsum. It should be noted that although there is no conclusive evidence to support the hypothesis, the results were consistent with previous studies that the biogenic release of acid degrades the cementitious material in concrete, generating gypsum in various states of hydration and ettringite. As none of the water bodies of visited bridges has strong physical action (splash and tidal waves) to remove surface concrete and paste, the deterioration observed is more likely caused by chemical action from biogenic release of acid and degradation of hydration products. Gypsum is soluble and can wash away and ettringite easily absorbs water, resulting in surface expansion and deterioration of the concrete cover surface.

CHAPTER 5:

MICROBIAL ATTACK IDENTIFICATION PROCEDURE

CONSISTENCIES OF *IN SITU* AND LABORATORY TESTS

One of the goals of this project was to evaluate the effectiveness of various test methods in identifying MID and assessing the extent of deterioration. However, before any evaluation of MID could be attempted, the self-consistency of different *in situ* and laboratory measurements had to be justified. In this project, measurements performed on different columns at each visited bridge, together with results obtained from repeated visits on the same bridge were evaluated.

The results indicate that although variations exist within different types of measurements; in general, the results from the rebound hammer, UPV, covering thickness, half cell corrosion potential and *in situ* phenolphthalein tests obtained from different columns within each individual bridge match well with each other and exhibit similar trends. In addition, the visual inspection and hammer test indicate that columns from the same or adjacent spans, i.e., columns experiencing similar environmental conditions, generally show comparable levels of deterioration. Results from microbial and chemical analyses indicated that although a very limited amount of data are available for comparison, results from pH, sulfate and chloride content, and *in situ* hydration measurements of microbial community population generally showed similar trends within each bridge. Details of *in situ* test and laboratory results can be found in Chapter 3, Chapter 4 and Appendices B, C, D and E.

In order to evaluate the self-consistency of tests performed at different visitation times, Bridge 1 (NBI: 20-146-0813-01-009) was chosen for repeat visits based on site condition and accessibility. In addition to the first visit on November 5th, 2009, Bridge 1 was revisited on April 15th, 2011. As shown in Appendix B, a visual inspection indicated that despite a one and a half year interval between the two visits and significantly different weather conditions, no noticeable change in condition was observed. While the widened sections appear to have a loss of paste and a low level of deterioration, the original section appears to be in fairly good condition. A comparison of results from *in situ* tests indicates that while the variation in the rebound hammer test is relatively high, there is no significant difference of results from the rebound hammer test, covering thickness test, and UPV test between the two visits. Due to limited accessibility, no

comparison can be made regarding half-cell corrosion potential measurements. Between the two visits, there were however, significant differences observed from microbial analysis. DAPI from *in situ* hydration tests showed a very different population of microbial community; with results from the second visit showing an approximate 80% lower population when compared to the first visit. The difference is likely due to seasonal changes and moisture content, as the site was experiencing extremely low water exposure because of drought conditions in the state of Texas in 2011. While both visits show a low acid water environment, the water body from the second visit showed a slightly higher pH. Chemical analysis from surface concrete sample showed comparable amounts of sulfate and chloride content obtained from both visits. As mineralogical and petrographic analyses provide a more qualitative rather than quantitative estimation, no recommendation can be made regarding the self-consistency of these two methods.

In summary, although microbial and chemical analysis may show slightly different results because of seasonal changes and water condition, similar trends observed from each analysis indicated that both microbial and chemical analysis can provide consistent results in general. Regarding *in situ* measurement, as results from different columns within each visit and from visits of bridges at different time show relatively consistent results, these tests included in this study can all provide reliable evaluation of MID in general.

EFFICIENCY OF *IN SITU* AND LABORATORY TESTS

As stated earlier in Chapter 2, test methods for the evaluation of concrete degradation under aggressive microbial attack in previous studies were found to be either time consuming or not accurate enough to reflect changes in concrete physical properties. An effective test procedure is therefore necessary for a rational evaluation of deterioration due to microbial attack of concrete. In addition, methods (procedures) are needed, in the field, to identify markers associated with microbial attack.

Based on results from *in situ* tests and laboratory tests performed in this study, the effectiveness of different test methods in identifying MID and estimating the level of deterioration were evaluated. Visual inspection was found to be necessary to give an overall estimation of the extent of deterioration and provide background information for further analysis. Based on the mechanism of MID and observations from the twelve bridges visited, visual inspection should focus on loss of paste, exposure of aggregate, cracks, and corrosion of steel.

As the microbial colonization generally results in reduction of pH, *in situ* measurement of pH (with either a pH meter or litmus paper) and of the water near the concrete surface is recommended in order to provide an indication of potential MID. The UPV test gives a good indication of overall concrete condition; however, the test is not applicable on round shaped columns. It should be noted that as the test requires sufficient contact between transducers and the concrete surface, results from this test might not be reliable if the surface deterioration level is high. The rebound hammer test was not found to be very effective in the evaluation of MID due to the fairly common rough surface with exposure of aggregate or spalling associated with concrete, and therefore is not recommended. Since the covering thickness of concrete can directly reflect the existing concrete thickness (over reinforcement), through a comparison with readings taken away from water level (i.e., high or further away from water), the cover meter can be used as a very effective tool in evaluating overall structural integrity under MID. The *in situ* phenolphthalein pH test over fresh fractured concrete can also provide a good indication of the level of deterioration as MID will result in reducing the pH. However, the examiner needs to bear in mind that carbonation could also result in a similar effect. The half-cell corrosion potential test provides a good indication of the corrosion potential of reinforcement inside concrete due to MID; however, the test is time consuming and requires directly exposing the steel; therefore, it is only recommended when used with core sampling.

Laboratory phenolphthalein pH tests performed with core specimens obtained from bridge columns can provide a good indication of the level of deterioration at or near the surface of the concrete. In addition, core samples obtained from the field can provide a good resource for laboratory chemical, biological, and petrographic analyses to further analyze the mechanism of deterioration and quantify the level of deterioration. Biological analysis, together with chemical analysis can provide valuable information in identifying MID, information on microbial population and identity and serve as a predictor of service life. However, both analyses are laboratory based and require special knowledge, training and equipment, which are not commonly available for TxDOT personnel. Petrographic and mineralogical analyses provide valid information in regard to the extent of deterioration and can be used to indirectly identify the mechanism of deterioration. However, the process is time consuming and should only be considered when necessary, i.e., when there is a suspicion of significant deterioration of service life. The effort required to conduct the various tests, the nature of the test, whether quantitative

or qualitative ,whether the test can identify MID, and the overall effectiveness of different test methods are summarized in Table 6.

Table 6. Effectiveness of Test Methods in Identifying and Quantifying MID.

	Measurement	Effort in Conducting Tests	Quantitative /Qualitative	MID Identification	Overall Effectiveness
Field	Visual inspection	Low	Qualitative	Indirect	High
	In situ phenolphthalein pH	Low	Quantitative	Indirect	High
	Rebound hammer	Low	Quantitative	No	Low
	Covering thickness	Low	Quantitative	No	High
	Half-Cell	Medium	Quantitative	No	High
	UPV	Medium	Quantitative	No	Medium
	In situ water pH	Low	Quantitative	Indirect	High
Lab	Lab phenolphthalein pH	Low	Quantitative	Indirect	High
	In situ hybridization	High	Quantitative	Yes	Medium
	SO_4^{2-} and Cl^- content	High	Quantitative	Indirect	Medium
	Mineralogy Analysis	High	Qualitative	Indirect	Medium
	Petrographic Analysis	High	Qualitative	Indirect	Medium

RECOMMENDED PROCEDURE

Based on the effectiveness of each of the tests, a two-stage approach is recommended to identify MID and evaluate the extent of MID for TxDOT structures. With Stage I as a preliminary survey to roughly evaluate the extent of MID, Stage II should serve as an extension of Stage I when needed, in order to confirm the MID and to further identify the extent of defects revealed by Stage I. A flow chart with tests recommended during the different stages is shown in Figure 25:

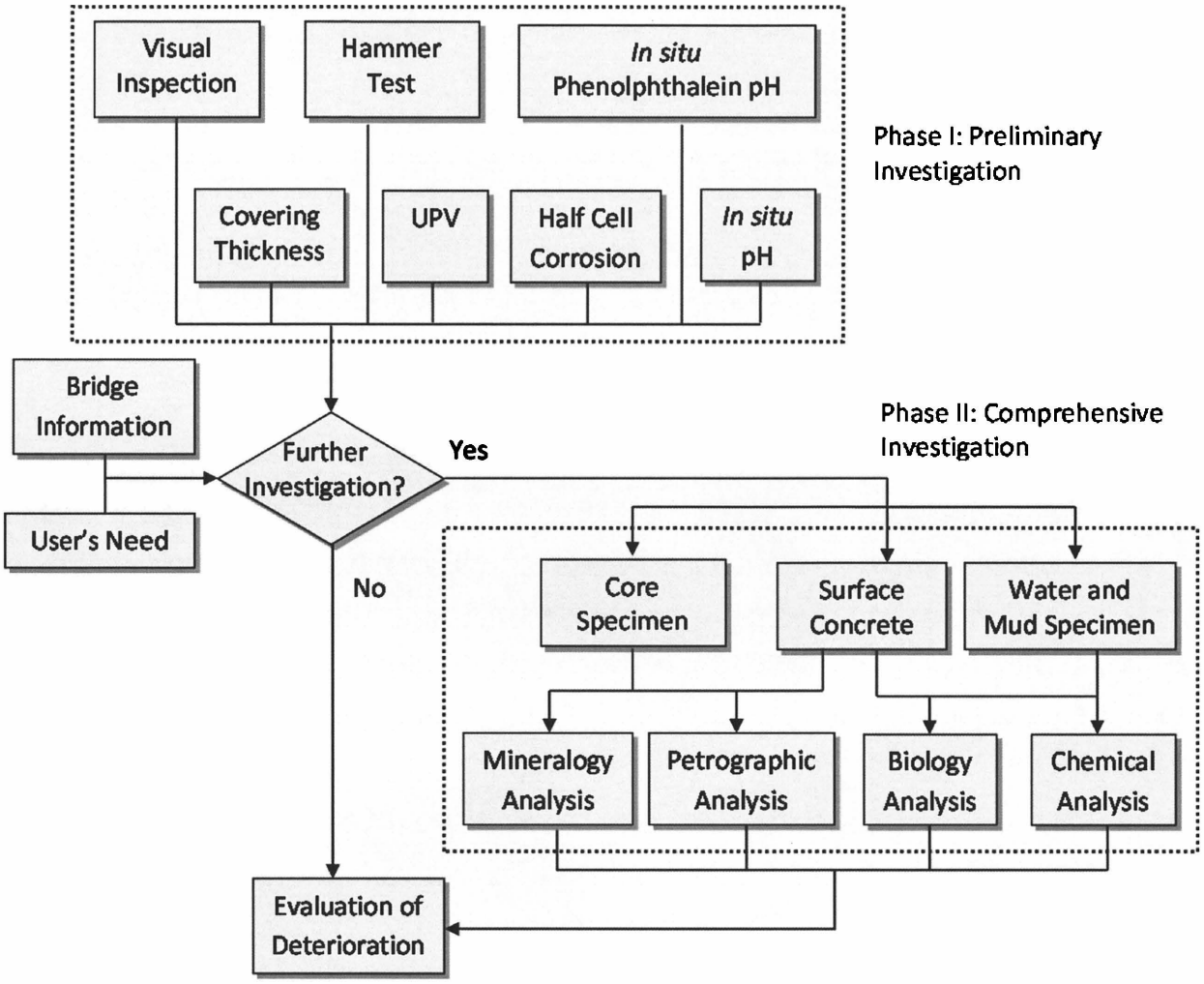

Figure 25. Flow Chart of Recommended MID Identification and Evaluation Procedure.

Within the preliminary investigation stage (Stage I), while there is no rapid test to identify MID in the field, visual inspection, nondestructive tests (including hammer test, covering thickness, UPV, half cell corrosion potential) together with *in situ* phenolphthalein measurements provide a good indication of level of deterioration. The *in situ* measurement of pH of water (using either a pH meter or litmus paper) near the concrete surface is recommended to access potential microbial involvement. Bridge information including the age of bridges, expected service life, mix design of concrete and environmental conditions (chemical, weather, etc.) together with results obtained from the above mentioned field tests, can then be used by users and owners of the infrastructure to determine whether further evaluation is needed. Signs of low covering thickness (for example, less than 1 inch) and a significant reduction in pH

(extending to 10mm from the core surface) can generally lead to a recommendation of further analysis.

Provided owners have a concern about the integrity of bridge structures, a Stage II examination encompassing a more comprehensive study is recommended. Surface concrete, water and mud specimens together with core specimens should be obtained before this stage II examination is conducted. Laboratory tests including microbial, chemical, mineralogical and petrographic analyses should be used to further evaluate the severity of deterioration and aggressiveness of the environment. A comprehensive evaluation of the level of deterioration can be conducted with this extensive study and used to evaluate the significance of MID in the structure, and provide guidance in predicting the service life of the structure under different microbial deterioration conditions. This two-stage procedure can serve as a guideline for TxDOT personnel in identifying MID and evaluating the extent of deterioration through both field procedures and laboratory evaluations. An early warning approach would be helpful in determining concrete structures that might be susceptible to failure and appropriate for remediation.

CHAPTER 6:
FEASIBILITY STUDY TO PREVENT AND REMEDIATE CONCRETE DEGRADATION

CONCRETE AND MORTAR MIXTURE PREPARATION

Materials

In this study, Type I and Type V portland cement conforming to TxDOT DMS-4600 (Hydraulic Cement) were used. SCMs conforming to TxDOT DMS-4610 (Fly Ash) and DMS-4630 (Silica Fume) were used in different mixtures respectively. A local limestone aggregate, conforming to TxDOT Item 421 "*Hydraulic Cement Concrete*" Grade 4 (No. 57 according to ASTM C33 "*Standard Specification for Concrete Aggregates*"), was used as the coarse aggregate (CA). Manufactured limestone sand (FA1) together with silica sand (FA2) were used as fine aggregates. It should be noted that the two fine aggregates were applied in an 85:15 ratio in order to obtain fine aggregate gradation conforming to TxDOT Item 421 Grade 1. Chemical admixtures including high range water reducer (HRWR), Glenium® 7700, and air entraining agent (AEA), AE90, conforming to TxDOT DMS-4640 were employed in this study. In addition, a water repellent admixture, RheoPel® Plus was used in selected mixtures. To study the potential means of remediation of existing concrete structures, a commercially available concrete preservation treatment solution (CPTS), Aquron® CPT-2000, was used as coating agent in selected mixtures.

Concrete Mix Designs and Specimen Preparation

In order to evaluate microbial attack resistance of commonly used cementitious material, six different concrete mixtures were selected in accordance with the PD and PMC of the project. The six mixes are: C-I (with Type I portland cement only, that served as a reference mix), C-V (with Type V cement only), C-I-CFA (with 20% Class C fly ash replacement), C-I-FFA (with 20% Class F fly ash replacement), C-I-SF (with 7% silica fume replacement), C-I-RPP (with water repellent admixture) and C-I-CPTS (C-I coated with CPTS). AE90 was used in all mix designs to obtain the appropriate air content. In mix C-I-SF, Glenium® 7700 was employed to provide the concrete with appropriate workability. The water-to-binder ratio (w/b) used in the mixes ranged from 0.48 to 0.49. It should be noted that a slightly higher w/c (compared to TxDOT Item 421) was selected here to prepare mixtures that would be more vulnerable to an

aggressive environment. Details with respect to the designs of concrete mixtures and mix proportions can be found in Appendix F.

All concrete mixtures were prepared according to the procedure described in ASTM C192 "*Standard Practice for Making and Curing Concrete Test Specimens in the Laboratory*". Slump, air content, and unit weight were measured according to ASTM C143 "*Standard Test Method for Slump of Hydraulic Cement Concrete*", ASTM C231 "*Standard Test Method for Air Content of Freshly Mixed Concrete by the Pressure Method*", and ASTM C138 "*Standard Test Method for Density (Unit Weight), Yield, and Air Content (Gravimetric) of Concrete*" respectively. Fifteen 4"x8" concrete cylinder specimens were prepared according to ASTM C192 "*Standard Test Method for Compressive Strength of Cylindrical Concrete Specimens*" for each mix design. Compressive strength tests were performed according to ASTM C39 at the age of 56 days. Details of slump, air content, unit weight and compressive strength from each mixture can be found in Appendix F.

Mortar Mix Designs and Specimen Preparation

Similar to concrete mixtures as described in the previous section, five different mortar mixes with different cementitious materials were prepared. The five mixes are: M-I (with Type I portland cement only, that served as a reference mix), M-V (with Type V cement only), M-I-CFA (with 30% Class C fly ash replacement), M-I-FFA (with 30% Class F fly ash replacement), M-I-SF (with 10% silica fume replacement) and M-I-CPTS (M-I coated with concrete preservation treatment solution). AE90 at a rate of 2.30 fl oz/cwt was used in all mixtures. Water-to-binder ratio (w/b) and sand-to-binder ratio was fixed at 0.45 and 2.50 respectively in all mix designs. The fine aggregate (sand) to binder ratio (s/b) was 2.50. Design details of the mortar mixtures and mix proportions can be found in Appendix F.

All mortar mixtures were mixed according to the procedure as described in ASTM C305 "*Standard Practice for Mechanical Mixing of Hydraulic Cement Pastes and Mortars of Plastic Consistency*". Two different types of mortar specimens, 2"x2"x2" mortar cubes and 1"x1"x11" mortar prisms were prepared. Seventy five 2"x2"x2" mortar cubes and ten 1"x1"x11" mortar prisms were prepared according to ASTM C109 "*Standard Test Method for Compressive Strength of Hydraulic Cement Mortars (Using 2 in. or [50 mm] Cube Specimens)*" and ASTM C157 "*Standard Test Method for Length Change of Hardened Hydraulic Cement Mortar and*

Concrete" respectively for each mix design. In addition to unit weight of each mixture, compressive strength tests were performed according to ASTM C109 at the age of 90 days. Details of unit weight and compressive strength tests from each mixture can be found in Appendix F.

As specimens were prepared within a four weeks' time span, in order to eliminate the effect of specimen age, concrete and mortar specimens were cured for 205±16 days and 264±12 days respectively in a curing room conforming to ASTM C511 "*Standard Specification for Mixing Rooms, Moist Cabinets, Moist Rooms, and Water Storage Tanks Used in the Testing of Hydraulic Cements and Concretes*" until being place into different MID simulation environments.

MICROBIAL ATTACK SIMULATION

Laboratory Simulation

Since microbial attack in a natural environment can take years to cause a noticeable deterioration, it is practically impossible to study MID resistance in the natural environment as the microbial attack is generally caused by secretions generated by microbes (Vincke et al. 2002, Shook and Bell 1998), sulfuric solutions with higher aggressiveness were therefore used to simulate the microbial attack occurring under natural conditions.

To select the proper solutions for MID simulation, sulfuric acid solutions with four different concentrations (1%, 3%, 5%, and 10%) were prepared. Dummy specimens were placed in these four different solutions and monitored on a daily based. After a 36-day observation, 1% and 3% sulfuric solutions were eventually selected to simulate microbial attack. The selection was made based on adequate aggressiveness yet a sufficient time to evaluating deteriorations in a manageable manner. Details of this simulation can be found in Appendix F.

In the laboratory simulation, concrete and mortar specimens were fully submerged in sulfuric acid solutions. Regular five gallon buckets and rectangular containers (approximately 15"x3"x4" in dimension) were used for storing the concrete and mortar specimens respectively. In order to maintain consistent exposure conditions, two 4"x8" concrete cylinders, fifteen 2"x2"x2" mortar cubes, and four 1"x1"x11" mortar prisms were stored in each of the containers. It should be noted that specimens were grouped in a manner such that only specimens from the same mix design were placed in the same container. It should also be noted that due to the

different size of specimens, exposure conditions for the different specimens, i.e., solution volume vs. total specimen surface area ratio was different; the concrete specimen exposure is approximately five times higher than that of mortar specimens. Each container was labeled with information concerning the specimen, and the concentrations of the solution to distinguish different specimens and conditions. Due to the aggressiveness of solutions used in this study, all the containers were placed in a secured storage area as shown in Figure 26. As the release of substances from concrete and mortar specimens can cause the reduction of acidity, with the pH value of the solutions changing with time, the pH values of solutions were monitored on a regular basis. In order to maintain relatively stable simulation conditions, when the pH values increased by 1, new solutions were prepared and replaced the earlier solutions. More information of solution selection, preparation, and measured pH values can be found in Appendix F.

(a)

(b)

Figure 26. Laboratory specimen placement.
(a) Secured Storage Area, (b) Concrete Cylinder Specimens in Sulfuric Solution.

Field Simulation

In addition to the laboratory simulation, field exposure was also used for microbial attack simulation. Site A, a water body that hosts Bridge 1 (FM 787@ Tarkington Bayou) was carefully chosen because of the easy accessibility and relatively aggressive water body (with pH between 5.4 and 6.1 during the first visit). It should be noted that because of drought condition in Texas, the water level was low and did not fully cover the specimen and therefore specimens were relocated to Site B after 62 days of exposure at Site A. Site B, a water body that hosts Bridge 10, is located approximately a quarter mile east of Site A. Site B and Site A were essentially the same water body, with a pH of approximately 7 and a water level of approximately five feet. The pH values of field water were measured each time the site was visited and the pH values were found to be relatively stable. Detailed information on the pH values during the field exposure trials can be found in Appendix F.

During the site exposure, specimens were wrapped in prefabricated plastic laminated wire cages to allow the full exposure of the specimens. Similar to laboratory exposure, only specimens with the same mix design, usually two concrete cylinders or two mortar prisms or eight mortar cubes, were placed in each cage. All cages were labeled with plastic laminated tags with information related to the mix design and exposure conditions. Cages with the same type of mixture and exposure condition were tied together with ropes and then tied to adjacent bridge columns for tracking purpose. Figure 27 shows the placement and exposure of specimens in the field.

(a)

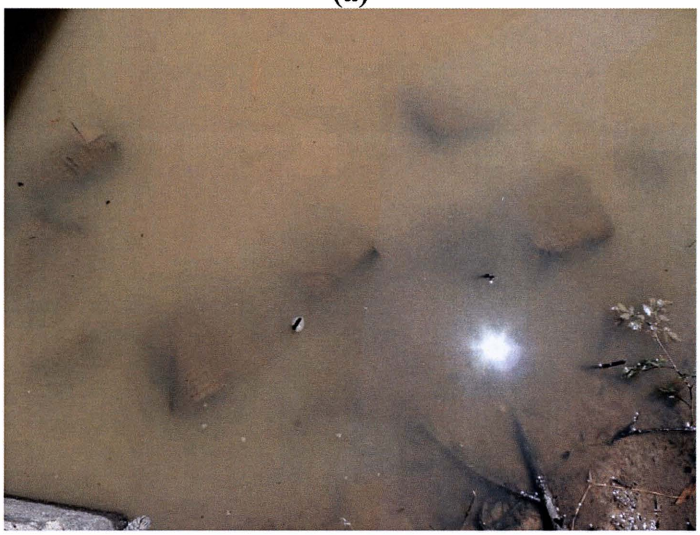

(b)

Figure 27. Field Specimen Placement.
(a) Specimen Placement; (b) Exposure of Specimens.

In order to simulate the deterioration of concrete and mortar specimens under different level of microbial attack, a total of five different exposure conditions with laboratory or field exposure, or combinations of laboratory or field exposures were employed in this study. The five different scenarios of MID simulation are summarized in Table 7.

Table 7. Scenarios of MID Simulation.

Scenario	Description	Laboratory Exposure (days)	Field Exposure (days)
I	Field	NA	Continuous
II	1% sulfuric solution	Continuous	NA
III	1% sulfuric solution to field	57	Continuous
IV	3% sulfuric solution	Continuous	N/A
V	3% sulfuric solution to field	15	Continuous

The five different scenarios were: Scenario I with continuous exposure in the field, Scenario II with continuous exposure in 1% sulfuric acid solution, Scenario III with 57 days of 1% sulfuric acid solution exposure followed by continuous exposure in the field, Scenario IV with continuous exposure in 3% sulfuric acid, and Scenario V with 15 days of 3% sulfuric solution acid followed by continuous exposure in the field.

TEST METHODS AND RESULTS

Visual Inspection

A visual inspection of the level of deterioration of specimens exposed to different scenarios was conducted on a regular basis. It was observed that soft and white reaction products were generated on the surface of specimens after being placed into the sulfuric acid solution. In general, the longer the specimens were exposed to the sulfuric acid solution, the more reaction products were generated. As expected, specimens in Scenario IV (3% sulfuric acid solution) were found to have a higher level of deterioration comparing to those stored in Scenario II (1% sulfuric acid solution). Examples of concrete deterioration observed during different exposure scenarios are shown in Figure 28.

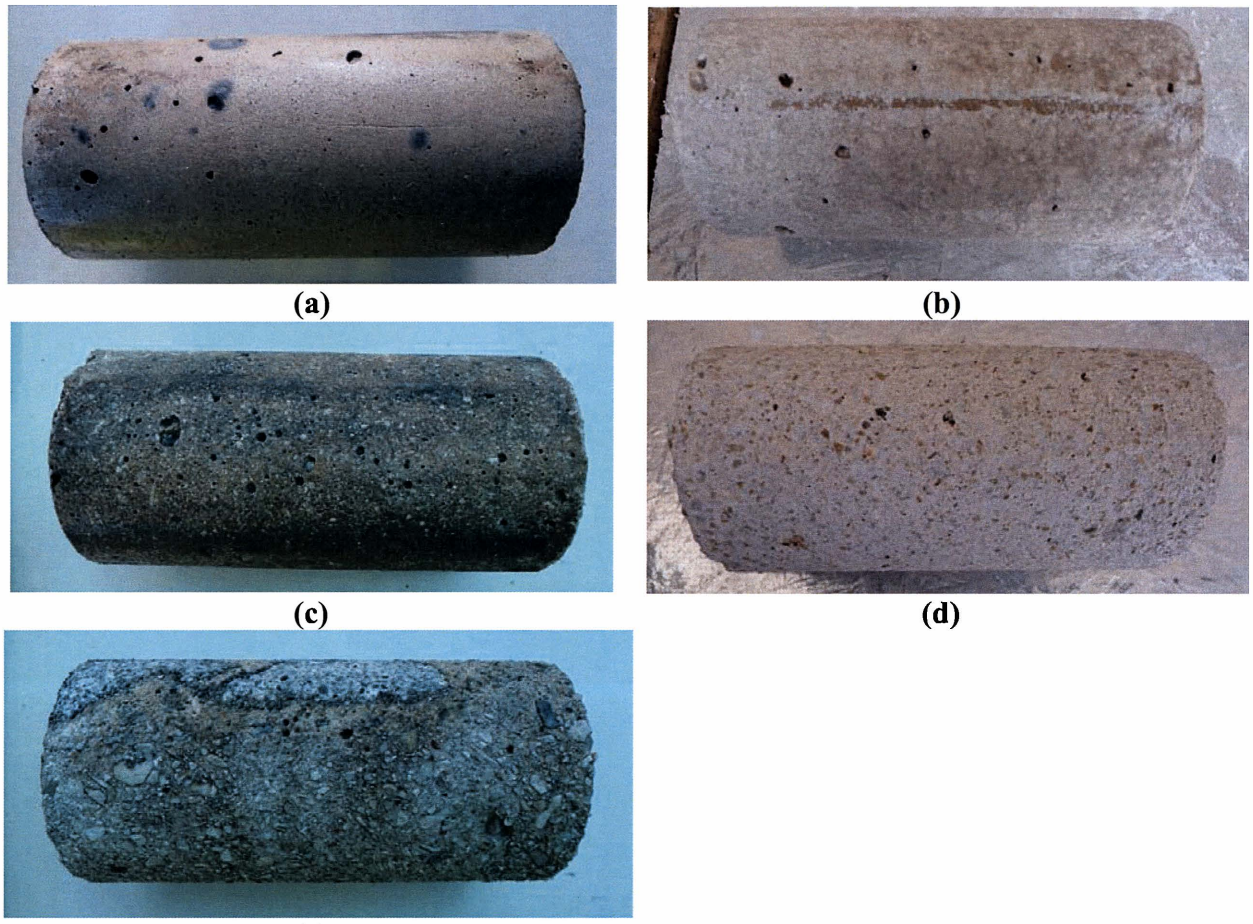

Figure 28. Examples of Concrete Deterioration under Different Exposure Conditions. (a) C-I in Scenario I after 96 Days of Exposure, (b). C-I in Scenario II after 126 Days of Exposure, (c) C-I in Scenario III after 96 Days of Exposure, (d) C-I in Scenario IV after 102 Days of Exposure, (e) C-I in Scenario V after 34 Days of Exposure.

Examples of concrete deterioration (from mixture C-I, i.e. mixes with Type I cement only) under different exposure conditions are shown in Figure 28. As expected, no noticeable change in the specimen was observed after 96 days of site exposure (Scenario I). After 126 days of exposure under Scenario II, specimens were still in fairly good condition; there were minor signs of a loss of paste and a small amount of exposed aggregate. Within the different mixtures, C-I/M-I, C-V/M-V, C-I-FFA/M-I-FFA, and C-I-SF/M-I-SF had smoother surfaces than other mixes; within which C-I-FFA/M-I-FFA had the smoothest surface when compared to all the other mixes.

As shown in Figure 28, as expected, a much higher level of deterioration was observed with specimens exposed in Scenario IV (3% sulfuric acid solution). Even though specimens were

exposed for a shorter period of time, very clear signs of loss of surface paste and aggregate exposure were observed. The exposure of coarse aggregate can be observed on concrete surfaces from all the mix designs. Within the different mixtures, similar results were observed under scenario II, with mixes C-V/M-V, C-I-FFA/M-I-FFA, and C-I-SF/M-I-SF performing the best.

Results also showed that there was no significant difference observed on the surfaces of specimens exposed in Scenario I, III and V after they were placed in the field. Darker sections observed on specimen surfaces were likely caused by the direct contact of mud during field exposure. Comparing specimens exposed in Scenario I for 96 days to specimens in the curing room, except for a surface color change, there were no significant differences in surface smoothness. Similar results from specimens exposed in Scenarios III and V were found.

Comparing specimens in Scenario III and V for 96 days and 34 days exposure respectively, to specimens in Scenario II and IV at approximately the same age, surface conditions were essentially the same except for some visible color changes. Comparing the condition of specimens to the condition of field bridge columns, which can be considered exposed to Scenario I for more than seventy years, specimens in scenario I performed better than bridge columns because of the much shorter exposure time; specimens in scenario III were found to be similar to the bottom sections of the columns that were close to the water level, while specimens in Scenario V showed a higher level of deterioration compared to those observed in field bridge columns.

Length change

After mortar prism specimens were placed into different scenarios, changes of lengths were measured with a length comparator on a regular basis. Results of length changes of specimens under different exposure conditions are summarized in Figure 29. As expected, all specimens experienced different levels of expansions, which was likely due to reaction between sulfuric acid and cement hydration products, which resulted in the production of ettringite and gypsums and a volume increases.

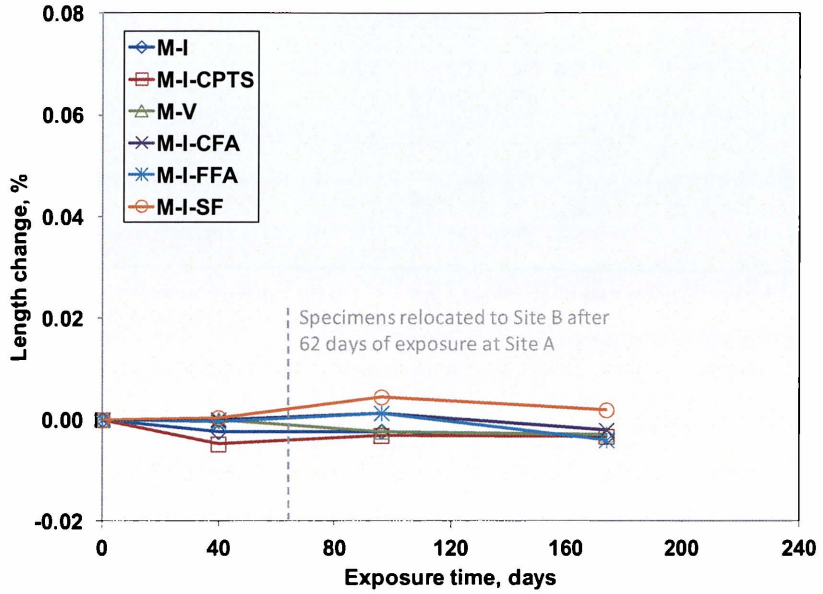

(a)

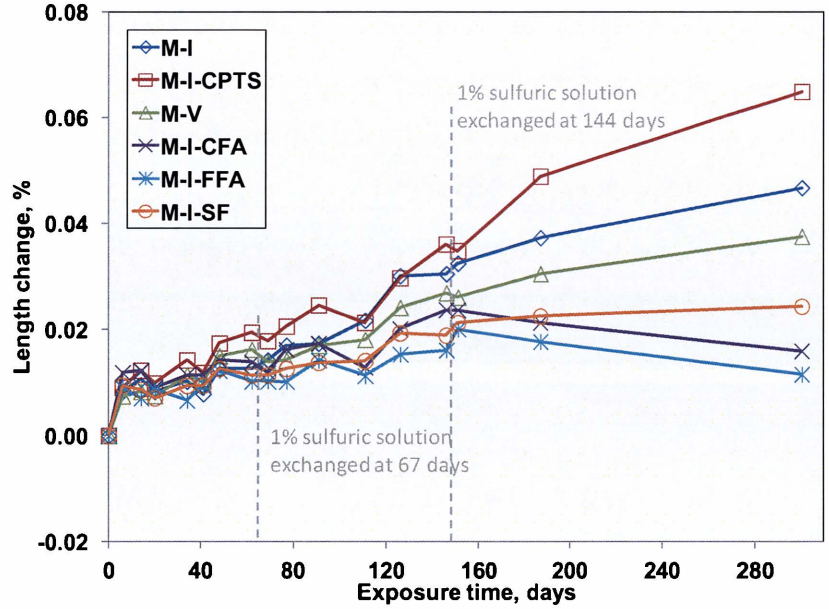

(b)

Figure 29. Length Change of Mortar Prism Specimens under Different Scenarios. (a). Scenario I, (b). Scenario II.

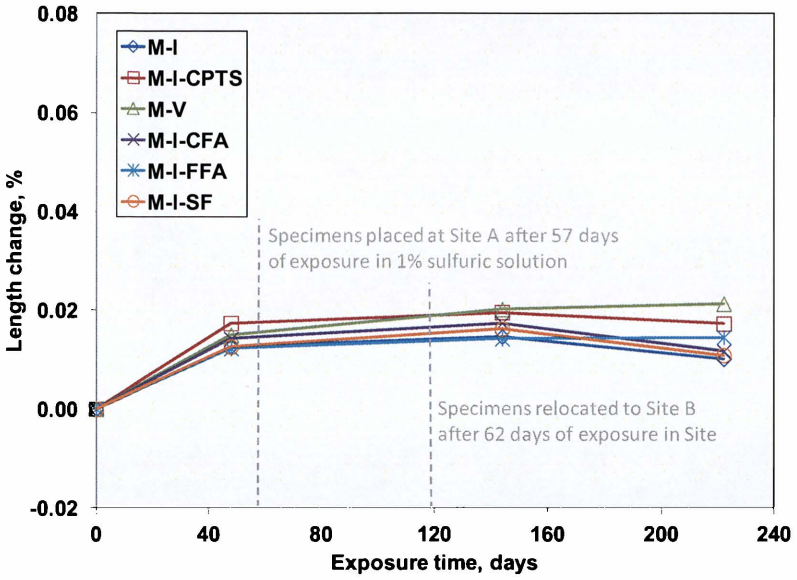

(c)

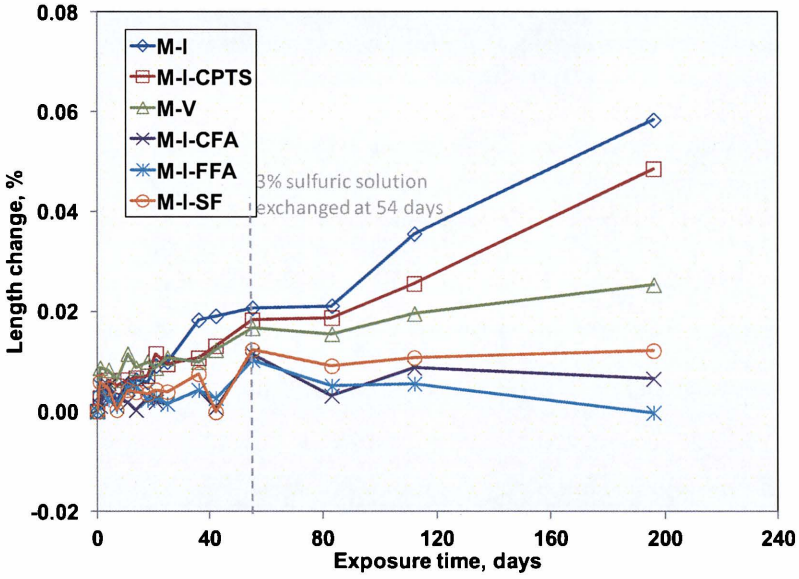

(d)

Figure 29. Length Change of Mortar Prism Specimens under Different Scenarios (continuous). (c). Scenario III, (d). Scenario IV.

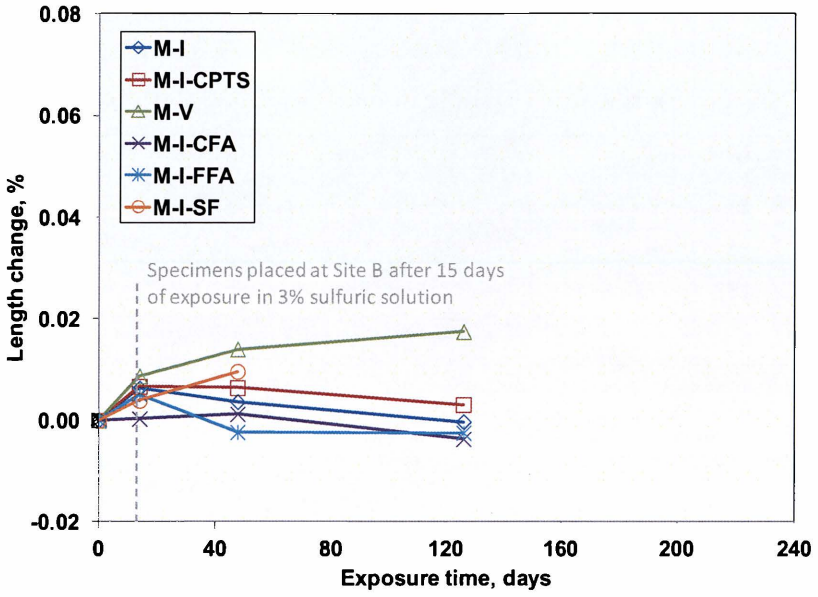

(e)

Figure 29. Length Change of Mortar Prism Specimens under Different Scenarios (continuous). (e). Scenario V.

Figure 29 shows that length changes were within 0.005% when exposed under scenario I over 180 days; the length change was small when compared to the change in length of specimens in Scenarios II and IV. After the mortar prism specimen was placed in the field after laboratory (sulfuric acid) exposure, i.e., Scenarios III and V, further length increases were very limited, with less than 0.005% in most cases. The results indicate that there is no significant apparent reaction taking place after the specimens are placed in the field. In selected specimens, a length decrease was even observed, which is likely caused by changes in the environment including temperature and humidity.

Within the different mixtures, while there is no clear trend observed for specimens in Scenario I, specimens from M-I-FFA, M-I-SF, and M-I-CFA in Scenarios II and IV showed less expansion compared to other mixes, which indicated these SCMs might provide better resistance against MID. There was no significant improvement with the use of CPTS observed.

In general, the expansion for all the specimens was found to be relatively small, as most of the expansions were less than 0.04%, including under the most aggressive conditions of Scenario IV. Considering the size of bridge columns in the field, and the fact that the reaction and expansion happened only on concrete surfaces, the effect on expansion caused by sulfuric acid or field exposure was not significant.

Mass Loss

It is well known that a series of reactions take place after concrete is exposed to a sulfuric acid environment. Reactions between cement hydration products and sulfuric acid create gypsum and ettringite, which generally results in volume increases. Gypsum and ettringite not only can dissolve and be removed from a concrete surface, but when enough gypsum and ettringite are accumulated on concrete surfaces, internal stresses can lead to surface cracking and a further loss of paste and fine aggregate, resulting in mass loss. In this study, mass losses for both concrete and mortar specimens were measured.

Results of mass losses of both concrete and mortar specimens are summarized in Figure 30 and Figure 31 respectively. Similar trends are observed in concrete and mortar, with different levels of mass losses observed under different scenarios. As expected, among the five scenarios, specimens in Scenario IV show the highest level of mass loss. While mass losses in most scenarios are relatively low (less than 5%), a much higher level of mass loss (up to 15%) was observed after approximately 120 days of exposure in Scenario IV. Results were consistent with visual observation as shown earlier in the chapter. One interesting observation is mass increases (negative mass losses) are observed in some scenarios, which is likely due to the expansion of specimens and absorption of water and solution into voids generated by expansion.

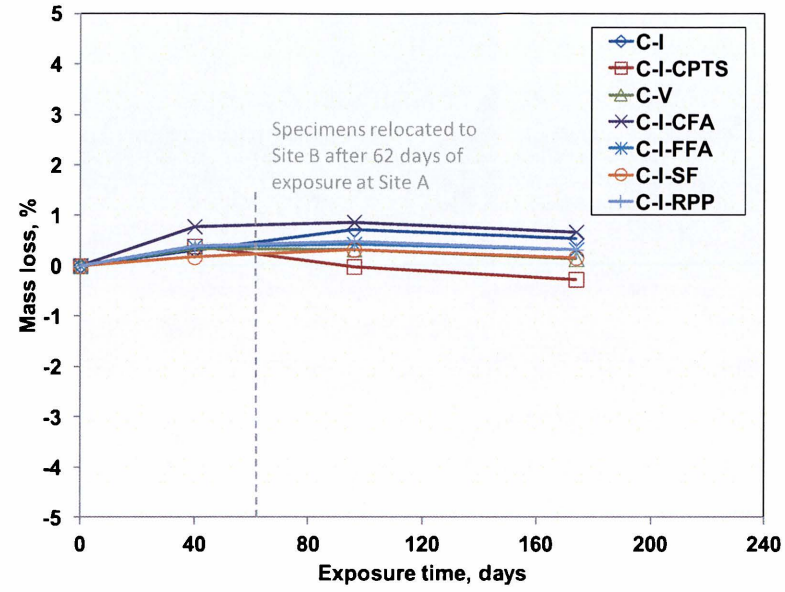

(a)

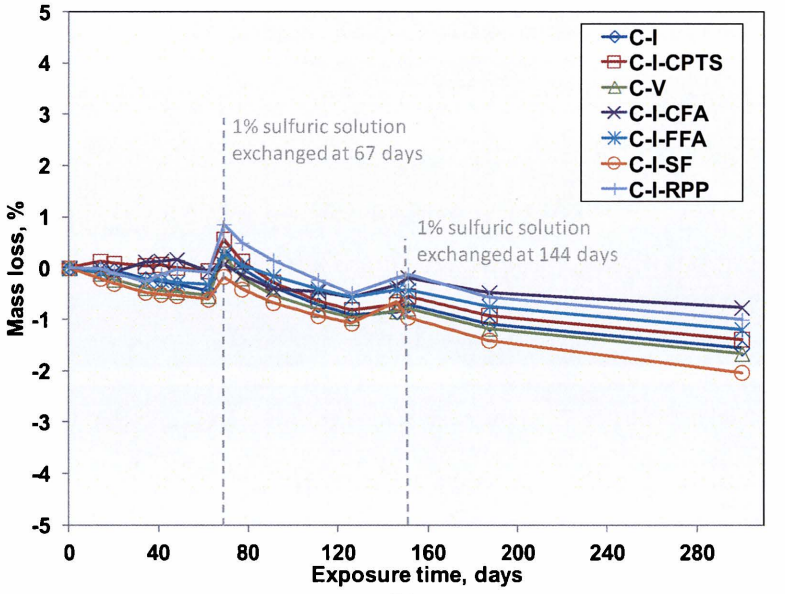

(b)

Figure 30. Mass Loss of Concrete Specimens under Different Scenarios. (a). Scenario I, (b). Scenario II.

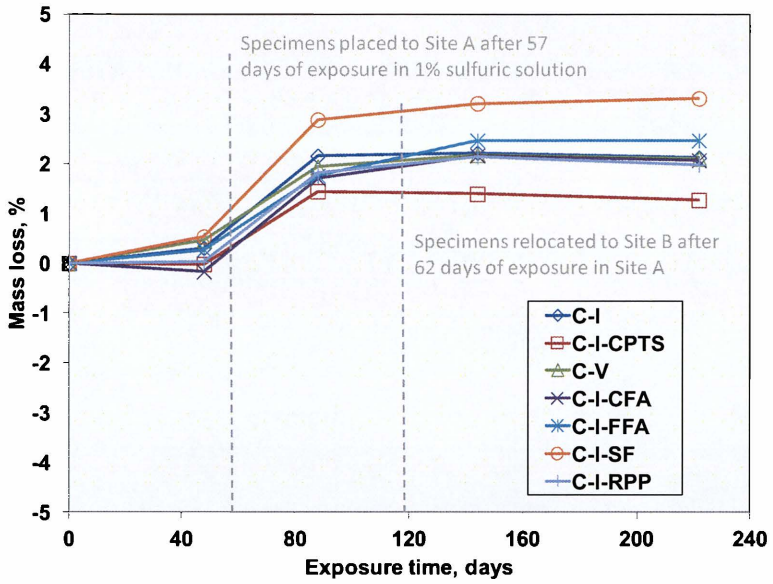

(c)

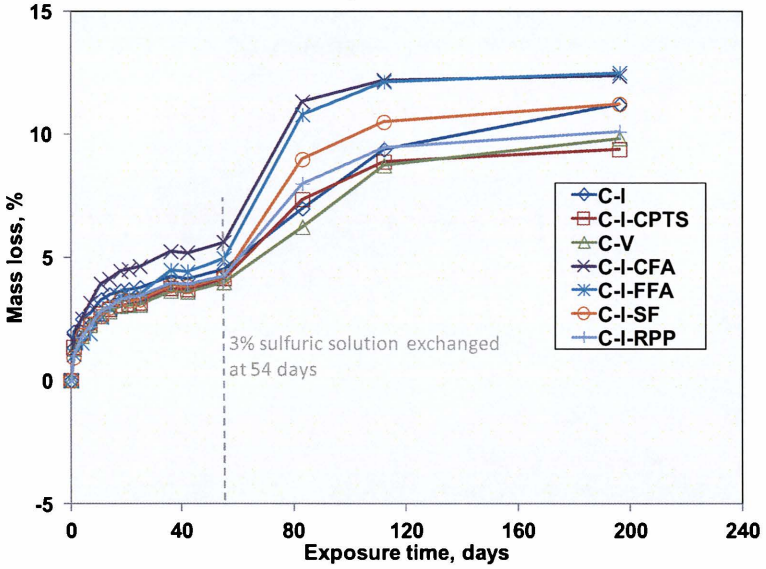

(d)

Figure 30. Mass Loss of Concrete Specimens under Different Scenarios (continuous). (c). Scenario III, (d). Scenario IV

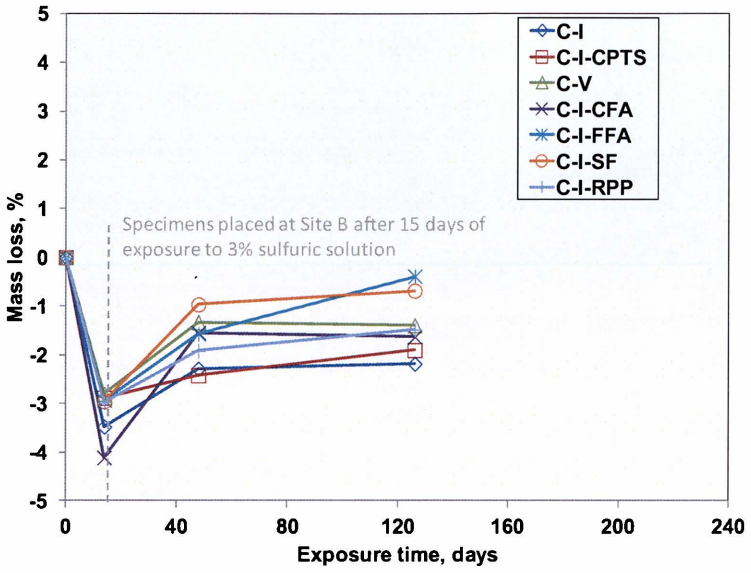

(e)

Figure 30. Mass Loss of Concrete Specimens under Different Scenarios (continuous). (e). Scenario V.

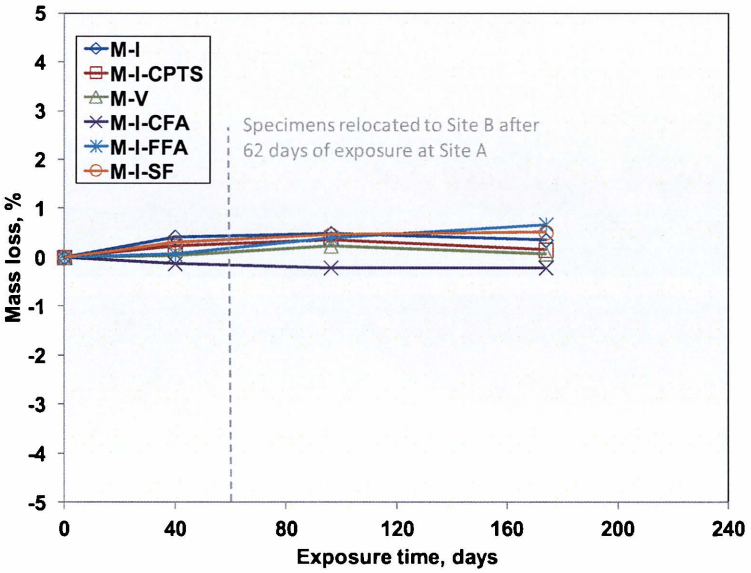

(a)

Figure 31. Mass Loss of Mortar Specimens under Different Scenarios. (a). Scenario I.

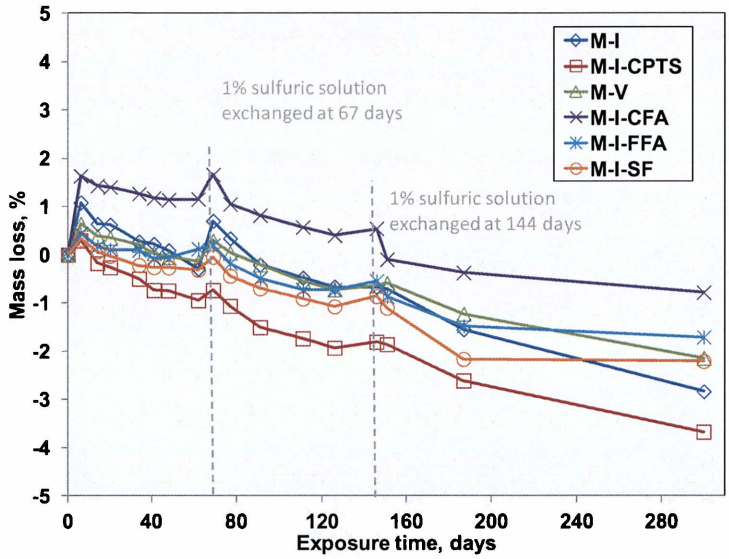

(b)

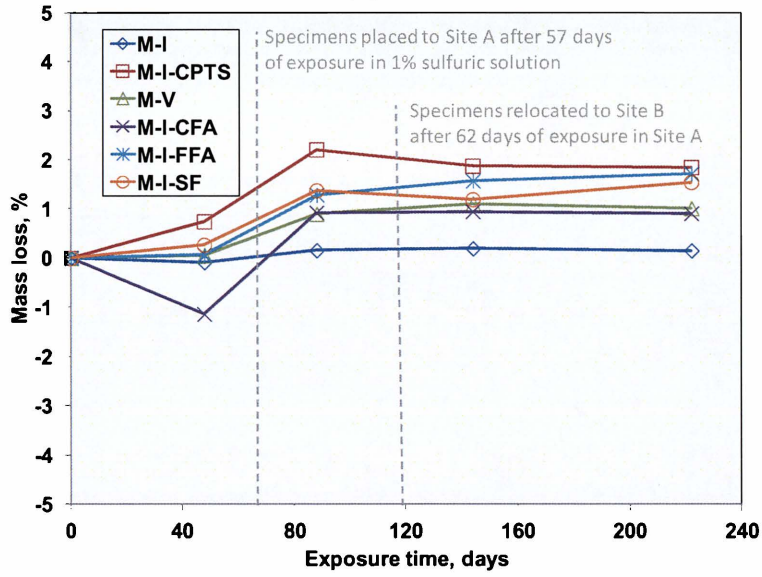

(c)

Figure 31. Mass Loss of Mortar Specimens under Different Scenarios (continuous). (b). Scenario II, (c). Scenario III.

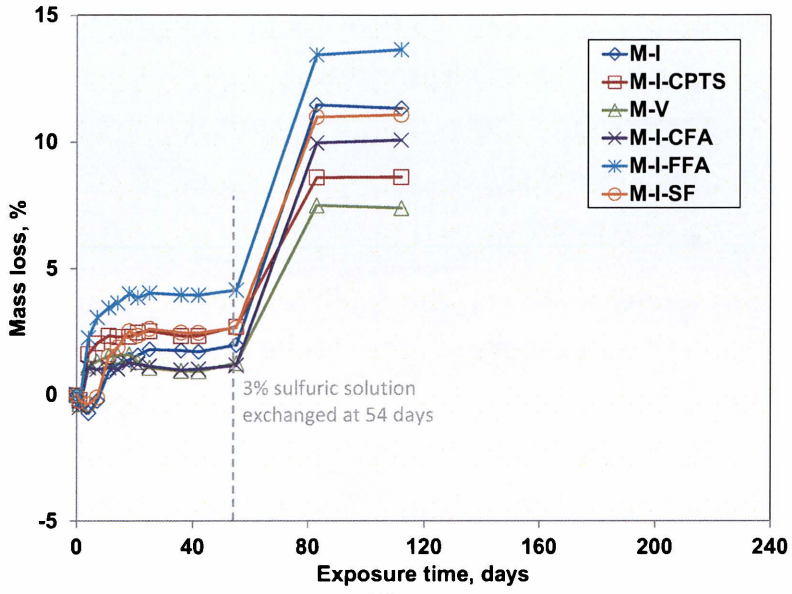

(d)

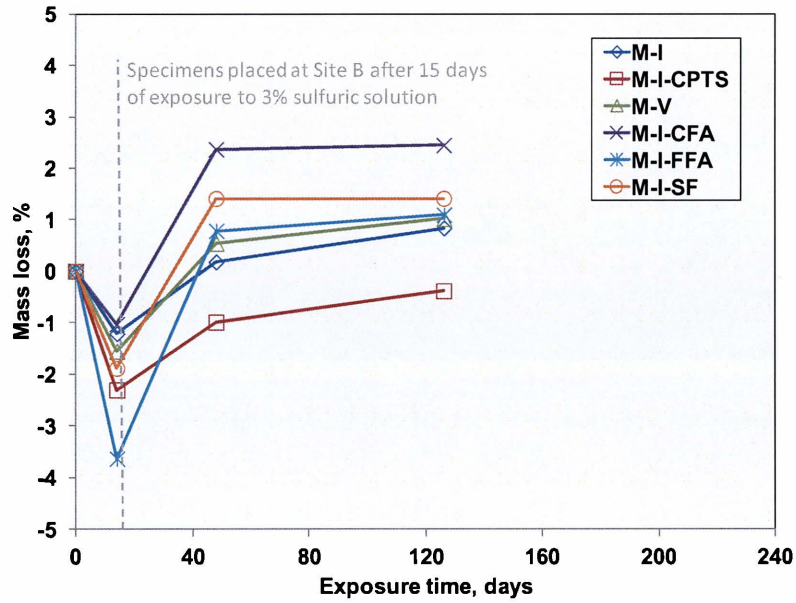

(e)

Figure 31. Mass Loss of Mortar Specimens under Different Scenarios (continuous). (d). Scenario IV, (e). Scenario V.

Among the all different mixtures, mixes with Type V cement or silica fume show a higher resistance with a lower amount of weight loss. While there is no significant improvement from mixtures with water repellent admixture (C-RPP), mixtures with coating agents (C-CPTS and M-CPTS) show slightly less mass loss when compared to reference mixtures (M-I and C-I) under aggressive environment conditions.

Compressive Strength

Compressive strength tests were performed after mortar specimens were exposed to different scenarios. Results as summarized in Figure 31 indicated that while there is no significant strength loss for the mortar cube specimens in Scenarios I, II, and III after 90 days exposure, in Scenario IV and IV for even fewer days. The results show up to a 15% loss of compressive strength. The reduction in compressive strength is likely due to the loss of surface substances. Within the different mixtures, M-I-CPTS and M-V show a slower rate of strength loss. This result is coincident with the results from visual observation and the mass loss test.

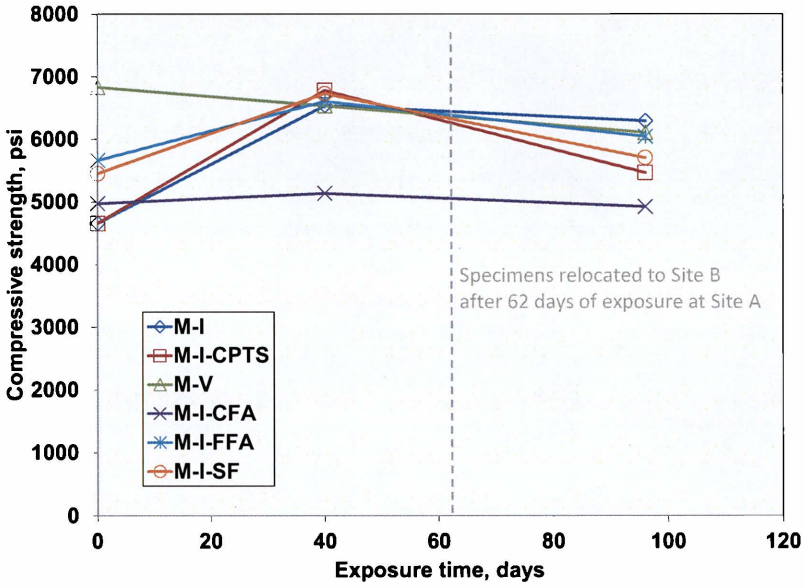

(a)

Figure 32. Compressive Strength of Mortar Specimens under Different Scenarios. (a). Scenario I.

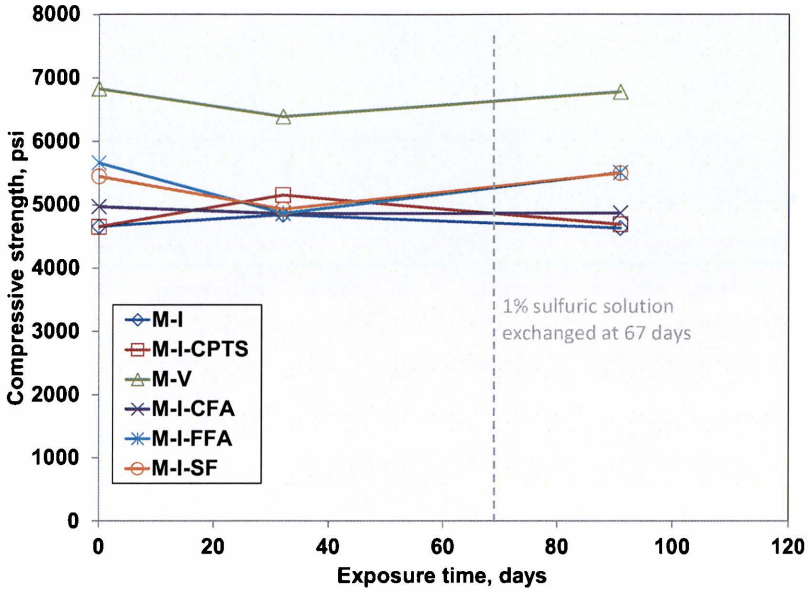

(b)

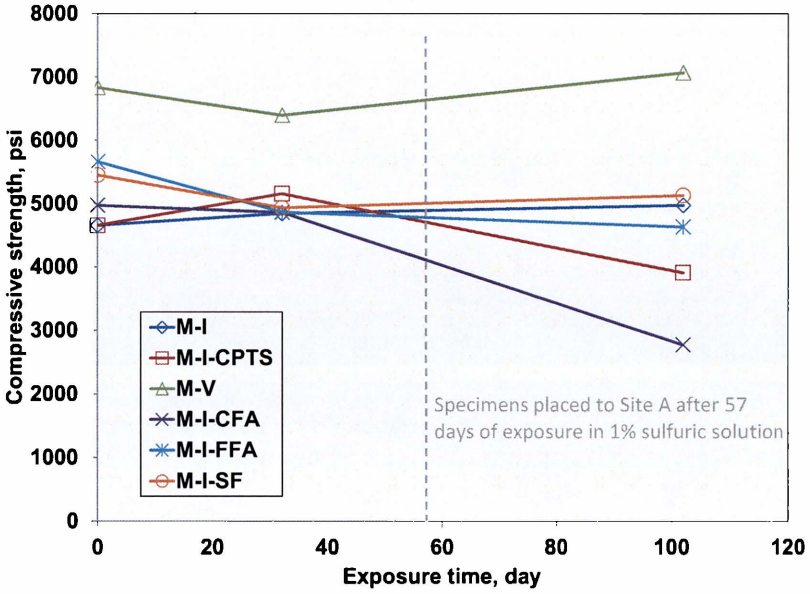

(c)

Figure 32. Compressive Strength of Mortar Specimens under Different Scenarios (continuous). (b). Scenario II, (c). Scenario III.

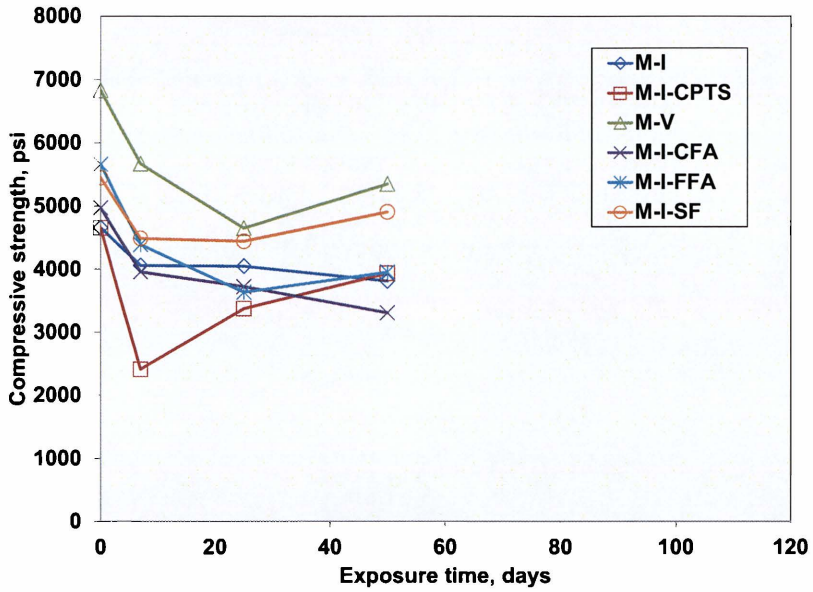

(d)

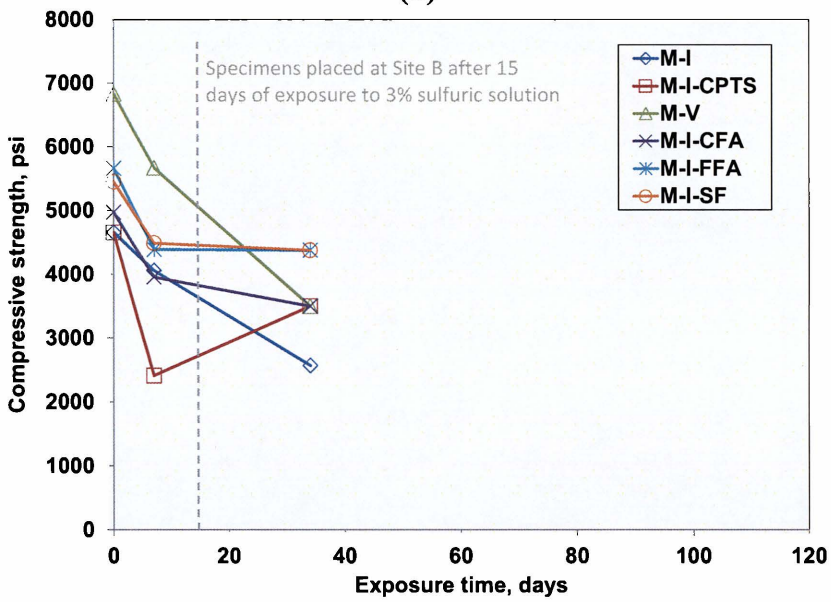

(e)

Figure 32. Compressive Strength of Mortar Specimens under Different Scenarios (continuous). (d). Scenario IV, (e). Scenario V.

Phenolphthalein pH

As an aggressive environment such as a sulfuric acid solution may result in a reduction of pH (and a color change from pink to clear), phenolphthalein indicators were used to evaluate the level of deterioration of the surface and near surface concrete. After specimens were removed from field or laboratory solutions, an automatic masonry saw was used to process selected mortar and concrete specimens and expose the internal surfaces. Examples of the results of

concrete specimen exposure to Scenarios II and IV are shown in Figure 33. Results show that despite the higher level of surface deterioration observed in specimens from Scenario IV due to the more aggressive environment, there were only a few millimeters of neutralized layer observed in the remaining concrete. Results were consistent with field evaluations, which regardless of different levels of surface deterioration, a low pH level only was observed a few millimeters beneath the concrete surface.

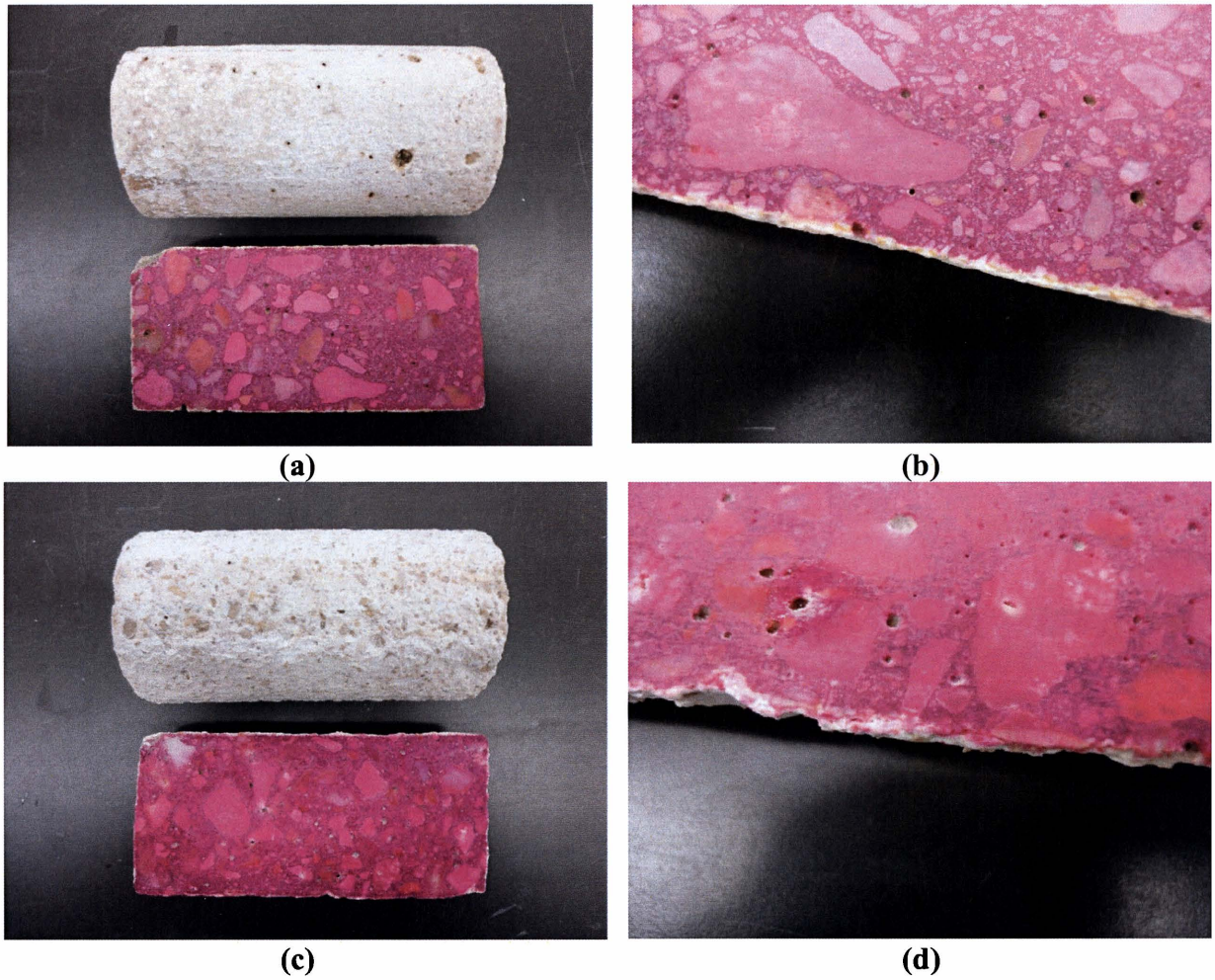

Figure 33. Examples of Deterioration and Phenolphthalein Color Change Tests. (a) Scenario II 238 days exposure (overview), (b). Scenario II 238 days exposure (close up), (c) Scenario IV 55 days exposure (overview), (d). Scenario IV 55 days exposure (close up).

A study was also conducted with mortar specimens exposed to different scenarios over different periods of time. As shown in Figure 34, while exposure in Scenario IV shows a higher level of deterioration, the depth of neutralized concrete proceeding from the surface is very low (generally less than 1mm), which indicates that the remaining concrete is unaffected. The phenolphthalein color changes associated with other samples are shown in Appendix F.

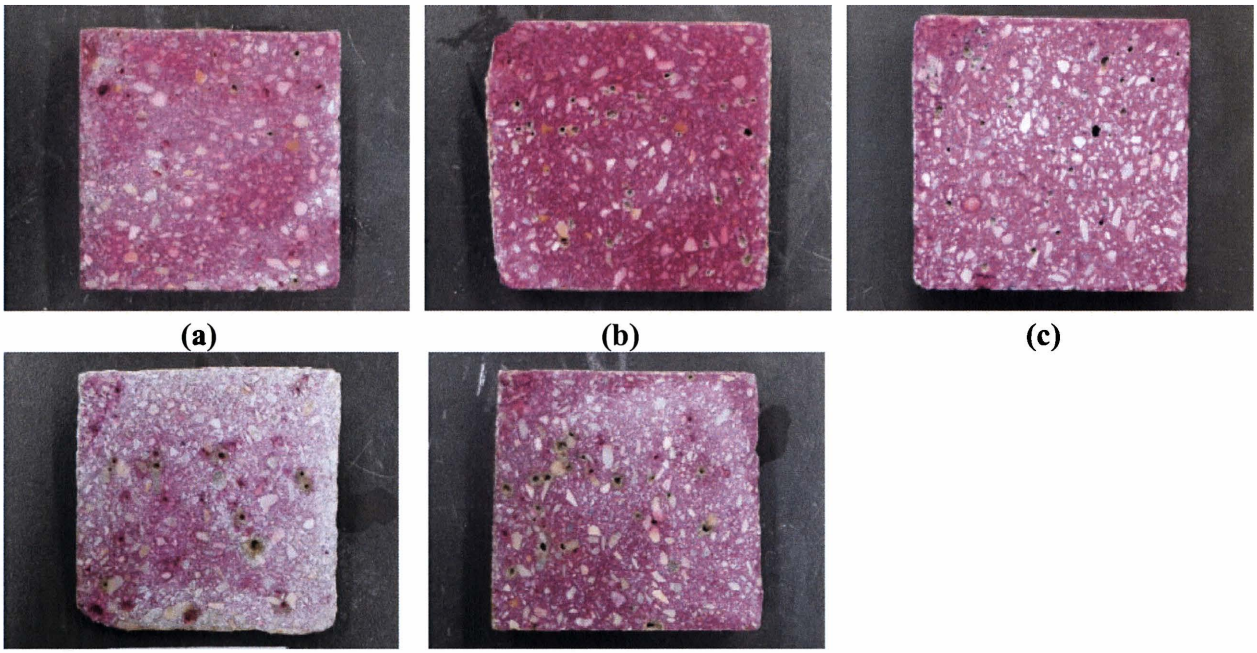

Figure 34. Examples of Phenolphthalein pH Test.
(a) M-I in scenario I with 96 days of exposure, (b) M-I in scenario II with 221 days of exposure, (c) M-I in scenario III with 96 days of exposure, (d) M-I in scenario IV with 50 days exposure , (e) M-I in scenario IV with 34 days of exposure.

Results from the measurement of neutralized thickness are summarized in Table 8. As shown in the table, while longer periods of exposure results in greater neutralized thickness, Scenarios II and IV generally result in greater neutralized thickness when compared to other scenarios. As the neutralized thicknesses were all very small, there was not enough information to draw any conclusions regarding the effect of different mixtures.

Table 8. Neutralized Thickness of M-I Specimens Exposed to Different Scenarios.

	Lab (days)	Field (days)	M-I	M-I-CPTS	M-V	M-I-CFA	M-I-FFA	M-I-SF
Scenario I	NA	96	~ 0	~ 0	~ 0	~ 0	~ 0	~ 0
Scenario II	28	NA	~ 0	~ 0	~ 0	~ 0	~ 0	~ 0
	91	NA	~ 0	~ 0	<0.25	<0.25	<0.25	<0.25
	221	NA	<0.25	<0.25	<0.5	<1	<1	<0.5
Scenario III	57	96	~ 0	~ 0	~ 0	<0.25	~ 0	~ 0
Scenario IV	7	NA	<0.25	~ 0	~ 0	<0.5	<0.25	~ 0
	25	NA	<0.75	<0.75	<0.75	<0.75	<0.75	<0.75
	50	NA	<1	<1	<1	<1	<1	<1
Scenario V	15	34	<0.25	<0.25	<0.5	<0.5	<0.5	<0.25

In summary, results from visual observation, length change, and mass loss indicated that while most mixtures present fairly good resistance against MID simulation, Type V cement, together with SCMs such as Class F fly ash, and silica fume can significantly improve MID resistance and therefore are recommended to be employed into the mix design in order to mitigate exposure to microbial attack. Despite of fact that mixtures with water repellent admixtures (C-RPP) were expected to improve performance under aggressive environmental conditions because of the reduced permeability, such a trend was not observed based on the mixtures included in this study. Further study is needed to verify the effectiveness of water repellent admixtures. Mixtures with a coating agent, i.e. concrete preservation treatment solution (C-CPTS and M-CPTS) did exhibit improved performance in this study. The sealant solution formed over the surface of concrete can prevent or slow down the penetration of aggressive agents. The CPTS provides protection to the existing concrete structure and it can be considered as a remediation method for deteriorated concrete.

CHAPTER 7:
CONCLUSIONS AND RECOMMENDATIONS

CONCLUSIONS

The research team performed an extensive literature search to collect information on (a) the mechanism of Microbial Induced Deterioration (MID), (b) test methods to identify and evaluate MID, (c) factors that affect the corrosion generated by MID, and (d) state-of-the-practice MID remediation methods. MID is a process of deterioration induced through the microbial production of acids, usually sulfuric acid, produced by sulfate-reducing bacteria and sulfur-oxidizing bacteria. This deterioration involves a chemical reaction between hydration products in the hardened concrete and biologically produced sulfuric acid, which alter the concrete chemical composition leading to early deterioration and loss of mass and strength. While a considerable number of chemical and microbial methods and procedures have been developed and used to identify MID in concrete, methods for field site identification of microbial induced degradation are still very limited.

Twelve selected TxDOT bridges with suspected MID issues were investigated. Visual inspection together with a number of *in situ* tests including rebound hammer, ultrasonic pulse velocity, cover thickness, half-cell corrosion potential and phenolphthalein pH analyses were performed to evaluate the integrity of these bridge columns. Water, mud, core and surface concrete samples of columns were also collected for laboratory analyses including microbial, chemical composition, mineralogy and petrographic analysis to investigate the potential cause and extent of the deterioration. Results from this comprehensive study were used to provide evidence of concrete degradation and ascertain the degree of deterioration caused by microbial attack. The study also evaluated effectiveness and consistency of various measurements used in this study and provided a suggested *in situ* and laboratory test procedure to identify microbial attack on concrete and evaluate the integrity of deteriorated concrete due to the attack.

In addition, a preliminary evaluation of the microbial attack resistance of concrete containing different types of cement, supplemental cementitious materials (SCMs) and coating agents was performed. A series of typical TxDOT concrete mixes were prepared and subjected to field and/or sulfuric acid solution exposure. Resistance against microbial attack from selected TxDOT mixes was evaluated.

The research and work documented herein generated the following conclusions:

1. The comprehensive inspection of twelve bridges in this study indicated that despite the different levels of surface spalling observed, mostly with softening of surface and near surface concrete and light to medium levels of scaling (penetration depth of less than half an inch), the deterioration of concrete mostly stays on the surface. Covering thickness measurements revealed sufficient concrete covers over existing reinforcements and the remaining concrete structures were still sound in general. Considering the fact that most of the bridges visited were more than forty years old, rates of deterioration are slow and MID should not be considered to post an immediate threat to the integrity of these structures.

2. pH measurements of water, mud and surface concrete indicate that most of the bridge columns are in contact with water having a pH of approximately 6, while the pH of the surface concrete scraping samples is higher and neutral to basic ranging from about 7 to 9. The reduction of pH together with traces of sulfate on the concrete surface based on chemical analysis indicates microbial growth. With respect to elevation along a concrete column, no clear trend emerges with respect to the concentration of sulfate or chloride.

3. Microbial analysis indicated that the detectability of organisms was high with essentially all organisms detectable. However, the microbes identified by *in situ* hybridization on these bridge columns are not comparable to those found in sewer systems. The deterioration observed in these structures is believed to result from the production of gypsum and ettringite from the biogenic release of sulfuric acid and dissolution of substituents in concrete (particularly C-S-H) due to the low acid environment that concrete experiences over time.

4. Differences in the level of deterioration with different concrete mixtures exposed to the same water body observed for selected bridges suggests that the role of aggregate and mix design may have an effect on resistance against microbial attack. Based on visual inspection and petrographic analysis of the mineralogy of aggregate, concrete with limestone as aggregate might be more susceptible to MID than gravel as aggregate.

5. While there is no quick test to identify MID in the field, visual inspection, and nondestructive tests together with *in situ* phenolphthalein (pH) measurements provide a good indication of level of deterioration. Laboratory tests including microbial, chemical, mineralogy and petrographic analysis can be used to further evaluate the severity of deterioration. A two-stage approach is recommended to evaluate the level of MID for TxDOT structures. Stage one

would be a preliminary survey to roughly evaluate the extend of MID, while stage two would serve as an extension of stage when needed, in order to confirm the MID and to identify the extent of defects revealed by stage one.

6. The preliminary evaluation of the microbial attack resistance of typical TxDOT concrete materials indicates that mixtures with Type V cement and SCMs can provide better resistance to MID. A concrete preservation treatment solution may also provide protection to the concrete and can be considered as a remediation method for deteriorated concrete.

RECOMMENDATIONS

The following recommendations can be made based on the data generated and knowledge and experience gained in the present research work:

1. As it was observed that the microbes identified by *in situ* hybridization on the bridge columns visited are not comparable to those found in sewer systems, it will be beneficial to perform a direct comparison of specimens collected from bridge columns and sewer systems. Data including in situ measurements, chemical, microbial, mineralogy and petrographic analyses can be used to confirm the mechanism of deterioration and quantitatively evaluate the level of deterioration under these two different environments. Results will provide TxDOT with a better knowledge of the extent and rate of deterioration.

2. Although a significant amount of tests have been performed to evaluate MID resistance of different mixtures, the numbers of tests and variety of mixtures that were conducted in the present research were not adequate to provide recommended mixtures for better MID resistance. A further study of microbial attack resistance of concrete with different materials and mix design could point toward improved measures to prevent and remediate microbial attack, while a further examination to quantify the influence of aggregate and mix design on MID resistance is also needed. Mixtures with different types of aggregate and amount of SCMs are needed to generate a recommendation of mix design of concrete mixtures for better MID resistance.

3. Due to the limited time of the study and nature of MID, deterioration of concrete specimens prepared for MID simulation, particularly those already placed in the field yielded results that were not significant. As specimens are still placed at various sites or under laboratory

conditions, continuous monitoring of field and laboratory specimens over a longer period of time would be beneficial to determine long term MID resistance.

4. Although rates of deterioration of most of the bridges visited were found to be slow and even though MID should not be considered to post an immediate threat to the integrity of these structures, methods for repair or remediation of heavily deteriorated sections might still be needed. It would be beneficial for TxDOT to identify selected locations where commercially available repair measures were used, and from the literature review conducted in this research, determine the actual effectiveness of these measures in preventing or remediating microbial attack.

REFERENCES

1. ACI 201, *Guide to Durable Concrete*. ACI 201.2R-08, American Concrete Institute, 2008.
2. Akman, M. S., and A. Guner. Applicability of Sonreb Method on Damaged Concrete. *Materials and Structures/Materiaux et Constructions*, Vol. 17, No. 3, 1984, pp. 195-200.
3. Amann, R. I., B. J. Binder, R. J. Olsen, S. W. Chisholm, R. Devereux, and D. A. Stahl. Combination of 16S rRNA-Targeted Oligonucleotide Probes with Flow Cytometry for Analyzing Mixed Microbial Populations. *Applied and Environmental Microbiology*, Vol. 56, No. 6, 1990, pp. 1919-1925.
4. Amann, R. I., L. Krumholz, and D. A. Stahl. Fluorescent Oligonucleotide Probing of Whole Cells for Determinative, Phylogenetic, and Environmental Studies in Microbiology. *Journal of Bacteriology*, Vol. 172, No. 2, 1990, pp.762-770.
5. Anzelmo, J. A., and J. R. Lindsay. X-Ray Fluorescence Spectrometric Analysis of Geologic Materials. *Journal of Chemical Education*, Vol. 64, No. 9, 1987, pp. A200-A204.
6. Bakker, R. On the Cause of Increased Resistance of Concrete Made from Blast Furnace Cement to the Alkali-Silica Reaction and to Sulfate Corrosion. Master Thesis, pp. 118 (Translated from German), RWTH Aachen University, 1980.
7. Bassuoni, M. T., and M. L. Nehdu. Resistance of Self-Consolidating Concrete to Sulfuric Acid Attack with Consecutive pH Reduction. *Cement and Concrete Research*, Vol. 37, No. 7, 2007, pp. 1070-1084.
8. Bates, R.G. *Determination of pH, 2nd ed.* New York Wiley, 1973.
9. Beeldens, A., J. Monteny, E. Vincke, N. De Belie, D. Van Gemert, L. Taerwe, and W. Verstraete. Resistance to Biogenic Sulphuric Acid Corrosion of Polymer-Modified Mortars, *Cement and Concrete Research*, Vol. 23, No. 1, 2001, pp. 47-56.
10. Beklimyshev, V. I., I. I. Makhonin, M. M. Afanas'ev, A. A. Abramyan, V. A. Solodivnikov, and R. V. Vartanov. *Biocidal Coating Compositions Containing Biocide-Modified Bentonite Nanoparticles*. RU 2338765 C1, 2008.
11. Bell, L. W., W. E. Shook, and T. Norris. Mitigating the Corrosion of Concrete Pipe and Manholes. *Concrete Pipe for the New Millennium*, ASTM STP1368, J. I. Enyart and I. I.

Kaspar, Eds., American Society for Testing and Materials, West Conshohocken, PA, 1999.

12. Benson, R. L. Stains, *Coatings and Sealers for Treating Wood, Concrete, and Related Materials*. US Patent 20100093887 A1, 2010.
13. Berndt, M. L. Protection of Concrete in Cooling Towers from Microbiologically Influenced Corrosion. *Geothermal Resources Council Transactions*, Vol. 25, 2001, pp. 3-7.
14. Biczok, I. *Concrete Corrosion-Concrete Protection, 8th Edition*. Akademiai Kiado, Budapest, 1972.
15. Bock, E., and W. Sand. Applied Electron Microscopy on the Biogenic Destruction of Concrete and Blocks-Use of the Transmission Electron Microscope for Identification of Mineral Acid Producing Bacteria. Bayles, J., G. R.Gouda, A. Nisperos, Eds., *Proceedings of Eighth International Conference on Cement Microscopy*, International Cement Microscopy Association, Duncanville, Texas. 1986.
16. Bond, P. L., and J. F. Banfield. Design and Performance of rRNA Targeted Oligonucleotide Probes for in situ Detection and Phylogenetic Identification of Microorganisms Inhabiting Acid Mine Drainage Environments. *Microbial Ecology*, Vol. 41, No. 2, 2001, pp. 149-161.
17. Chatzinotas, A., R. A. Sandaa, W. Schönhuber, R. Amann, F. L. Daae, V. Torsvik, J. Zeyer, and D. Hahn. Analysis of Broad-Scale Differences in Microbial Communities of Two Pristine Forest Soils. *Systematic and Applied Microbiology*, Vol. 21, No. 4, 1998, pp. 579-587.
18. ConShield, http://www.conshield.com/site/. Accessed October 28, 2011.
19. Corrosion Club, http://www.corrosion-club.com/watermic.htm. Accessed October 28, 2011.
20. Cowan, D. A., T. Guevara, and G. F. Matz, *Lightweight Concrete Compositions Containing Antimicrobial Agents*. US Patent 7632348, 2009.
21. Daims, H., A. Brühl, R. Amann, K. H. Schleifer, and M. Wagner. The Domain-Specific Probe EUB338 is Insufficient for the Detection of All Bacteria: Development and Evaluation of a More Comprehensive Probe Set. *Systematic and Applied Microbiology*, Vol. 22, No. 3, 1999, pp. 434-444.

22. Daims, H., J. L. Nielsen, P. H. Nielsen, K-H. Schleifer, and M. Wagner. In situ Characterization of Nitrospira-like Nitrite-Oxidizing Bacteria Active in Wastewater Treatment Plants. *Applied and Environmental Microbiology*, Vol. 67, No. 11, 2001, pp. 5273-5284.
23. Davies R. Concrete Service in Aggressive Industrial Environments. *Concrete*, 2005, pp. 32-35.
24. Davis, J. L., D. Nica, K. Shields, and D. J. Roberts, Analysis of Concrete from Corroded Sewer Pipe. *International Biodeterioration and Biodegradation*, Vol. 42, No. 1, 1998, pp. 75-84.
25. De Belie, N. Evaluation of Methods for Testing Concrete Degradation in Aggressive Solutions, *Workshop on Performance of Cement-based Materials in Aggressive Aqueous Environments - Characterization, Modeling, Test Methods and Engineering Aspects*, 2008, pp. 79-92.
26. De Belie, N., W. De Muynck, and W. Verstraete. A Synergistic Approach to Microbial Presence on Concrete: Cleaning and Consolidating Effects. *Structure Concrete*, Vol. 7, No. 3, 2006, pp. 105-109.
27. De Belie, N., Biogenic Sulfuric Acid Corrosion (BSA). *Magnel Laboratory for Concrete Research Project Report*. http://www.ugent.be/ea/labomagnel/en/research/topics/bsa.pdf. Accessed October 28, 2011.
28. De Belie, N., J. Monteny, A. Beeldens, E. Vincke, D. Van Gemert, and W. Verstraete. Experimental Research and Prediction of Chemical and Biogenic Sulfuric Acid on Different Types of Commercially Produced Concrete sewer Pipes. *Cement and Concrete Research*, Vol. 34, No. 12, 2004, pp. 2223-2236.
29. De Belie, N., M. Debruyckere, D. Van Nieuwenburg, and B. De Blaere. Concrete Attack by Feed Acids: Accelerated Tests to Compare Different Concrete Compositions and Technologies. *ACI Materials Journal*, Vol. 94, No. 6, 1997, pp. 546-554.
30. De Belie, N., H. J. Verselder, B. De Blaere, D. Van Nieuwenburg, and R. Verschoore. Influence of the Cement Type on the Resistance of Concrete to Feed Acids. *Cement and Concrete Research*, Vol. 26, No. 11, 1996, pp. 1717-1725.

31. De Muynck, W., D. Debrouwer, N. De Belie, and W. Verstraete. Bacterial Carbonate Precipitation Improves the Durability of Cementitious Materials. *Cement and Concrete Research*, Vol. 38, No. 7, 2008, pp. 1005-1014.
32. Diercks M., W. Sand, and E. Bock. Microbial Corrosion of Concrete. *Cellular and Molecular Life Sciences*, Vol. 47, No. 6, 1991, pp.514-516.
33. Felsenstein, J. Confidence Limits of Phylogenies: an Approach Using the Bootstrap. *Evolution*, Vol. 39, No. 4, 1985, pp. 783-791.
34. Freed, W. W. *Reinforced Concrete Containing Antimicrobial-Enhanced Fibers*. US Patent 6162845, 2000.
35. Garuti, J. Jr., and L. M. Calvo. Sealing Compositions for Use in Construction and Construction Method. US Patent 20100034978 A1, 2008.
36. Giannantonio, D. J. *Molecular Characterization of Microbial Communities fouling Concrete Infrastructures*. Master Thesis, Georgia Institute of Technology, 2008.
37. Goncharov, V. V., Biocidal Mortars and Concretes. *Beton I Zhelezobeton*, Vol. 3, 1984, pp. 26-27.
38. Gran, G. Determination of the Rquivalence Point in Potentiometric Titrations. Part II. *Analyst*, Vol. 77, No. 920, 1952, pp. 661.
39. Hahn, D., J. Gaertner, M. R. Forstner, and F. L. Rose. High Resolution Analysis of Salmonellae from Turtles within a Headwater Spring Ecosystem. *FEMS Microbiology Ecology*. Vol. 60, No. 1, 2007, pp. 148-155.
40. Hahn, D., K. Zepp, and J. Zeyer. Whole Cell Hybridization as a Tool to Study Frankia Populations in Root Nodules. *Physiologia Plantarum*, Vol. 99, No. 4, 1997, pp. 696-706.
41. Hahn, D., R. I. Amann, and J. Zeyer. Detection of mRNA in Streptomyces Cells by Whole-Cell Hybridization with Digoxigenin-Labeled Probes. *Applied and Environmental Microbiology*, Vol. 59, No. 8, 1993, pp. 2753-2757.
42. Hahn, D., R. I. Amann, and J. Zeyer. Whole-Cell Hybridization of Frankia Strains with Fluorescence- or Digoxigenin-Labeled, 16S rRNA-Targeted Oligonucleotide Probes. *Applied and Environmental Microbiology*, Vol. 59, No. 6, 1993, pp. 1709-1716.
43. Hahn, D., R. I. Amann, W. Ludwig, A. D. Akkermans, and K. H. Schleifer. Detection of Microorganisms in Soil after in situ Hybridization with Ribosomal RNA-Targeted,

Fluorescently Labeled Oligonucleotides. *Journal of General Microbiology*, Vol. 138, No. 5, 1992, pp. 879-887.

44. Hillis, D. M., and J. J. Bull. An Empirical Test of Bootstrapping as a Method for Assessing Confidence in Phylogenetic Analysis. *Systematic Biology*, Vol. 42, No. 2, 1993, pp. 182-192.
45. Huelsenbeck, J. P., and F. Ronquist. MRBAYES: Bayesian Inference of Phylogenetic Trees. *Bioinformatics*, Vol. 17, No. 8, 2001, pp. 754-755.
46. Huelsenbeck, J. P., F. Ronquist., R. Nielsen., and J. P. Bolback. Bayesian Inference of Phylogeny and Its Impact on Evolutionary Biology. *Science*, Vol. 294, No. 5550, 2001, pp. 2310-2314.
47. Hyman, A. E. Inspection, Repair and Rehabilitation of Concrete Structures Due to Corrosion. *International Journal of Materials and Product Technology*, Vol. 23, No. 3/4, 2005, pp. 309-337.
48. Idorn, G. M., and D. M. Roy. *Opportunities with Alkalies in Concrete Testing, Research, and Engineering Practice. Alkalies in Concrete*, STP-930, American Standard of Testing Materials (ASTM), West Conshohocken, Pa., pp. 5-15. 1986.
49. Islander, R. L., J. S. Devinny, F. Mansfeld, A. Postyn, and H. Shih. Microbial Ecology of Crown Corrosion in Sewers. *Journal of Environmental Engineering*, Vol. 117, No. 6, 1991, pp. 751-770.
50. Ismail, N., T. Nonaka, S. Noda, and T. Mori. Effect of Carbonation on Microbial Corrosion of Concretes. *Journal of Construction Management and Engineering*, Vol. 20, 1993, pp. 133-138.
51. Jensen, H. S., A. H. Nielsen, T. Hvitved-Jacobsen, and J. Vollertsen. Survival of Hydrogen Sulfide Oxidizing Bacteria on Corroded Concrete Surfaces of Sewer Systems. *Water Science and Technology*, Vol. 57, No. 11, 2008, pp. 1721-1726.
52. Kalousek, G. L., L. C. Porter, and E. J. Benton. Concrete for Long-Time Service in Sulfate Environment. *Cement and Concrete Research*, Vol. 2, No. 1, 1972, pp. 79-89.
53. Kanagawa, T., Y. Kamagata, S. Aruga, T. Kohno, M. Horn, and M. Wagner. Phylogenetic Analysis of and Oligonucleotide Probe Development for Eikelboom Type 021N Filamentous Bacteria Isolated from Bulking Activated Sludge. *Applied and Environmental Microbiology*, Vol. 66, No. 11, 2000, pp. 5043-5052.

54. Kukanskis, K.A., Z. Siddiquee, R. V. Shohet, and H. R. Garner. Mix of Sequencing Technologies for Sequence Closure: an Example. *BioTechniques*, Vol. 28, 1999, No. 4, pp. 630-634.

55. Lauer, K. R. Classification of Concrete Damage Caused by Chemical Attack. *Materials and Structures*, Vol. 23, No. 3, 1990, pp. 223-229.

56. Lea, F. M. *The Chemistry of Cement and Concrete, 1st American Edition.* Chemical Publishing Co., New York, 1971.

57. Liskowitz, J. W., M. Wecharatana, C. Jaturapitakkul, and A. E. Cerkanowica, *Sulfate and Acid Resistant Concrete and Mortar*, US Patent 5772752, 1998.

58. Maddison, W. P., and D. R. *Maddison. MacClade: Analysis of Phylogeny and Character Evolution.* Sinauer Associates, Sunderland, MA. 1999.

59. Maeda T., A. Negishi, H. Komoto, Y. Oshimna, K. Kamimura, and T. Sugio. Isolation of Iron-Oxidizaing Bacteria from Corroded Concretes of Sewage Treatment Plants. *Journal of Bioscience and Bioengineering*, Vol. 88, No. 3, 1999, pp. 300-305.

60. Maidak, B. L., J. R. Cole, C. T. Parker Jr, G. M. Garrity, N. Larsen, B. Li, T.G. Lilburn, M. J. McCaughey, G. J. Olsen, R. Overbeek, S. Pramanik, T. M. Schmidt, J. M. Tiedje, and C. R. Woese. A New Version of the RDP (Ribosomal Database Project). *Nucleic Acids Research*, Vol. 27, No. 1, 1999, pp. 171-173.

61. Malhotra, V. M. and N. J. Carino. *Handbook on Nondestructive Testing of Concrete.* 2nd Ed., ASTM International, CRC Press, 2004.

62. Malorny, B., J. Hoorfar, C. Bunge, and R. Helmuth. Multicenter Validation of the Analytical Accuracy of Salmonella PCR: Towards and International Standard. *Applied and Environmental Microbiology*, Vol. 69, No. 1, 2003, pp. 290-296.

63. Manz, W., R. Amann, W. Ludwig, M. Vancanneyt, and K. H. Schleifer. Application of a Suite of 16S rRNA-Specific Oligonucleotide Probes Designed to Investigate Bacteria of the Phylum Cytophaga-Flavobacter-Bacteroides in the Natural Environment. *Microbiology*, Vol. 142, No. 5, 1996, pp. 1097-1106.

64. Manz, W., R. Amann, W. Ludwig, M. Wagner, and K-H. Schleifer. Phylogenetic Oligodeoxynucleotide Probes for the Major Subclasses of Proteobacteria: Problems and Solutions. *Systematic and Applied Microbiology*, Vol. 15, No. 4, 1992, pp. 593-600.

65. Mather, B. Field and Laboratory Studies of the Sulfate Resistance of Concrete, *Performance of Concrete-Resistance of Concrete to Sulfate and Other Environmental Conditions, Thorvaldson Symposium*, University of Toronto Press, Toronto, 1968, pp. 66-76..
66. McPolin, D. O., P. A. M. Basheer, A. E. Long, K. T. V. Grattan, and T. Sun. New Test Method to Obtain pH Profiles due to Carbonation of Concretes Containing Supplementary Cementitious Materials. *Journal of Materials in Civil Engineering*, Vol. 19, No. 936, 2007, pp. 936-946.
67. Meier, H., R. I. Amann, W. Ludwig, and K-H. Schleifer. Specific Oligonucleotide Probes for in situ Detection of a Major Group of Gram-Positive Bacteria with Low DNA G+C Content. *Systematic and Applied Microbiology*, Vol. 22, No. 2, 1999, pp. 186-196.
68. Metha, P.K. Sulfate Resistance of Blended Portland Cements Containing Pozzolans and Granulated Blast-Furnace Slag. *Proceedings, 5th International Symposium on Concrete Technology*, Universidad Autonoma de Nuevo Leon, Monterry, N. L., Mexico, pp. 35-50. 1981.
69. Metha, P.K. Discussion of "Combating sulfate attack in Corps of Engineers concrete construction". *ACI Journal, Proceedings*, Vol. 73, No. 4, 1976, pp. 237-238.
70. Milde, K., W. Sand, W. Wolff, and E. Bock, Thiobacilli of the Corroded Concrete Walls of the Hamburg Sewer System. *Journal of General Microbiology*, Vol. 129, No. 5, 1983, pp. 1327-1333.
71. Monteny, J., N. De Belie, E. Vincke, W. Verstraete, and L. Taerwe, Chemical and Microbiological Tests to Simulate Sulfuric Acid Corrosion of Polymer-Modified Concrete. *Cement and Concrete Research*, Vol. 31, No. 9, 2001, pp. 1359-1365.
72. Mori, T., T. Nonaka, K. Tazak, M. Koga, Y. Hikosaka, and S. Nota. Interactions of Nutrients, Moisture and pH on Microbial Corrosion of Concrete Sewer Pipes. *Water Research*. Vol. 26, No. 1, 1992, pp. 29–37.
73. Mori, T., M. Koga, Y. Hikosaka, T. Nonaka, F. Mishina, Y. Sakai, and J. Koizumi. Microbial Corrosion of Concrete Sewer Pipes, H2S Production from Sediments and Determination of Corrosion. *Water Science Technology*, Vol. 23, 1991, pp. 1275-1282.

74. Moter, A., and U. B. Goebel. Fluorescence in situ Hybridization (FISH) for Direct Visualization of Microorganisms. *Journal of Microbiology Methods*, Vol. 41, No. 2, 2000, pp. 85-112.

75. Neef, A., R. Amann, H. Schlesner, and K-H. Schleifer. Monitoring a Widespread Bacterial Group: in situ Detection of Planctomycetes with 16S rRNA-Targeted Probes. *Microbiology*, Vol. 144, 1998, pp. 3257-3266.

76. Nicomrat, D., W. A. Dick, and O.H. Tuovinen. Microbial Populations Identified by Fluorescence in situ Hybridization in a Constructed Wetland Treating Acid Coal Mine Drainage. *Journal of Environmental Quality*, Vol. 35, No. 4, 2006, 1329-1337.

77. Nonaka, M., and T. Sato. *Cement Admixtures for Manufacture of Antibacterial Cement.* JP 2001031461 A, 2001.

78. Okabe, S., M. Odagiri, T. Ito, and H. Satoh. Succession of Sulfur-Oxidizing Bacteria in the Microbial Community on Corroding Concrete in Sewer Systems. *Applied and Environmental Microbiology*, Vol. 73, No. 3, 2007, pp. 971-980.

79. Padival, N. A., W. A. Kimbell, J. A. Redner. Use of Iron Salts to Control Dissolved Sulfide in Trunk Sewers. *Journal of Environmental Engineering*, Vol. 121, No. 11, 1995, pp. 824-829.

80. Page, R. D. TreeView: an Application to Display Phylogenetic Trees on Personal Computers. *Computer Applications in the Biosciences*, Vol. 12, No. 4, 1996, pp. 357-358.

81. Paiva, D. M., M. Singh, K. S. Macklin, S. B. Price, J. B. Hess, and D. E. Conner. Antimicrobial Activity of Commercial Concrete Sealant against Salmonella Spp: A Model for Poultry Processing Plants. *International Journal of Poultry Science*, Vol. 8, No. 10, 2009, pp. 939-945.

82. Parande, A. K., P. L. Ramsamy, S. Ethirajan, C. R. K. Rao, and N. Palanisamy, Deterioration of Reinforced Concrete in Sewer Environments. *Proceedings of the Institution of Civil Engineers, Municipal Engineer*, Vol. 159, No. 1, 2006, pp. 11-20.

83. Parande, A. K., and N. Palaniswamy. Influence of Microbiologically Induced Corrosion of Steel Embedded in Ordinary Portland Cement and Portland Possolona Cement. *Anti-Corrosion Methods and Materials*, Vol. 52, No. 3, 2005, pp. 148-153.

84. Parker, C. The Corrosion of Concrete - Isolation of Species of Bacterium Associated with the Corrosion of Concrete Exposed to Atmospheres Containing Hydrogen Sulphide.

Australian Journal of Experimental Biology and Medical Science, Vol. 23, No. 3, 1945, pp. 14-17.

85. Peccia, J., E. A. Marchand, J. Silverstein, and M. Hernandez. Development and Application of Small-Subunit rRNA Probes for Assessment of Selected Thiobacillus Species and Members of the Genus Acidiphilium. *Applied and Environmental Microbiology*, Vol. 66, No. 7, 2000, pp. 3065-3072.
86. Rabus, R, M. Fukui, H. Wilkes, and F. Widdel. Degradative Capacities and 16S rRNA-Targeted Whole-Cell Hybridization of Sulfate-Reducing Bacteria in an Anaerobic Enrichment culture Utilizing Alkylbenzenes from Crude Oil. *Applied and Environmental Microbiology*, Vol. 62, No. 10, 1996, pp. 3605-3613.
87. Ramirez, T. H.; G. D. De Leon. *Concrete-Based Floors and Wall Coverings with Antimicrobial Effect*. European Patent Application EP 1428806 A1, 2004.
88. Ramsburg, P., Preventing Sewer Corrosion. *Public Works*, No. 10, 2004.
89. Redner, J.A., E. J. Esfandi, and R. P. His. Evaluating Protective Coatings for Concrete Exposed to Sulfide Generation in Wastewater Treatment Facilities. *Journal of Protective Coatings and Linings*, Vol. 8, 1991, pp. 48-58.
90. Rigdon, J. H., and C. W. Beardsley. Corrosion of Concrete by Autotrophes. *Corrosion*, Vol. 5, 1956, pp. 60-62.
91. Roberts, D. J., D. Nica, G. Zuo, and J. L. Davis. Quantifying Microbially Induced Deterioration of Concrete: Initial Studies. *International Biodeterioration and Biodegradation*, Vol. 49, No. 4, 2002, pp. 227-234.
92. Roller, C., M. Wagner, R. Amann, W. Ludwig, and K-H. Schleifer. In situ Probing of Gram-Positive Bacteria with a High DNA G+C Content Using 23S rRNA-Targeted Oligonucleotides. *Microbiology*, Vol. 140, 1994, pp. 2849-2858.
93. Roy, D. M., and G. M. ldorn. Hydration, Structure, and Properties of Blast Furnace Slag Cements, Mortars, and Concrete. *ACI Journal, Proceedings*, Vol. 79, No. 6, 1982, pp. 444-457.
94. Sambrook, J., E. F. Fritsch, and T. Maniatis. *Molecular Cloning: a Laboratory Manual*. Cold Spring Harbor Press, Cold Spring Harbor, 1989.

95. Sand, W. Microbial Mechanisms of Deterioration of Inorganic Substrates – a General Mechanistic Overview. *International Biodeterioration and Biodegradation*, Vol. 40, No. 2-4, 1997, 183-190.

96. Sand, W., and E. Bock. Biodeterioration of Mineral Materials by Microorganisms – Biogenic Sulfuric and Nitric Acid Corrosion of Concrete and Natural Stone. *Geomicrobiology Journal*, Vol. 9, No. 2-3, 1991, pp. 129-138.

97. Sand, W. Importance of Hydrogen Sulfide, Thiosulfate, and Methylmercaptan for Growth of Thiobacilli during Simulation of Concrete Corrosion. *Applied and Environmental Microbiology*. Vol. 53, No. 7, 1987, pp. 1645-1648.

98. Saricimen, H., M. Shameem, M. S. Barry, M. Ibrahim, and T.A. Abbasi. Durability of Proprietary Cementitious Materials for Use in Wastewater Transport System. *Cement and Concrete Composites*, Vol. 25, No. 4-5, 2003, pp. 421-427.

99. Shimatani, H., H. Izawa, M. Wakasugi, and S. Nagaoka. *Cement Admixtures for Suppressing Alkali Aggregate Reaction*, Japanese Patent Application JP 62128954 A2. 1987.

100. Shook, W. E., and L. W. Bell. Corrosion Control in Concrete Pipe and Manholes, Technical Presentation. *Water Environmental Federation*, Orlando, 1998.

101. Sinanen Zeomic Co., LTD., www.zeomic.co.jp/english/, Accessed October 28, 2011.

102. Small, H., S. S. Timothy, and W. C. Bauman, Novel Ion Exchange Chromatographic Method using Conductimetric Detection, *Analytical Chemistry*, Vol. 47, No. 11, 1975, 1801-1809.

103. Solis, H. A. Cementitious Mix with Highly Improved Physicochemical and Bacteriological Characteristics, which Contains Dopamelanin, Its precursors, Analogs, or Derivatives as an Additive. Patent Cooperation Treaty (PCT) International Application, WO 2010062155 A1, 2010.

104. Specifier, www.specifier.com.au, Accessed October 28, 2011.

105. Stahl, D. A., R. I. Amann. Development and Application of Nucleic Acid Probes. Stackebrandt, E, M. Goodfellow, M Ed., *Nucleic acid techniques in bacterial systematics*. John Wiley & Sons, New York, 1991, pp. 205-248.

106. Stamatakis, A., Phylogenetic Models of Rate Heterogeneity: A High Performance Computing Perspective, Proceeding of IPDP, Rhodos, Greece, 2006.
107. Stamatakis, A., RAxML-VI-HPC: Maximum Likelihood-Based Phylogenetic Analyses with Thousands of Taxa and Mixed Models. *Bioinfomatics*, Vol. 22 No. 21, 2006, pp. 2688-2790.
108. Swofford, D. L. PAUP*. *Phylogenetic Analysis Using Parsimony (* and other methods)*. Sinauer Associates, Sunderland, MA. 2002.
109. Sydney, R., E. Esfandi, , S. Surapancni, Control Concrete Sewer Corrosion via the Crown Spray Process. *Water Environment Research*, Vol. 68, No. 3, 1996, pp. 338-347.
110. Tamura, K., J. Dudley, M. Nei, and S. Kumar. Molecular Evolutionary Genetics Analysis (MEGA) Software Version 4. *Molecular Biology and Evolution*, Vol. 24, 2007, pp. 1596-1599.
111. Taniuchi, Y., A. Murakami, and K. Ohki. Whole-Cell Immunocytochemical Detection of Nitrogenase in Cyanobacteria: Improved Protocol for Highly Fluorescent Cells. *Aquatic Microbial Ecology*, Vol. 51, 2008, pp. 237-247.
112. Thompson, J. D., T. J. Gibson, F. Plewniak, F. Jeanmougin, and D. G. Higgins. The CLUSTAL_X Windows Interface: Flexible Strategies for Multiple Sequence Alignment Aided by Quality Analysis Tools. *Nucleic Acids Research*, Vol. 25, No. 24, 1997, pp. 4876-4882.
113. Trejo, D., P. de Figueiredo, M. Sanchez, C. Gonzalez, S. Wei, and L. Li. *Analysis and Assessment of Microbial Biofilm-Mediated Concrete Deterioration*. Technical Report, U.S. Department of Transportation, 2008.
114. Trejo, D., and K. Reinschmidt. Justifying Materials Selection for RC Structures in Corrosive Environments; Part I – Sensitivity Analysis. *Journal of Bridge Engineering*, Vol. 12, No. 1, 2007, pp. 38-44.
115. Tsudome, T., K. J. Man, C. K. Sun, *Antibacterial, Antifungal, and Antifouling Compositions Containing Poly (Hexamethyleneguanidine Phosphate)*, Japanese Patent 2004149496 A, 2004.
116. Utrobin, N. P., A. S. Titarenko, and A. E. Balakirev. *Additive for Concrete Mixes*, RU 2377208 C1, 2009.

117. Vaidya, S. Use of Nanomaterials for Concrete Pipe Protection. *Advances And Experiences With Trenchless Pipeline Projects - Proceedings Of The ASCE International Conference On Pipeline Engineering And Construction*, Pipelines, 2007.

118. Vanden Bosch, V. D. *Performance of Mortar Specimens in Chemical and Accelerated Marine Exposure, Performance of Concrete in Marine Environment, SP-65, V. M. Malhotra, ed.*, American Concrete Institute, Farmington Hills, Mich.,1980, pp. 487-507.

119. Vincke, E., E. Van Wanseele, J. Monteny, A. Beeldens, N. De Belie, L. Taerwe, D. Van Gemert, and W. Verstraete. Influence of Polymer Addition on Biogenic Sulfuric Acid Attack of Concrete. *International Biodeterioration and Biodegradation*, Vol. 49, No. 4, 2002, pp. 283-292.

120. Vincke, E., N. Boon, and W. Verstraete. Analysis of the Microbial Communities on Corroded Concrete Sewer Pipes--a Cast Study. *Applied and Environmental Microbiology*, Vol. 57, No. 5-6, 2001, pp. 776-785.

121. Wagner, M., R. Amann, P. Kämpfer, B. Assmus, A. Hartmann, P. Hutzler, N. Springer, and K-H. Schleifer. Identification and in situ Detection of Gram-Negative Filamentous Bacteria in Activated Sludge. *Systematic and Applied Microbiology*, Vol. 17, 1994, pp. 405-417.

122. Welton, R. G., M. Ribas Silva, C. Gaylarde, L. K. Herrera, X. Anleo, N. De Belie, and S. Modry. Techniques Applied to the Study of Microbial Impact on Building Materials. *Materials and Structures*, Vol. 38, No. 10, 2005, pp. 883-893.

123. Widmer, F., B. T. Shaffer, L. A. Porteous, and R. J. Seidler. Analysis of nifH Gene Pool Complexity in Soil and Litter at a Douglas Fir Forest Site in the Oregon Cascade Mountain Range. *Applied and Environmental Microbiology*, Vol. 65, No. 2, 1999, pp. 374-380.

124. Xiong, G., X. Chen, G. Li, and L. Chen. Sulphuric Acid Resistance of Soluble Soda Glass-Polyvinyl Acetate Latex-Modified Cement Mortar. *Cement and Concrete Research*, Vol. 31, No. 1, 2001, pp. 83-86.

125. Yamanaka, T., I. Aso, S. Togashi, M. Tanigawa, K. Shoji, T. Watanabe, N. Watanabe, K. Maki, and H. Susuki. Corrosion by Bacteria of Concrete in Sewerage

Systems and Inhibitory Effects of Formates on Their Growth. *Water Research*, Vol. 36, No. 10, 2002, pp. 2636-2642.

126. Yang, W., and T. Nonaka. A Study on Estimation of Deterioration Depth on Microbial Corrosion of Concrete. *JCA Proceedings of Cement and Concrete*, No. 52, 1998, pp. 726-733.

127. Zarda, B., D. Hahn, A. Chatzinotas, W. Schoenhuber, A. Neef, R. I. Amann, and J. Zeyer. Analysis of Bacterial Community Structure in Bulk Soil by in situ Hybridization. *Archives of Microbiology*, Vol. 168, No. 3, 1997, pp. 185-192.

128. Zhang, X., and X. Zhang. Mechanism and Research Approach of Microbial Corrosion of Concrete. *Journal of Building Materials*, Vol. 9, No. 1, 2006, pp. 52-58.

APPENDIX A:

COMMERCIALLY AVAILABLE TECHNOLOGIES FOR MID REMEDIATION

Following is a summary of commercially available technologies for MID remediation:

Ziomighty produced by Sinanen Zeomic Co., LTD (Zeomic 2011) is a zeolite that has aluminum substituted into silica oxide structure. The resultant positive charge resulting from this substitution (aluminum +3 substituted for a silica + 4) is compensated by copper and silver counter ions. The copper and silver ions provide the efficacy of bacteria attack. These ions are not fugitive because of the ionic association with the zeolite. The effectiveness of Ziomighty in concrete is at the 1% level. Because of the chemical nature of the zeolite and its particle size, it is readily assimilated into concrete formulas. The technology is reported to not compromise compressive strength of concrete.

Synthetic Industries, Inc. (Chicamauga, GA) has a developed fiber technology that contains an antimicrobial agent which is dispersed into the concrete to produce a fiber reinforced concrete product (Freed 2000). Polyolefins (polyethylene and polypropylene) are the preferred polymer for the fiber. Microban B (a phenolic based antibacteria agent) is the preferred additive for the polymer fibers (0.005 % loading) to kill the bacteria. The fibers are reported to reduce shrinkage cracking in the concrete in addition to killing the bacteria. Concern about the long term durability of the polymer fibers in the concrete is justified.

BioSealed for ConcreteTM produced by GreenSealed Solutions Inc, Johns Creek, GA., was evaluated as an antibacterial coating on concrete by spraying the product onto the concrete with a paint sprayer. The product proved to be an effective treatment for concrete remediation of bacteria attack (Paiva et al. 2009).

Deflecta Stabilizer Antimicrobial produced by Deflecta Crete Seals (Specifer 2011), Victoria, Australia, is a coating that penetrates the concrete to at least 150 mm to form a silicate hydrogel. No volatile organic solvents are associated with this water based coating. The coating provides an effective moisture barrier and antibacterial coating. It is reported to increase the structural strength of the concrete.

Elemix concrete additive manufactured by Syntheon (Moon Township, PA) is an expanded polymer spherical particle that is a light weight additive which can contain a antibacteria agent (Cowan et al. 2009). The product is claimed to deliver an energy efficient concrete with crack resistance and antibacterial performance.

Cemex has a patent application (Ramirez and De Leon 2004) that describes the antibacterial effectiveness for mixing quaternary ammonium ions directly with the preparation of

the concrete. The quat type that is mentioned in the patent application is alkylbenzyldimethyl chlorides. These quats are well known as effective antibacterial agents in hand soaps.

Con Shield (ConShield 2011) manufactured by CONSHIELD Technologies Inc., Atlanta, GA, is a liquid additive for concrete that claims a product "uninhabitable for bacteria growth". The chemistry of the technology is not described. An EPA registration number, 75174-2-47000 is supplied.

Formulated Solutions LLC, Largo, Florida, provides custom sealing compositions for concrete with antibacterial activity (Garuti and Calvo 2008). The patent application includes quats, metal salts, and organic antibacterial compounds. Some of the additives are very toxic and not suitable for environmental applications.

Timber Ox, Inc., Cicero, IN., produces a concrete sealer that contains Troysan Polyphase 60B as the antibacterial agent in the coating (Benson 2010). The agent is a bio-based, deep penetrating, film forming wet look or satin finished sealer that can be applied for concrete, bricks and many other cementitious materials.

APPENDIX B:

DETAILED SITE VISIT RECORD

Figure B. 1. Overview of Bridge Deterioration (Bridge 1).

Table B. 1. General Information and Summary of Visual Inspection (Bridge 1).

Location	FM 787 @ Tarkington Bayou (Liberty County)
Date of Visit	11/5/2009
Weather Condition	73.5°F, 55% RH
GPS	Latitude - 30.35467624; Longitude - 095.05299129
Bridge ID	NBI: 20-146-0813-01-009; CSJ: 0813-01-036
General Information	Originally built in 1930, widened in 1973
Summary of Visual Inspection	Originally section (gravel as aggregate) appears to be in good condition; widening section (limestone as aggregate) appears to have loss of paste issue (with low level of deterioration). Bottom section of columns are softer (i.e., easier to be scraped off) comparing to upper section.

Table B. 2. Specimen Collection Record (Bridge 1).

Specimen ID	Sampling Height (in.)	Specimen Type	Notes
1-C1-1	6	Core (1.5")	SW End Column
1-C1-2	22	Core (1.5")	SW End Column
1-C2-1	20	Core (1.5")	West End Expansion
1-C2-2	27	Core (1.5")	West End Expansion
1-C2-3	34	Core (1.5")	West End Expansion
1-C3-1	38	Core (1.5")	West End Middle Span Section
1-C3-2	28	Core (1.5")	West End Middle Span Section
1-C3-3	21	Core (1.5")	West End Middle Span Section
1-C4-1	26	Core (1.5")	SW Side Column
1-C4-2	14	Core (1.5")	SW Side Column
1-C4-3	10	Core (1.5")	SW Side Column
1-Water1	NA	Water	
1-Water2	NA	Water	
1-Water3	NA	Water	
1-C1-1C	6	Surface Scraping	Deteriorated
1-C1-2C	22	Surface Scraping	Semi-deteriorated
1-C2-1C	20	Surface Scraping	Semi-deteriorated
1-C3-2C	21	Surface Scraping	Semi-deteriorated
1-C1-1B	6	Surface Scraping	Deteriorated
1-C1-2B	30	Surface Scraping	Semi-deteriorated
1-C1-3B	66	Surface Scraping	Non-deteriorated

Table B. 3. Rebound Hammer Test Record (Bridge 1).

Test Location	Test Height (in)	Estimate Strength (psi)	Rebound Number								
			Average	Standard Deviation	Individual Results						
1-C1-1	6	3050	31.20	7.48	29	26	15	31	35	35
1-C1-1	22	2625	29.50	5.89	27	26	21	32	34	37
1-C1-1	38	5150	39.60	6.91	42	38	25	38	45	35
1-C1-1	54	3917	34.67	3.61	35	41	33	34	35	30
1-C1-1	70	4458	36.83	3.66	33	43	38	35	34	38
1-C1-2	6	2250	28.00	8.00	20	28	36			
1-C1-2	22	5000	39.00	7.00	39	39	25	39		
1-C1-2	38	5750	42.00	9.87	43	41	25			
1-C1-2	54	4750	38.00	4.00	34	42	38			
1-C1-2	70	5500	41.00	6.56	34	47	42			
1-C2-1	6	188	19.75	4.57	23	13	21	22		
1-C2-1	20	2833	30.33	4.51	26	35	30			
1-C2-1	27	2563	29.25	8.14	31	40	24	22		
1-C2-1	34	NA	16.25	2.36	18	13	16	18		
1-C2-2	6	4833	38.33	6.03	44	39	32			
1-C2-2	20	5167	39.67	4.73	45	38	36			
1-C2-2	27	4167	35.67	0.58	36	36	35			
1-C2-2	34	4250	36.00	1.00	36	35	37			
1-C2-2	40	5500	41.00	4.58	40	37	46			
1-C2-2	54	4750	38.00	4.36	40	33	41			
1-C2-2	70	4583	37.33	3.06	34	40	38			
1-C3-1	6	583	21.33	2.89	18	23	23			
1-C3-1	21	1333	24.33	2.08	26	25	22			
1-C3-1	28	1667	25.67	0.58	25	26	26			
1-C3-1	38	1313	24.25	4.11	25	19	29	24		
1-C3-1	50	4833	38.33	5.69	40	43	32			
1-C3-1	70	6250	44.00	6.08	40	41	51			
1-C3-2	6	3375	32.50	5.97	26	40	30	34		
1-C3-2	21	2167	27.67	2.52	28	25	30			
1-C3-2	28	1500	25.00	3.00	22	25	28			
1-C3-2	38	2313	28.25	9.03	19	40	24	30		
1-C3-2	50	4417	36.67	2.52	39	37	34			
1-C3-2	70	5333	40.33	0.58	40	41	40			

Table B. 4. Ultrasonic Pulse Velocity (UPV) Test Record (Bridge 1).

Test location	Test Height (in)	Calculated UPV (ft/s)			
		Average	Standard Deviation	Individual Results	
1-C1	6	16556	N/A	16556	
1-C1	22	13838	271	13646	14029
1-C3	50	13995	N/A	13995	

Table B. 5. Halfcell Test Record (Bridge 1).

Test Location	Test Height (in)	Corrosion Potential (mV)						
		Average	Standard Deviation	Individual Results				
1-C3	6	-147	NA	-147				
1-C3	21	-199	42.91	-145	-218	-225	-163	-245
1-C3	28	-137	11.05	-137	-119	-137	-147	-145
1-C3	38	-165	22.77	-138	-157	-154	-187	-191
1-C3	50	-178	13.01	-157	-189	-183	-175	-187
1-C3	70	-162	11.59	-152	-160	-154	-181	-165

Table B. 6. Covermeter Test Record (Bridge 1).

Test Location	Test Height (in.)	Rebar Size (in)	Covering thickness (in)				
			Average	Standard Deviation	Individual Results		
1-C3	36	11	2.40	0.14	3	2.3	2.5

Figure B. 2. Overview of Bridge Deterioration (Bridge 2)

Table B. 7. General Information and Summary of Visual Inspection (Bridge 2).

Location	SH 21 @ Navasota River (Robertson County)
Date of Visit	11/19/2009
Weather Condition	74°F, 49% RH
GPS	Latitude - 30.86970776; Longitude 096.19254394
Bridge ID	NBI: 17-154-0117-03-065; CSJ: N/A
General Information	1959
Summary of Visual Inspection	Column (precast) part appears to be in good condition; center wall span (site cast) appears to have loss of paste issue (with low level of deterioration), bottom part of wall span appeared to be repaired.

Table B. 8. Specimen Collection Record (Bridge 2).

Specimen ID	Sampling Height (in.)	Specimen Type	Notes
2-C1	N/A	Core (1.5")	Column closed to the center wall span
2-C1	N/A	Core (1.5")	Column closed to the center wall span
2-C1	N/A	Core (1.5")	Column closed to the center wall span
2-Wall	Footing	Core (1.5")	Center wall span, sample crumbled
2-Wall	18	Core (1.5")	Center wall span
2-Wall	32	Core (1.5")	Center wall span
2-C2	N/A	Core (1.5")	Column away from center wall span
2-C2	N/A	Core (1.5")	Column away from center wall span
M-1	NA	Concrete	3" diameter and 24" long (in soil)
M-2	NA	Concrete	Pole stand
2-Water	NA	Water	
2-Water	NA	Water	
2-Water	NA	Water	
2-Mud	NA	Mud	
2-C1C	6	Surface scraping	Deteriorated
2-C1C	12	Surface scraping	Semi-deteriorated
2-C1C	36	Surface scraping	Non-deteriorated
2-FootingC	0	Surface scraping	Deteriorated
2-C1-1B	6	Surface scraping	Deteriorated
2-C1-2B	12	Surface scraping	Semi-deteriorated
2-C1-3B	36	Surface scraping	Non-deteriorated

Table B. 9. Rebound Hammer Test Record (Bridge 2).

Test Location	Test Height (in)	Estimate Strength (psi)	Rebound Number											
			Average	Standard Deviation	Individual Results									
2-C1-1	6	1375	24.50	5.93	36	20	24	26	28					
2-C1-1	18	2150	27.60	3.85	32	22	26	2	30					
2-C1-1	30	3250	32.00	5.10	30	40	34	28	28					
2-C1-1	42	6250	44.00	3.16	42	40	44	46	48					
2-C1-1	54	8050	51.20	4.60	44	50	52	54	56					
2-C1-1	68	8550	53.20	4.82	48	56	48	56	58					
2-C1-2	6	1833	26.33	5.85	16	24	30	30	32	26				
2-C1-2	18	3350	32.40	7.13	22	38	40	30	32					
2-C1-2	30	8643	53.57	12.63	22	46	56	32	60	55	56	50	52	
2-C1-2	42	6350	44.40	9.10	34	36	46	54	52					
2-C1-2	54	6350	44.40	6.23	34	44	48	46	50					
2-C1-2	68	8550	53.20	7.95	40	52	56	58	60					
2-C2-1	0	5150	39.60	6.78	24	36	38	40	42	42				
2-C2-1	6	7050	47.20	11.64	20	42	46	50	52	46				
2-C2-1	18	4450	36.80	4.38	32	36	36	36	44					
2-C2-1	30	3450	32.80	8.52	30	18	40	40	28	26				
2-C2-1	42	6833	46.33	9.91	36	48	40	38	58	58				
2-C2-1	54	7050	47.20	6.42	42	48	50	56	40					
2-C2-1	68	6150	43.60	9.10	30	40	46	48	54					
2-C2-2	6	4375	36.50	8.67	32	32	20	42	40					
2-C2-2	18	3250	32.00	6.32	32	40	36	28	24					
2-C2-2	30	1650	25.60	4.34	20	26	24	26	32					
2-C2-2	42	7000	47.00	17.92	18	32	58	60	62	52				
2-C2-2	54	6050	43.20	8.32	30	40	48	48	50					
2-C2-2	68	4350	36.40	5.37	32	32	34	44	40					
2-C2-3	0	1350	24.40	5.90	26	34	20	22	20					
2-C2-3	6	2500	29.00	8.07	36	40	22	32	22	22				
2-C2-3	18	7875	50.50	14.59	52	56	42	52	20					
2-C2-3	30	1850	26.40	2.19	26	26	30	24	26					
2-C2-3	42	2500	29.00	10.26	50	28	36	26	26					
2-C2-3	54	2950	30.80	6.57	38	34	26	34	22					
2-C2-3	68	5450	40.80	7.43	30	36	46	46	46					
2-C3-1	6	1550	25.20	4.15	20	22	28	30	26					
2-C3-1	18	1250	24.00	4.24	20	24	20	30	26					
2-C3-1	30	2050	27.20	3.03	22	30	28	28	28					
2-C3-1	42	750	22.00	1.41	22	22	22	20	24					
2-C3-1	54	1650	25.60	4.10	22	26	22	26	32					
2-C3-1	68	4500	37.00	9.70	40	48	26	24	42	42				

Table B. 9. Rebound Hammer Test Record (Bridge 2).

Test Location	Test Height (in)	Estimate Strength (psi)	Rebound Number										
			Average	Standard Deviation	Individual Results								
2-C3-1	80	5550	41.20	6.42	32	38	42	48	46				
2-C3-2	6	1350	24.40	4.34	20	20	30	26	26				
2-C3-2	18	2250	28.00	3.74	34	24	28	26	28				
2-C3-2	30	3350	32.40	9.84									
2-C3-2	42	3083	31.33	11.98									
2-C3-2	54	3417	32.67	7.55									
2-C3-2	68	2458	28.83	8.26									
2-C3-2	80	6950	46.80	11.88									
2-Wall	6	2833	30.33	10.23									
2-Wall	18	7500	49.00	12.20									
2-Wall	30	5150	39.60	6.54									
2-Wall	42	5450	40.80	7.29									

Table B. 10. Ultrasonic Pulse Velocity (UPV) Test Record (Bridge 2).

Test Location	Test Height (in)	Calculated UPV (ft/s)					
		Average	Standard Deviation	Individual Results			
2-C1	6	14671	116	14602	14805	14606	
2-C1	18	15435	4451	13550	22096	12806	13288
2-C1	30	13173	38	13213	13168	13138	
2-C1	42	13068	10	13059	13079	13065	
2-C2	6	10625	1428	8792	12065	10270	11371
2-C2	18	13179	348	12778	13364	13395	
2-C2	30	13052	1315	11079	13677	13725	13725
2-C2	42	11665	3645	6198	13456	13503	13503
2-C3	6	14004	1029	13456	13364	15191	
2-C3	18	14369	1649	16271	13503	13333	
2-C3	30	13109	115	12977	13183	13168	
2-C3	42	13460	282	13138	13582	13661	

Table B. 11. Halfcell Test Record (Bridge 2).

Test Location	Test Height (in)	Corrosion Potential (mV)				
		Average	Standard Deviation	Individual Results		
2-C1	4	-111	N/A	-111		
2-C1	12	-60	N/A	-60		
2-C1	18	-58	N/A	-58		
2-C1	24	-15	N/A	-15		
2-C1	31	16	N/A	16		
2-C1	34	34	N/A	34		
2-C1	42	53	N/A	53		
2-C1	50	90	N/A	90		
2-C1	57	95	N/A	95		
2-C1	64	120	N/A	120		
2-C1	68	133	N/A	133		
2-C2	12	-117	6.56	-124	-116	-111
2-C2	24	-82	12.66	-84	-68	-93
2-C2	36	-23	12.53	-35	-24	-10
2-C2	48	-24	4.00	-20	-28	-24
2-C2	50	-9	9.24	-14	-14	2
2-C2	62	27	3.21	26	31	25
2-C3	12	-91	N/A	-91		
2-C3	24	-18	N/A	-18		
2-C3	26	31	N/A	31		
2-C3	48	79	N/A	79		
2-C3	50	164	N/A	164		
2-C3	62	188	N/A	188		
2-C3	74	206	N/A	206		

Figure B. 3. Overview of Bridge Deterioration (Bridge 3).

Table B. 12. General Information and Summary of Visual Inspection (Bridge 3).

Location	SH 276 @ Lake Tawakoni (Hunt County)
Date of Visit	12/10/2009
Weather Condition	36°F, 41% RH
GPS	Latitude - 32.90405349; Longitude - 095.99853246
Bridge ID	NBI: N/A; CSJ: N/A
General Information	Built 1959
Summary of Visual Inspection	Area close to water level appeared to have medium level of deterioration. Heavy deterioration sections underneath water level was not accessible Water level at testing column was approximate 5 feet from bottom of bridge, 32 feet from bottom of lake.
Other Information	Two trips (first trip – surface and water sample collection, in situ tests; second trip – core sample collection). Very cold and windy on first trip. Water level very high (6-7 feet higher than summer 2009 season). Columns at the center section of the bridge were chosen to allow the access of boat.

Table B. 13. Specimen Collection Record (Bridge 3).

Specimen ID	Sampling Height (in.)	Specimen Type	Notes
3-C131-1	6	Core (1.5")	NW, column
3-C131-2	24	Core (1.5")	NW, column
3-C131-3	6	Core (1.5")	SE, column
3-C131-4	24	Core (1.5")	SE, column
3-C131-5	48	Core (1.5")	SE, column
3-C131-6	60	Core (1.5")	SE, column
3-Water	NA	Water	
3-Water	NA	Water	
3-C131C	6	Surface scraping	Deteriorated
3-C131C	24	Surface scraping	Semi-deteriorated
3-C131C	48	Surface scraping	Non-deteriorated
3-C131B	6	Surface scraping	Deteriorated
3-C131B	24	Surface scraping	Semi-deteriorated
3-C131B	48	Surface scraping	Non-deteriorated

Table 1. Rebound Hammer Test Record (Bridge 3).

Test Location	Test Height (in)	Estimate Strength (psi)	Rebound Number				
			Average	Standard Deviation	Individual Results		
3-C131	6	3250	32.00	N/A	32		
3-C131	12	3750	34.00	N/A	34		
3-C131	18	3500	33.00	1.41	34	32	
3-C131	24	4250	36.00	3.46	40	34	34
3-C131	30	4750	38.00	0.00	38	38	
3-C131	36	4250	36.00	2.83	38	34	
3-C131	42	3750	34.00	2.83	36	32	
3-C131	52	5000	39.00	4.24	42	36	
3-C131	62	4000	35.00	4.24	38	32	

Table B. 14. Halfcell Test Record (Bridge 3).

Test Location	Test Height (in)	Corrosion Potential (mV)				
		Average	Standard Deviation	Individual Results		
3-C131	6	69	1.15	70	68	68
3-C131	18	116	19.40	126	129	94
3-C131	30	123	12.58	135	125	110
3-C131	42	129	33.23	130	127	71
3-C131	54	117	8.08	122	122	108
3-C131	66	113	5.03	108	112	118

Table B. 15. Covermeter Test Record (Bridge 3).

Test Location	Test Height (in.)	Rebar Size (in)	Covering Thickness (in)				
			Average	Standard Deviation	Individual Results		
3-C131	36.00	N/A	2.55	0.21	4	2.4	2.7

Figure B. 4. Overview of Bridge Deterioration (Bridge 4).

Table B. 16. General Information and Summary of Visual Inspection (Bridge 4).

Location	SH 82 @ Alligator Bayou (Jefferson County)
Date of Visit	4/30/2010
Weather Condition	75°F, 81% RH
GPS	Latitude - 29.87770685; Longitude - 093.97911691
Bridge ID	NBI: N/A; CSJ: N/A
General Information	Built 1952
Summary of Visual Inspection	Severe deterioration was observed on the bridge. Visual observation confirms rebar corrosion. Big chunks of concrete on the main rebar direction were peeled off from concrete column (height: up to 4 feet from the water level). However, except surface deterioration and rebar corrosion, core concrete specimens remain in relative good condition.

Table B. 17. Specimen Collection Record (Bridge 4).

Specimen ID	Sampling Height (in.)	Specimen Type	Notes
4-C6	45	Core (1.5")	Span 1, column 6 (semi-deteriorated)
4-C6	85	Core (1.5")	Span 1, column 6 (semi-deteriorated)
4-C6	34	Core (1.5")	Span 1, column 6 (semi-deteriorated)
4-C3	4	Core (1.5")	Span 1, column 3 (deteriorated)
4-C3	8	Core (1.5")	Span 1, column 3 (deteriorated)
4-C3	28	Core (1.5")	Span 1, column 3 (semi-deteriorated)
4-C03	16	Core (1.5")	Span -1, column 3 (non-deteriorated)
4-C03	40	Core (1.5")	Span -1, column 3 (non-deteriorated)
4-Water1	NA	Water	
4-Water2	NA	Water	
4-Mud1	NA	Mud	Underwater (span 1)
4-Mud2	NA	Mud	Bank
4-C3C	6	Surface scraping	Span 1, column 5 (deteriorated)
4-C5C	15	Surface scraping	Span 1, column 5 (deteriorated)
4-C6C	18	Surface scraping	Span 1, column 6 (deteriorated)
4-C05C	46	Surface scraping	Span 1, column 5 (non-deteriorated)
4-C3B	6	Surface scraping	Span 1, column 3 (deteriorated)
4-C5B	48	Surface scraping	Span 1, column 5 (semi-deteriorated)
4-C5B	58	Surface scraping	Span 1, column 5 (non-deteriorated)
4-C5B	15	Surface scraping	Span 1, column 5 (deteriorated)
4-C6B	55	Surface scraping	Span 1, column 6 (semi-deteriorated)
4-C6B	15	Surface scraping	Span 1, column 6 (deteriorated)
4-C6B	65	Surface scraping	Span 1, column 6 (non-deteriorated)

Table B. 18. Rebound Hammer Test Record (Bridge 4).

Test Location	Test Height (in)	Estimate Strength (psi)	Rebound Number							
			Average	Standard Deviation	Individual Results					
4-C2	6	1375	24.50	5.74	24	32	24	18		
4-C2	12	1850	26.40	4.16	28	20	28	31	25	
4-C2	24	4667	37.67	9.83	32	24	48	42	32	48
4-C2	36	3813	34.25	7.60	19	37	30	38	32	
4-C2	48	5100	39.40	7.33	33	50	34	36	44	
4-C2	60	5800	42.20	5.22	36	50	40	44	41	
4-C4	6	750	22.00	3.54	24	27	20	18	21	
4-C4	12	1850	26.40	1.82	24	28	27	25	28	
4-C4	24	4042	35.17	4.58	38	30	36	29	40	38
4-C4	36	2550	29.20	2.59	31	26	30	32	27	
4-C4	48	3417	32.67	2.50	28	34	35	34	33	32
4-C4	60	6700	45.80	1.79	43	46	48	46	46	
4-C5	6	1650	25.60	5.41	32	30	22	25	19	
4-C5	12	1800	26.20	5.50	22	24	22	28	35	
4-C5	24	5150	39.60	7.57	27	44	45	44	38	
4-C5	36	3292	32.17	5.38	30	32	42	30	26	33
4-C5	48	3500	33.00	2.55	29	32	35	35	34	
4-C5	60	7550	49.20	3.70	45	46	51	54	50	
4-S0-C2	36	3750	34.00	4.60	28	38	36	34	29	39
4-S0-C2	48	4708	37.83	6.91	46	35	40	31	45	30
4-S0-C2	60	6125	43.50	4.14	48	45	39	39	42	48
4-S0-C4	36	5250	40.00	4.24	45	43	34	39	39	
4-S0-C4	48	2083	27.33	4.18	23	34	24	30	28	25
4-S0-C4	60	4600	37.40	4.56	40	32	33	40	42	
4-S0-C6	24	4650	37.60	7.92	28	44	42	30	44	
4-S0-C6	36	5708	41.83	5.60	43	34	44	36	46	48
4-S0-C6	48	3700	33.80	2.59	38	33	33	34	31	
4-S0-C6	60	4750	38.00	5.34	35	42	36	32	45	

Table B. 19. Ultrasonic Pulse Velocity (UPV) Test Record (Bridge 4).

Test Location	Test Height (in)	Calculated UPV (ft/s)				
		Average	Standard Deviation	Individual Results		
4-S0-C4	48	13130	24	13116	13158	13116
4-S0-C4	48	12691	36	12665	12716	
4-S0-C4	48	13338	228	13470	13470	13075
4-S0-C4	36	12922	54	12860	12953	12953
4-S0-C4	36	12922	8	12927	12913	12927
4-S0-C4	36	12913	81	13007	12860	12873
4-S0-C4	24	13513	0	13513	13513	13513
4-S0-C4	24	12817	167	12663	12994	12794
4-S0-C4	24	13251	8	13256	13242	13256
4-C2	48	13130	24	13116	13158	13116
4-C2	48	12691	36	12665	12716	
4-C2	48	13338	228	13470	13470	13075
4-C2	36	12922	54	12860	12953	12953
4-C2	36	12922	8	12927	12927	12913
4-C2	36	13271	345	13470	13470	12873
4-C2	24	13513	0	13513	13513	13513
4-C2	24	12818	166	12665	12994	12794
4-C2	24	13251	8	13256	13256	13242

Table B. 20. Halfcell Test Record (Bridge 4).

Test Location	Test Height (in)	Corrosion Potential (mV)									
		Average	Standard Deviation	Individual Results							
4-S0-C3	6	-252	20.46	-278	-275	-228	-237	-247	-244		
4-S0-C3	12	-185	15.19	-191	-213	-177	-178	-180	-171		
4-S0-C3	24	-128	16.08	-145	-141	-109	-133	-131	-107		
4-S0-C3	36	-17	10.46	-19	-29	-22	-15	-20	2		
4-S0-C3	48	35	21.29	16	12	27	41	46	69		
4-S0-C3-2	6	-275	N/A	-275							
4-S0-C3-2	12	-106	N/A	-106							
4-S0-C3-2	18	-92	N/A	-92							
4-S0-C3-2	30	-27	N/A	-27							
4-S0-C3-2	42	-141	N/A	-141							
4-S0-C3-2	54	-226	N/A	-226							
4-S0-C3-2	66	22	N/A	22							
4-C3	6	-385	16.56	-379	-401	-403	-376	-392	-360		
4-C3	12	-297	13.47	-270	-301	-303	-300	-306	-303		
4-C3	18	-261	34.24	-249	-289	-295	-288	-224	-220		
4-C3	30	-154	21.35	-160	-164	-122	-132	-168	-175		
4-C3	42	-128	40.33	-92	-100	-95	-123	-182	-173		
4-C3	54	11	14.51	16	14	22	23	6	-16		
4-C3	66	91	8.76	88	92	101	98	91	76		
4-C3-2	6	-158	101.85	-275	-106	-92					
4-C3-2	30	-115	N/A	-115							
4-C3-2	42	-141	N/A	-141							
4-C3-2	54	-226	N/A	-226							
4-C3-2	66	22	N/A	22							
4-C6	6	-393	50.09	-407	-428	-444	-446	-333	-338	-353	
4-C6	12	-301	16.07	-288	-308	-312	-291	-283	-324		
4-C6	24	-202	41.86	-144	-218	-257	-250	-181	-196	-169	
4-C6	36	-162	30.50	-138	-138	-227	-184	-144	-145	-163	-156
4-C6	48	-57	17.83	-84	-67	-51	-27	-71	-71	-60	-25

Figure B. 5. Overview of Bridge Deterioration (Bridge 5).

Table B. 21. General Information and Summary of Visual Inspection (Bridge 5).

Location	FM 276 @ Patroon Bayou (Sabine County)
Date of Visit	12/3/2010
Weather Condition	52°F, 76% RH
GPS	Latitude - 31.52276283; Longitude - 093.79931811
Bridge ID	NBI: N/A; CSJ: N/A
General Information	Built 1967
Summary of Visual Inspection	Highly scaled, aggregate pop out. Deterioration reaches approximately 7-8 feet about bottom of piers. No visual rebar exposure. Low water level – 3 feet lower than the bottom of column (foundation exposed)

Table B. 22. Specimen Collection Record (Bridge 5).

Specimen ID	Sampling Height (in.)	Specimen Type	Notes
5-C1B	74	Surface scraping	Non-deteriorated
5-C1B	64	Surface scraping	Semi-deteriorated
5-C1B	12	Surface scraping	Deteriorated
5-C2B	85	Surface scraping	Non-deteriorated
5-C2B	75	Surface scraping	Semi-deteriorated
5-C2B	10	Surface scraping	Deteriorated
5-C1-2	72	Surface scraping	Non-deteriorated
5-C1-2	12	Surface scraping	Deteriorated
5-C2-2	65	Surface scraping	Non-deteriorated
5-C2-2	24	Surface scraping	Deteriorated
5-Water1	NA	Water	West
5-Water2	NA	Water	East
5-Mud1	NA	Mud	West
5-Mud2	NA	Mud	East

Table B. 23. Rebound Hammer Test Record (Bridge 5).

Test Location	Test Height (in)	Estimate Strength (psi)	Rebound Number								
			Average	Standard Deviation	Individual Results						
5-C2	6	500	21.00	7.77	20	28	20	32	14	12	
5-C2	18	1821	26.29	10.23	16	44	16	26	28	20	34
5-C2	30	1679	25.71	11.40	24	18	12	16	38	42	30
5-C2	42	-286	17.86	5.61	16	10	26	14	22	22	15
5-C2	54	2750	30.00	9.45	32	30	42	42	22	24	18
5-C2	66	3464	32.86	10.51	50	16	32	26	36	38	32
5-C2	78	3393	32.57	4.86	28	30	34	30	40	38	28
5-C2	90	6071	43.29	6.40	38	42	36	46	40	46	55
5-C1	6	714	21.86	5.43	21	15	17	23	31	26	20
5-C1	18	1321	24.29	10.86	41	26	37	17	15	14	20
5-C1	30	964	22.86	6.28	16	24	33	29	22	18	18
5-C1	42	1107	23.43	8.08	36	22	19	14	33	22	18
5-C1	54	2929	30.71	7.18	34	40	38	28	28	28	19
5-C1	66	1750	26.00	6.14	27	16	26	26	29	36	22
5-C1	78	6536	45.14	5.40	44	48	42	56	42	44	40
5-C1	90	6536	45.14	4.41	52	44	38	44	43	48	47

Table B. 24. Covermeter Test Record (Bridge 5).

Test Location	Test Height (in.)	Rebar Size (in)	Covering Thickness (in)								
			Average	Standard Deviation	Individual Results						
5-C2	6	10	2.76	0.20	2.70	3.10	2.50	2.70	2.85	2.85	2.60
5-C2	18	10	2.27	0.19	2.55	2.15	2.10	2.05	2.35	2.45	2.25
5-C2	30	10	2.42	0.48	2.30	2.15	1.65	2.70	2.85	2.85	
5-C2	42	10	2.76	0.59	2.95	2.25	1.95	2.40	2.85	3.50	3.45
5-C2	54	10	2.69	0.65	3.05	2.10	1.70	2.35	2.85	3.25	3.50
5-C2	66	10	2.73	0.64	3.00	2.05	1.85	2.40	2.95	3.50	3.35
5-C2	78	10	2.63	0.48	3.15	2.40	2.00	2.40	2.60	3.25	
5-C2	90	10	2.69	0.41	3.10	2.45	2.25	2.45	2.60	3.30	
5-C1	6	10	2.07	0.42	1.70	2.20	2.75	2.45	2.00	1.70	1.70
5-C1	18	10	2.71	0.33	2.60	2.95	3.05	2.40	3.10	2.25	2.60
5-C1	30	10	2.99	0.26	2.90	3.20	3.10	2.50	3.10	3.15	
5-C1	42	10	2.89	0.53	3.40	3.40	2.75	2.25	2.20	2.85	3.40
5-C1	54	10	2.97	0.62	3.15	3.80	2.50	2.15	2.75	3.45	
5-C1	66	10	2.64	0.53	3.35	3.05	2.30	2.15	2.35		
5-C1	78	10	2.82	0.66	3.65	2.90	2.35	2.00	3.20		

Table B. 25. In Situ Phenolphthalein Test Record (Bridge 5).

Test Location	Test Height (in)	Depth of Low pH Covering (mm)
5-C2	6	NA
5-C2	18	NA
5-C2	48	2

Figure B. 6. Overview of Bridge Deterioration (Bridge 6).

Table B. 26. General Information and Summary of Visual Inspection (Bridge 6).

Location	SH 21 @ Carrice Creek (Sabine County)
Date of Visit	12/3/2010
Weather Condition	71°F, 59% RH
GPS	Latitude - 31.45585875; Longitude - 093.76156541
Bridge ID	NBI: N/A; CSJ: N/A
General Information	Built 1967. Small bridge, only four spans
Summary of Visual Inspection	Highly deteriorated with exposed corroded rebar (column 3). More corrosion was observed on south. Suspected construction defects (no enough mortar covering in original concrete). Pier foundation appeared to use low quality concrete.

Table B. 27. Specimen Collection Record (Bridge 6).

Specimen ID	Sampling Height (in.)	Specimen Type	Notes
6-C1B	108	Surface scraping	Non-deteriorated
6-C1B	96	Surface scraping	Semi-deteriorated
6-C1B	6	Surface scraping	Deteriorated
6-C3B	106	Surface scraping	Non-deteriorated
6-C3B	96	Surface scraping	Semi-deteriorated
6-C3B	6	Surface scraping	Deteriorated
6-C1-2C	108	Surface scraping	Non-deteriorated
6-C1-2C	96	Surface scraping	Semi-deteriorated
6-C3-2C	6	Surface scraping	Deteriorated
6-C3-2C	106	Surface scraping	Non-deteriorated
6-Backfill	NA	Concrete	Concrete from column 3 foundation
6-Water1	NA	Water	West
6-Water2	NA	Water	East
6-Mud1	NA	Mud	West
6-Mud2	NA	Mud	East

Table B. 28. Rebound Hammer Test Record (Bridge 6).

Test Location	Test Height (in)	Estimate Strength (psi)	Rebound Number								
			Average	Standard Deviation	Individual Results						
6-C1	18	NA	18.86	4.85	15	16	15	22	28	16	20
6-C1	30	NA	18.86	4.74	13	19	16	23	18	27	16
6-C1	42	3607	33.43	9.86	25	24	44	50	28	31	32
6-C1	54	500	21.00	7.26	16	14	20	21	15	27	34
6-C1	66	1250	24.00	7.23	25	20	35	18	26	14	30
6-C1	78	214	19.86	4.30	16	23	23	16	24	14	23
6-C1	90	2000	27.00	5.72	20	24	25	30	38	25	27
6-C1	102	5321	40.29	7.78	42	34	36	52	30	40	48
6-C1	114	7179	47.71	5.94	42	54	50	48	54	48	38
6-C2	6	1583	25.33	10.05	23	45	28	25			
6-C2	18	500	21.00	9.56	16	20	13	19	42	18	19
6-C2	30	821	22.29	5.65	17	29	15	23	26	28	18
6-C2	42	2143	27.57	5.50	28	21	20	27	32	35	30
6-C2	54	607	21.43	5.53	21	15	26	18	30	24	16
6-C2	66	2036	27.14	5.49	24	23	20	28	32	27	36
6-C2	78	929	22.71	5.09	26	23	17	26	21	30	16
6-C2	90	1929	26.71	6.55	24	14	34	28	29	26	32
6-C2	102	3536	33.14	7.73	46	30	32	26	42	28	28

Table B. 29. Halfcell Test Record (Bridge 6).

Test Location	Test Height (in)	Corrosion Potential (mV)								
		Average	Standard Deviation	Individual Results						
6-C3	6	-149	44.15	-130	-162	-190	-188	-128	-68	-180
6-C3	18	-95	35.49	-94	-71	-106	-139	-118	-39	
6-C3	30	-32	13.76	-14	-19	-39	-29	-51	-38	
6-C3	42	-20	21.27	-53	5	-20	0	-32	-22	
6-C3	54	21	54.12	-21	29	118	60	60	-23	
6-C3	66	13	43.83	-29	67	14	-32	63	-7	
6-C3	78	67	49.91	64	120	54	85	102	-22	
6-C3	90	58	42.80	102	22	78	-2	29		
6-C3	102	86	78.39	144	166	90	25	129	-38	

Table B. 30. Covermeter Test Record (Bridge 6).

Test Location	Test Height (in)	Rebar Size (in)	Covering Thickness (in)								
			Average	Standard Deviation	Individual Results						
6-C1	18	10	2.21	0.97	1.5	1.2	1.7	1.7	3.5	3.5	2.5
6-C1	30	10	2.10	0.90	1.1	1.2	1.7	2.8	2.1	3.6	2.3
6-C1	42	10	1.60	1.08	0.9	0.8	1	1.4	3.6	2.1	
6-C1	54	10	1.74	1.30	1.8	0.7	0	1.9	2.5	3.7	
6-C1	66	10	2.23	1.22	2	0.9	0.9	1.5	3.6	3.4	3.4
6-C1	78	10	2.07	0.94	2	1.2	1	1.4	2.9	2.5	3.5
6-C1	90	10	2.17	0.96	1.9	1.3	1.3	1.9	3	3.7	
6-C1	102	10	2.54	0.90	3.5	2.1	1.5	1.7	2.8	3.9	2.6
6-C3	6	10	1.50	N/A	1.5						
6-C3	18	10	1.77	0.98	1.7	1.3	1.2	1.1	1.6	3.7	
6-C3	30	10	2.21	1.25	1.4	0.9	0.9	2	3.1	3.7	3.6
6-C3	42	10	2.61	1.15	1.2	1	2.2	3.2	3.6	3.6	3.6
6-C3	54	10	1.96	1.36	1.7	1.1	0	1.2	3.7	2.6	3.6
6-C3	66	10	1.59	1.41	1.5	0	0	1	3.5	2	3.3
6-C3	78	10	2.01	1.65	1.2	0	0	2.2	3.3	3.8	3.7
6-C3	90	10	1.94	1.52	1.5	0	0	2.4	3.7	2.5	3.5
6-C3	102	10	2.16	1.28	1.3	1	3.7	2.8			

Table B. 31. In Situ Phenolphthalein Test Record (Bridge 6).

Test Location	Test Height (in)	Depth of Low pH Covering (mm)
6-C3	90	1 to 2
6-C3	32	1 to 2
6-C1	90	NA
6-C1	30	NA

Figure B. 7. Overview of Bridge Deterioration (Bridge 7).

Table B. 32. General Information and Summary of Visual Inspection (Bridge 7).

Location	FM 3121 @ Palo Gaucho Bayou (Sabine County)
Date of Visit	12/3/2010
Weather Condition	78°F, 54% RH
GPS	Latitude - 31.41320518; Longitude - 093.78129968
Bridge ID	NBI: N/A; CSJ: N/A
General Information	Built 1968
Summary of Visual Inspection	Deterioration was similar to Bridge 5. Heavily scaled, pop out aggregate Deterioration reaches all the way up to the top of columns (approximately 7 feet in total). No visual rebar or corrosion (original some suspected exposed rebar, turn out just water lines). Tested columns (span #1 – east side), column 1 (north) and column 3 (south)

Table B. 33. Specimen Collection Record (Bridge 7).

Specimen ID	Sampling Height (in.)	Specimen Type	Notes
7-C3	90	Surface scraping	Span #1 (east side, south end) (Non-deteriorated)
7-C3	6	Surface scraping	Span #1 (east side, south end) (Deteriorated)
7-C1	90	Surface scraping	Span #1 (east side, north end) (Non-deteriorated)
7-C1	6	Surface scraping	Span #1 (east side, north end) (Deteriorated)
7-Water	NA	Water	North
7-Water	NA	Water	South
7-Mud	NA	Mud	North
7-Mud	NA	Mud	South

Table 2. Rebound Hammer Test Record (Bridge 7).

Test Location	Test Height (in)	Estimate Strength (psi)	Rebound Number								
			Average	Standard Deviation	Individual Results						
7-C3	6	71	19.29	6.47	16	12	22	23	15	31	16
7-C3	18	536	21.14	2.91	24	22	21	21	18	17	25
7-C3	30	321	20.29	3.68	15	22	20	23	18	18	26
7-C3	42	786	22.14	4.41	24	16	26	25	22	26	16
7-C3	54	786	22.14	6.26	18	32	29	18	23	20	15
7-C3	66	1607	25.43	5.29	25	28	16	32	24	30	23
7-C3	78	2893	30.57	4.12	36	34	28	32	32	28	24
7-C3	90	2036	27.14	4.14	28	24	22	24	30	34	28
7-C1	6	607	21.43	6.29	16	16	28	22	14	24	30
7-C1	18	893	22.57	9.36	30	40	18	20	18	20	12
7-C1	30	NA	18.00	4.16	14	24	14	18	22	20	14
7-C1	42	536	21.14	2.79	24	24	16	20	22	22	20
7-C1	54	143	19.57	5.16	21	14	20	16	14	26	26
7-C1	66	964	22.86	2.48	24	26	21	21	26	22	20
7-C1	78	2000	27.00	4.76	24	31	20	31	24	33	26
7-C1	90	3893	34.57	6.16	33	46	38	34	33	26	32

Table B. 34. Covermeter Test Record (Bridge 7).

Test Location	Test Height (in.)	Rebar Size (in)	Covering Thickness (in)								
			Average	Standard Deviation	Individual Results						
7-C3	6	10	2.24	0.32	2.7	2.2	1.9	2.1	2.9		
7-C3	18	10	2.32	0.41	2.9	2.3	2.1	2	2.2	2.9	
7-C3	30	10	2.37	0.41	2.8	2.2	2.1	1.8	2.9	2.4	2.9
7-C3	42	10	2.40	0.43	2.6	2.4	2	2	2	2.5	2.9
7-C3	54	10	2.32	0.34	2.8	2.5	2.3	2.1	2.5	2.7	
7-C3	66	10	2.45	0.28	2.5	2.6	2.5	2.4	2.3	2.1	2.5
7-C3	78	10	2.40	0.17	2.4	2.6	2.5	2.7	2	2.5	2.4
7-C3	90	10	2.42	0.22	2.9	2.8	2.6	2.2	1.8	1.6	2.3
7-C1	6	10	2.28	0.48	2.8	2.6	2.3	2.2	2.1	2	2.3
7-C1	18	10	2.31	0.28	2.7	2.3	2	2.4	2.4	2.7	
7-C1	30	10	2.40	0.27	2.1	2.3	2.5	2.2	2.9	2.6	2.6
7-C1	42	10	2.41	0.27	2.6	2	2.1	2.5	2.5	2.7	2.7
7-C1	54	10	2.41	0.28	2.7	2.1	2.2	2.3	2.5	2.6	2.6
7-C1	66	10	2.41	0.21	2.2	2.2	2.7	2.7	2.6	2.7	2.6
7-C1	78	10	2.49	0.22	2.3	2.1	2.2	2.7	2.3	2.5	

Table B. 35. In Situ Phenolphthalein Test Record (Bridge 7).

Test Location	Test Height (in)	Depth of Low pH Covering (mm)
7-C3	6	NA
7-C3	80	7
7-C1	6	NA
7-C1	80	4

Figure B. 8. Overview of Bridge Deterioration (Bridge 8).

Table B. 36. General Information and Summary of Visual Inspection (Bridge 8).

Location	SH 31 WB @ Kickapoo Creek (Henderson County)
Date of Visit	4/14/2011
Weather Condition	80°F, 63% RH
GPS	Latitude - 32.30112370; Longitude - 095.50136160
Bridge ID	NBI: 10-108-0164-03-018; CSJ: N/A
General Information	Built 1930s (west bound), 2 spans
Summary of Visual Inspection	Moderate scaling (1/4"-1/2" penetration) along water line of most concrete piles. Severe scaling of column #4 and #5 at waterline – penetration up to 3". The bridge columns from water line to about 30" above scaling and pop out aggregate. From about 30" to about 42" above waterline, mild scaling was observed. Visual rebar corrosion on the column 4. Water level was up to 3 feet deep on span 1

Table B. 37. Specimen Collection Record (Bridge 8).

Specimen ID	Sampling Height (in.)	Specimen Type	Notes
8-C2	6	Surface scraping	span #1 west end, column 2 (north)
8-C2	18	Surface scraping	span #1 west end, column 2 (north)
8-C2	30	Surface scraping	span #1 west end, column 2 (north)
8-C2	54	Surface scraping	span #1 west end, column 2 (north)
8-C4	6	Surface scraping	span #1 west end, column 4 (south)
8-C4	18	Surface scraping	span #1 west end, column 4 (south)
8-C4	30	Surface scraping	span #1 west end, column 4 (south)
8-C4	54	Surface scraping	span #1 west end, column 4 (south)
8-Water1	NA	Water	South
8-Water2	NA	Water	North
8-Water3	NA	Water	Middle
8-Mud	NA	Mud	South
8-Mud	NA	Mud	North

Table B. 38. Rebound Hammer Test Record (Bridge 8).

Test Location	Test Height (in)	Estimate Strength (psi)	Rebound Number							
			Average	Standard Deviation	Individual Results					
8-C2	6	4583	37.33	17.42	20	28	34	60	58	24
8-C2	18	2625	29.50	11.11	27	13	22	36	35	44
8-C2	30	2000	27.00	15.45	28	57	25	19	15	18
8-C2	42	5042	39.17	1.83	41	41	37	39	40	37
8-C2	54	7292	48.17	4.26	45	46	46	55	52	45
8-C2	66	7708	49.83	3.97	45	47	48	55	50	54
8-C4	6	-833	15.67	7.81	10	10	19	30	11	14
8-C4	18	-2042	10.83	3.66	9	11	9	18	8	10
8-C4	30	4167	35.67	6.56	43	32	31	39	27	42
8-C4	42	7167	47.67	3.88	42	50	52	50	48	44
8-C4	54	8550	53.20	2.86	50	53	51	57	55	

Table B. 39. Halfcell Test Record (Bridge 8).

Test Location	Test Height (in)	Corrosion Potential (mV)							
		Average	Standard Deviation	Individual Results					
8-C4	6	-23	8.39	-11	-31	-23	-31	-27	-15
8-C4	18	16	37.45	-18	-16	-8	19	39	77
8-C4	30	24	16.67	23	33	-13	15	19	31
8-C4	42	42	27.13	22	38	4	46	61	80

Table B. 40. Covermeter Test Record (Bridge 8).

Test Location	Test Height (in.)	Rebar Size (in)	Covering Thickness (in)								
			Average	Standard Deviation	Individual Results						
8-C2	6	11	2.46	0.57	3.5	2.9	2.3	2.3	2.4	1.9	2
8-C2	18	11	2.41	0.54	3.3	3	2.6	2.1	1.9	1.9	2.3
8-C2	30	11	2.30	0.50	3.1	2.9	2.3	2.1	1.9	1.7	2.3
8-C2	42	11	2.08	0.52	2.9	2.7	2.2	2	1.7	1.5	1.8
8-C2	54	11	1.61	0.66	2.4	2.3	1.9	2	1	1	0.9
8-C2	66	11	1.50	0.44	1.4	1.3	2.2	0.8	1.7	1.4	1.8
8-C4	6	11	2.36	0.22	2.6	2.3	2.5	2.7	2.2	2.2	2.1
8-C4	18	11	2.49	0.27	2.7	2.6	2.6	2.4	2.6	2.7	1.9
8-C4	30	11	2.38	0.60	3	2.6	2.8	2.7	2.3	2.3	1.1
8-C4	42	11	2.07	0.54	1.6	2.5	2.8	2.5	1.8	2.1	1.3

Table B. 41. In Situ Phenolphthalein Test (Bridge 8).

Test Location	Test Height (in)	Depth of Low pH Covering (mm)
8-C4	24	2 to 3
8-C2	12	2 to 3

Figure B. 9. Overview of Bridge Deterioration (Bridge 9).

Table B. 42. General Information and Summary of Visual Inspection (Bridge 9).

Location	SH 31 EB @ Kickapoo Creek (Henderson County)
Date of Visit	4/14/2011
Weather Condition	75°F, 81% RH
GPS	Latitude - 32.30112370; Longitude - 095.50136160
Bridge ID	NBI: 10-108-0164-03-018; CSJ: N/A
General Information	Built 1970s (east bound) , 7 spans
Summary of Visual Inspection	Moderate scaling (1/4"-1/2" penetration) along water line of most concrete piles. The bridge columns from water line to about 18" above scaling and pop out aggregate. From about 18" to about 42" above waterline, mild scaling was observed. No visual rebar corrosion observed. Water level was up to 1 foot deep on span 1.

Table B. 43. Specimen Collection Record (Bridge 9).

Specimen ID	Sampling Height (in.)	Specimen Type	Notes
9-C3	6	Surface scraping	span #2 from east, column 3 (from north)
9-C3	18	Surface scraping	span #2 from east, column 3 (from north)
9-C3	30	Surface scraping	span #2 from east, column 3 (from north)
9-C3	54	Surface scraping	span #2 from east, column 3 (from north)
9-C4	6	Surface scraping	span #2 from east, column 4 (from north)
9-C4	18	Surface scraping	span #2 from east, column 4 (from north)
9-C4	30	Surface scraping	span #2 from east, column 4 (from north)
9-C4	54	Surface scraping	span #2 from east, column 4 (from north)
9-Water1	NA	Water	North
9-Water2	NA	Water	South
9-Water3	NA	Water	Middle
9-Mud1	NA	Mud	North
9-Mud2	NA	Mud	South

Table B. 44. Rebound Hammer Test Record (Bridge 9).

Test Location	Test Height (in)	Estimate Strength (psi)	Rebound Number							
			Average	Standard Deviation	Individual Results					
9-C3	6	83	19.33	7.66	10	20	28	28	12	18
9-C3	18	2167	27.67	8.85	27	44	23	29	18	25
9-C3	30	6167	43.67	9.24	50	52	50	44	28	38
9-C3	42	7875	50.50	6.60	58	55	51	54	43	42
9-C3	54	7917	50.67	8.33	55	58	59	50	44	38
9-C3	66	7458	48.83	7.86	54	56	57	40	46	40
9-C4	6	125	19.50	5.36	25	17	15	19	14	27
9-C4	18	4833	38.33	7.45	35	42	42	40	46	25
9-C4	30	7542	49.17	2.99	46	45	52	52	50	50
9-C4	42	9208	55.83	2.56	56	56	52	55	60	56
9-C4	54	9375	56.50	2.66	57	58	60	56	52	56
9-C4	66	9875	58.50	2.43	60	60	56	55	61	59

Table B. 45. Halfcell Test Record (Bridge 9).

Test Location	Test Height (in)	Corrosion Potential (mV)							
		Average	Standard Deviation	Individual Results					
9-C4	6	-55	15.60	-55	-39	-49	-41	-76	-72
9-C4	18	-34	36.99	-17	-22	-11	5	-88	-72
9-C4	30	15	38.06	43	37	-50	-13	32	41
9-C4	42	85	33.38	61	61	128	127	67	63
9-C4	54	87	49.81	8	125	90	89	44	1

Table B. 46. Covermeter Test Record (Bridge 9).

Test Location	Test Height (in.)	Rebar Size (in)	Covering Thickness (in)					
			Average	Standard Deviation	Individual results			
9-C3	6	11	2.63	0.12	2.6	2.8	2.6	2.6
9-C3	18	11	2.56	0.11	2.4	2.6	2.7	2.6
9-C3	30	11	2.48	0.18	2.3	2.5	2.7	2.5
9-C3	42	11	2.61	0.11	2.5	2.7	2.7	2.7
9-C3	54	11	2.54	0.15	2.4	2.8	2.6	2.5
9-C3	66	11	2.64	0.15	2.5	2.7	2.9	2.6
9-C4	6	11	2.69	0.17	2.9	2.7	2.7	2.5
9-C4	18	11	2.63	0.15	2.6	2.8	2.8	2.5
9-C4	30	11	2.69	0.14	2.6	2.9	2.8	2.6
9-C4	42	11	2.50	0.19	2.6	2.4	2.8	2.4
9-C4	54	11	2.46	0.11	2.6	2.5	2.5	2.3
9-C4	66	11	2.41	0.17	2.6	2.2	2.6	2.4

Table B. 47. In Situ Phenolphthalein Test Record (Bridge 9).

Test Location	Test Height (in)	Average Depth of Low pH Covering (mm)
9-C4	6	<4
9-C4	18	2 to 3

Figure B. 10. Overview of Bridge Deterioration (Bridge 10).

Table B. 48. General Information and Summary of Visual Inspection (Bridge 10).

Location	FM 787 @ Tarkington Bayou (Liberty County)
Date of Visit	7/20/2011
Weather Condition	89°F, 54% RH
GPS	Latitude: - 30.35529000; Longitude - 95.05120000
Bridge ID	NBI: N/A; CSJ: N/A
General Information	Built 1930. Also known as Little Tarkington Bayou Relief Bridge
Summary of Visual Inspection	The columns are in good condition. No aggregate pops out. Surfaces above the ground for about 6", where is used to be covered by water, have deterioration, and still the paste covers the aggregate well.

Table B. 49. Specimen Collection Record (Bridge 10).

Specimen ID	Sampling Height (in.)	Specimen Type	Notes
10-C2	6	Surface scraping	Deteriorated
10-C2	42	Surface scraping	Semi-deteriorated
10-C2	78	Surface scraping	Non-deteriorated
10-C3	6	Surface scraping	Deteriorated
10-C3	42	Surface scraping	Semi-deteriorated
10-C3	78	Surface scraping	Non-deteriorated
10-Water1	NA	Water	South
10-Water2	NA	Water	North
10-Water3	NA	Water	Middle
10-Mud1	NA	Mud	South
10-Mud2	NA	Mud	North

Table B. 50. Rebound Hammer Test Record (Bridge 10).

Test Location	Test Height (in)	Estimate Strength (psi)	Rebound Number							
			Average	Standard Deviation	Individual Results					
10-C2	6	2792	30.17	3.76	25	30	34	29	28	35
10-C2	18	4042	35.17	4.62	35	42	28	36	37	33
10-C2	30	4375	36.50	4.55	35	31	35	34	43	41
10-C2	42	5667	41.67	3.67	44	44	45	41	35	41
10-C2	54	5708	41.83	5.71	49	48	38	37	36	43
10-C2	66	7625	49.50	7.34	50	56	55	42	39	55
10-C2	78	7833	50.33	3.98	55	45	49	48	50	55
10-C3	6	2417	28.67	2.80	25	28	26	30	31	32
10-C3	18	4750	38.00	2.10	40	40	35	36	38	39
10-C3	30	5458	40.83	3.66	38	38	39	46	39	45
10-C3	42	6208	43.83	1.94	42	43	42	47	45	44
10-C3	54	6667	45.67	2.73	42	48	44	49	44	47
10-C3	66	8000	51.00	2.00	53	49	54	50	50	50
10-C3	78	8583	53.33	3.50	48	54	58	56	52	52

Table B. 51. Ultrasonic Pulse Velocity (UPV) Test Record (Bridge 10).

Test Location	Test Height (in)	Calculated UPV (ft/s)				
		Average	Standard Deviation	Individual Results		
10-C2	6	12889	995	14302	14286	13998
10-C2	42	12238	732	12195	12340	12077
10-C2	78	12294	737	12575	12066	12160
10-C3	6	12159	811	12031	10927	13767
10-C3	42	12118	477	12165	12425	12531
10-C3	78	11862	580	12352	12013	11221

Table B. 52. Covermeter Test Record (Bridge 10).

Test Location	Test Height (in.)	Rebar Size (in)	Covering Thickness (in)							
			Average	Standard Deviation	Individual Results					
10-C2	6.00	11	2.72	0.21	2.7	3.1	2.6	2.5	2.7	2.8
10-C2	18.00	11	2.67	0.11	2.8	2.7	2.6	2.6	2.6	2.9
10-C2	30.00	11	2.13	0.82	2.8	0.8	1.4	2.6	2.6	2.6
10-C2	42.00	11	2.88	0.33	3	2.9	3.5	2.8	2.7	2.6
10-C2	54.00	11	2.60	0.03	2.6	2.6	2.6	2.6	2.6	2.7
10-C2	66.00	11	2.60	0.14	2.5	2.4	2.8	2.7	2.6	2.6
10-C2	78.00	11	2.72	0.14	2.6	2.6	2.9	2.9	2.7	2.8
10-C3	6.00	11	2.64	0.16	2.5	2.5	2.9	2.7	2.8	2.5
10-C3	18.00	11	2.73	0.08	2.8	2.8	2.6	2.8	2.8	2.7
10-C3	30.00	11	2.54	0.15	2.5	2.5	2.7	2.5	2.4	2.8
10-C3	42.00	11	2.68	0.11	2.8	2.8	2.8	2.6	2.6	2.7
10-C3	54.00	11	2.63	0.08	2.8	2.7	2.6	2.6	2.6	2.6
10-C3	66.00	11	2.56	0.04	2.6	2.6	2.6	2.6	2.5	2.5
10-C3	78.00	11	2.56	0.06	2.6	2.5	2.5	2.5	2.6	2.7

Table B. 53. In situ Phenolphthalein Test Record (Bridge 10).

Test Location	Test Height (in)	Average Depth of Low pH Covering (mm)
10-C4	24	2 to 3
10-C2	12	2 to 3

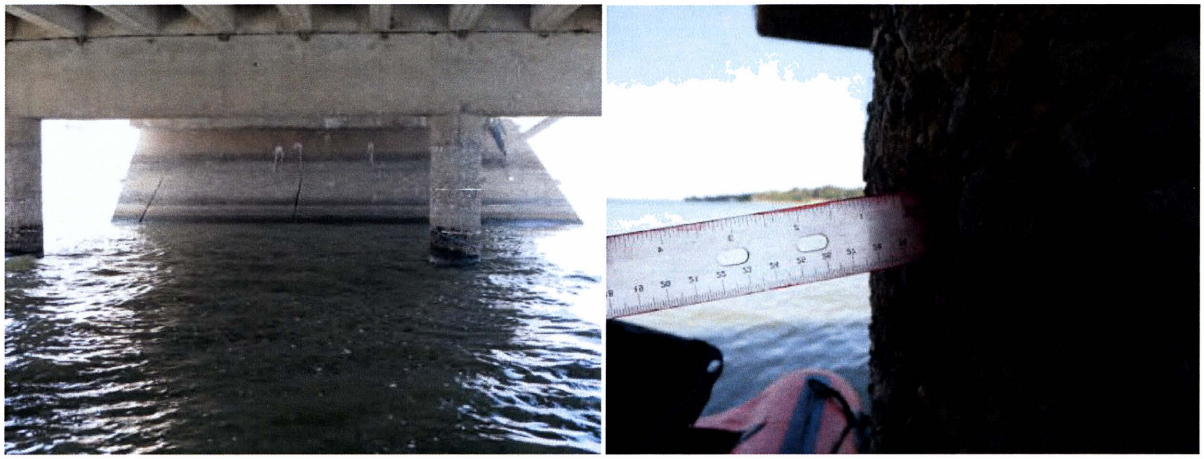

Figure B. 11. Overview of Bridge Deterioration (Bridge 11).

Table B. 54. General Information and Summary of Visual Inspection (Bridge 11).

Location	FM 751 @ Duck Creek (Hunt County)
Date of Visit	7/21/2011
Weather Condition	75°F, 81% RH
GPS	Latitude - 32.85147471; Longitude - 096.05812551
Bridge ID	NBI: 01-117-1017-04-009; CSJ: N/A
General Information	1959 South Side 429
Summary of Visual Inspection	The columns are in good condition. Surface aggregate can be seen without protection of cement paste. Organic product grows on the surface of the columns. There is no re-bar observed on the surface.

Table B. 55. Specimen Collection Record (Bridge 11).

Specimen ID	Sampling Height (in.)	Specimen Type	Notes
11-C1	6	Surface scraping	Deteriorated
11-C1	30	Surface scraping	Semi-deteriorated
11-C1	54	Surface scraping	Non-deteriorated
11-Water1	NA	Water	North
11-Water2	NA	Water	South
11-Water3	NA	Water	
11-Mud1	NA	Mud	
11-Mud2	NA	Mud	

Table B. 56. Rebound Hammer Test Record (Bridge 11).

Test Location	Test Height (in)	Estimate Strength (psi)	Rebound number							
			Average	Standard Deviation	Individual Results					
11-C1	6	2500	29.00	8.46	32	30	34	18	20	40
11-C1	18	2750	30.00	6.42	18	29	33	36	30	34
11-C1	30	4750	38.00	2.61	40	39	40	38	33	38
11-C1	42	2375	28.50	4.89	34	32	22	27	32	24
11-C1	54	3417	32.67	4.37	37	30	32	30	28	39
11-C2	6	2542	29.17	5.71	26	35	30	20	35	29
11-C2	18	4000	35.00	6.16	42	26	30	40	38	34
11-C2	30	4375	36.50	5.75	32	40	37	33	46	31
11-C2	42	2125	27.50	5.36	28	25	30	20	36	26
11-C2	54	3333	32.33	2.73	30	34	34	29	31	36

Table B. 57. Covermeter Test Record (Bridge 11).

Test Location	Test Height (in.)	Rebar Size (in)	Covering Thickness (in)					
			Average	Standard Deviation	Individual Results			
11-C1	6	11	2.83	0.44	3.1	3.3	2.5	2.4
11-C1	18	11	2.75	0.44	2.3	3	3.3	2.6
11-C1	30	11	2.84	0.22	3.1	3	2.6	2.7
11-C1	42	11	2.98	0.34	2.8	2.7	3	3.5
11-C1	54	11	2.64	0.34	3	2.9	2.2	2.6
11-C2	6	11	3.10	0.33	2.7	3.4	3.1	3.4
11-C2	18	11	3.19	0.67	3.5	3.4	2.2	3.7
11-C2	30	11	2.65	0.48	3.3	2.2	2.7	2.4
11-C2	42	11	2.89	0.61	3.4	2.1	3.3	2.9
11-C2	54	11	2.78	0.55	3.2	2	3.2	2.8

Table B. 58. In Situ Phenolphthalein Test Record (Bridge 11).

Test Location	Test Height (in)	Average Depth of Low pH Covering (mm)
11-C4	6	<4
11-C4	18	2 to 3

Figure B. 12. Overview of Bridge Deterioration (Bridge 12).

Table B. 59. General Information and Summary of Visual Inspection (Bridge 12).

Location	FM 751 @ S. Fork Sabine River (Hunt County)
Date of Visit	7/21/2011
Weather Condition	90°F, 63% RH
GPS	Latitude - 32.86086642; Longitude - 096.06713390
Bridge ID	NBI: 01-117-1017-04-008; CSJ: N/A
General Information	Built 1959
Summary of Visual Inspection	The columns are in good condition. Surface aggregate can be seen without protection of cement paste. Organic product grows on the surface of the columns. There is no re-bar observed on the surface.

Table B. 60. Specimen Collection Record (Bridge 12).

Specimen ID	Sampling Height (in.)	Specimen Type	Notes
12-C1	6	Surface scraping	Deteriorated
12-C1	30	Surface scraping	Semi-deteriorated
12-C1	54	Surface scraping	Non-deteriorated
12-Water1	NA	Water	East
12-Water2	NA	Water	West
12-Mud1	NA	Mud	East
12-Mud2	NA	Mud	West

Table B. 61. Rebound Hammer Test Record (Bridge 12).

Test Location	Test Height (in)	Estimate Strength (psi)	Rebound Number							
			Average	Standard Deviation	Individual Results					
12-C1	6	2917	30.67	9.63	26	45	35	22	36	20
12-C1	18	5167	39.67	10.84	38	34	40	56	46	24
12-C1	30	2958	30.83	3.71	28	30	28	35	36	28
12-C1	42	3375	32.50	3.21	29	32	30	32	34	38
12-C1	54	6208	43.83	8.50	42	41	57	45	47	31
12-C1	66	5458	40.83	2.32	40	44	41	39	43	38
12-C2	6	3250	32.00	7.59	34	36	24	34	22	42
12-C2	18	1958	26.83	4.67	24	22	31	24	26	34
12-C2	30	2875	30.50	6.38	31	24	26	36	26	40
12-C2	42	1917	26.67	3.33	29	24	32	24	27	24
12-C2	54	4250	36.00	5.90	38	32	32	41	44	29
12-C2	66	5125	39.50	3.51	34	45	39	40	39	40

Table B. 62. Covermeter Test Record (Bridge 12).

Test Location	Test Height (in.)	Rebar Size (in)	Covering Thickness (in)							
			Average	Standard Deviation	Individual Results					
12-C1	6	11	3.07	0.87	3.3	3.6	3.6	3.8	1.4	2.9
12-C1	18	11	2.37	0.82	1.7	2.9	3.3	1.5	3.2	1.7
12-C1	30	11	2.20	1.13	1.8	2.9	3.5	3.3	1	0.9
12-C1	42	11	2.48	1.05	1.8	3.2	3.3	3.8	1.8	1.2
12-C1	54	11	2.46	0.45	2.4	2.1	3.2	2.5	2.8	2
12-C1	66	11	2.73	0.54	2.8	2.8	3	3.4	2.8	1.8
12-C2	6	11	2.28	0.37	2.5	2.7	2.1	1.9		
12-C2	18	11	2.60	0.79	3.2	3.7	2.1	1.8	2.3	
12-C2	30	11	2.08	0.87	1.5	1.3	2.4	3.2		
12-C2	42	11	3.19	0.46	3.6	3.2	3.4	2.6		
12-C2	54	11	3.13	0.82	3.3	3.5	3.9	2		
12-C2	66	11	3.34	0.34	3.2	3	3.8	3.4		

Table B. 63. In Situ Phenolphthalein Test Record (Bridge 12).

Test Location	Test Height (in)	Average Depth of Low pH Covering (mm)
12-C2	30	<1
12-C3	30	<1

Figure B. 13. Overview of Bridge Deterioration (Bridge 1R).

Table B. 64. General Information and Summary of Visual Inspection (Bridge 1R).

Location	FM 787 @ Tarkington Bayou (Liberty County)
Date of Visit	4/15/2011
Weather Condition	75°F, 81% RH
GPS	Latitude - 30.35467624; Longitude - 095.05299129
Bridge ID	NBI: 20-146-0813-01-009; CSJ: 0813-01-036
General Information	Originally Built in 1930, Widened in 1973
Summary of Visual Inspection	No noticeable change comparing to visit 1 (on 11/5/2009)

Table B. 65. Specimen Collection Record (Bridge 1R).

Specimen ID	Sampling Height (in.)	Specimen Type	Notes
1R-W1	6	Surface scrapping	Deteriorated
1R-W1	18	Surface scrapping	Semi-deteriorated
1R-W1	42	Surface scrapping	Non-deteriorated
1R-C1	6	Surface scrapping	Deteriorated
1R-C1	18	Surface scrapping	Semi-deteriorated
1R-C1	42	Surface scrapping	Non-deteriorated
1R-Water1	NA	Water	
1R-Water2	NA	Water	
1R-Water3	NA	Water	Upstream
1R-Mud	NA	Mud	

Table B. 66. Rebound Hammer Test Record (Bridge 1R).

Test Location	Test Height (in)	Estimate Strength (psi)	Rebound Number								
			Average	Standard Deviation	Individual Results						
1R-Wall1	6	2000	27.00	5.22	28	32	33	26	19	24	
1R-Wall1	18	4250	36.00	6.77	34	20	38	36	38	34	
1R-Wall1	30	3750	34.00	5.55	28	27	34	38	36	41	
1R-Wall1	42	4429	36.71	3.59	36	36	34	36	42	41	32
1R-Wall1	54	4643	37.57	4.04	32	42	36	37	43	39	34
1R-C1	6	1500	25.00	5.18	18	25	26	33	27	21	
1R-C1	18	3167	31.67	3.56	27	29	35	36	30	33	
1R-C1	30	2417	28.67	3.93	27	24	34	31	25	31	
1R-C1	42	5250	40.00	4.24	38	36	48	41	38	39	
1R-C1	54	3708	33.83	2.71	34	32	34	39	32	32	
1R-C1	66	4583	37.33	2.34	35	35	36	38	40	40	
1R-C1	78	5550	41.20	5.76	28	42	40	42	44	38	

Table B. 67. Ultrasonic Pulse Velocity (UPV) Test Record (Bridge 1R).

Test Location	Test Height (in)	Calculated UPV (ft/s)				
		Average	Standard Deviation	Individual Results		
1R-Wall	6	12471	1479	13351	10764	13298
1R-Wall	42	12984	694	13587	12225	13141
1R-Wall	78	11862	580	12352	12013	11221
1R-C1	6	14595	171	14668	14717	14399
1R-C1	42	14461	16	14446	14461	14477
1R-C1	78	13632	413	14109	13400	13387

Table B. 68. Halfcell Test Record (Bridge 1R).

Test Location	Test Height (in)	Corrosion Potential (mV)					
		Average	Standard Deviation	Individual Results			
1R-Wall1	6	44	28.99	23	64		
1R-Wall1	18	137	2.12	138	135		
1R-Wall1	30	111	42.58	173	94	102	76
1R-Wall1	42	197	4.76	194	192	202	200
1R-Wall1	54	129	39.51	78	123	172	143
1R-Wall1	66	164	20.34	153	181	180	140

Table B. 69. Covermeter Test Record (Bridge 1R).

Test Location	Test Height (in.)	Rebar Size (in)	Covering Thickness (in)						
			Average	Standard Deviation	Individual Results				
1R-Wall1	6	11	2.08	0.49	2.1	2.8	1.6	1.9	
1R-Wall1	18	11	2.61	0.57	2.3	2.7	3.4	2.2	
1R-Wall1	30	11	2.38	0.29	2.3	2.3	2.2	2.8	
1R-Wall1	42	11	1.91	0.25	1.7	2.3	1.8	2	
1R-Wall1	54	11	2.03	0.58	2	2.2	1.3	2.7	
1R-Wall1	66	11	1.74	0.60	1.9	2	0.9	2.2	
1R-C1	6	11	2.82	0.39	3.1	3.2	2.9	2.2	2.9
1R-C1	18	11	2.71	0.08	2.8	2.8	2.7	2.7	
1R-C1	30	11	2.65	0.12	2.7	2.8	2.6	2.6	
1R-C1	42	11	2.60	0.18	2.8	2.7	2.5	2.4	
1R-C1	54	11	2.84	0.13	2.9	3	2.9	2.7	
1R-C1	66	11	2.70	0.26	2.9	3	2.5	2.5	

Table B. 70. In Situ Phenolphthalein Test Record (Bridge 1R).

Test Location	Test Height (in)	Average Depth of Low pH (mm)
1R-C1	12	2 to 3

APPENDIX C:

DETAILED MICROBIAL ANALYSIS PROCEDURES AND RESULTS

MICROBIAL ANALYSIS PROCEDURES

Sample Fixation

Subsamples from concrete (1 gram dry wt.) and from sediments (2 grams wet wt.) as well as pellets from water samples (40 ml centrifuged at 4,000 x g for 15 minutes) were fixed with 1 ml of 4% paraformaldehyde (PFA) in phosphate buffered saline (PBS, composed of 0.13 M NaCl, 7 mM Na_2HPO_4 and 3 mM NaH_2PO_4, pH 7.2 in water) (Hahn et al. 1992) at 4°C for 2 days, centrifuged at 14,000 x g for 2 minutes, and the pellets dispersed in PBS. After centrifugation at 14,000 x g for 2 minutes, the pellets were finally dispersed in 50% ethanol in PBS to a final volume of 1.5 ml and stored at -20°C until further use (Amann et al. 1990). Cells are preserved, remain intact and can be stored under these conditions for virtually unlimited time.

In Situ Hybridization

For in *situ* hybridization, 20 µl of the stored samples in 50% ethanol were dispersed in 980 µl of 0.1% sodium pyrophosphate in distilled water by mild sonication, and 10 µl (adjusted depending on the cell density) from each fixed and dispersed sample spotted onto gelatin-coated slides [0.1% gelatin, 0.01% $KCr(SO_4)_2$] and dried at 42°C for 20 minutes. Following dehydration in 50, 80 and 96% ethanol for 3 minutes each, the samples were treated with 10 µl of 0.1% lysozyme solution (Fluka, Buchs, Switzerland; 1 mg corresponding to 37,320U dissolved in 1 ml of distilled water) for 30 minutes to enhance the permeability of the cells. After an additional dehydration in 50, 80 and 96% ethanol for 3 minutes each, the preparations were pre-hybridized in 9 µl of hybridization buffer (0.9 M NaCl, 20 mM Tris/HCl, 5 mM EDTA, 0.01% SDS, pH 7.2) in the presence of 10 to 35% formamide depending on the probe and 0.05% blocking reagent (Roche) in 0.1 M maleic acid, pH 7.5, 0.15 M NaCl for 30 minutes (Hahn et al. 1997). After the addition of 1 µl of Cy3-labeled oligonucleotide probes (25 ng μl^{-1}), which included DAPI at a final concentration of 2 ng μl^{-1}), samples were hybridized at 42°C for 2 hours. The slides were subsequently washed in buffer containing 20 mM Tris/HCl, pH 7.2, 10 mM EDTA, 0.01% SDS and either 440, 308, 102 or 80 mM NaCl depending on the formamide concentration during hybridization (10, 20, 30 and 35%, respectively) for 15 min at 48°C, subsequently rinsed with distilled water, and air-dried (Zarda et al. 1997).

Table C. 1.Oligonucleotide Probes for Basic Community Structure Analyses.

Probe	Target	Sequence (5'-3') Formamide (%)	Reference
Eub338	Bacteria 16S rRNA, pos. 338-355	GCTGCCTCCCGTAGGAGT 30	(Daims et al. 1999)
Euk516	Eukarya 18S rRNA, pos. 502-516	ACCAGACTTGCCCTCC 20	(Amann et al. 1990)
Arch915	Archaea 16S rRNA, pos. 915-934	GTGCTCCCCCGCCAATTCCT 20	(Stahl and Amann 1991)
ALF1b	α-subdivision of Proteobacteria 16S rRNA, pos. 19-35	CGTTCGYTCTGAGCCAG 10	(Manz et al. 1992)
BET42a	β-subdivision of Proteobacteria 23S rRNA, pos. 1027-1043	GCCTTCCCACTTCGTTT 30	(Manz et al. 1992)
GAM42a	γ-subdivision of Proteobacteria 23S rRNA, pos. 1027-1043	GCCTTCCCACATCGTTT 30	(Manz et al. 1992)
SRBDb	δ-subdivision of Proteobacteria 16S rRNA, pos. 385-402	CGGCGTTGCTGCGTCAGG 35	(Rabus et al. 1996)
SRB385	δ-subdivision of Proteobacteria 16S rRNA, pos. 385-402	CGGCGTCGCTGCGTCAGG 35	(Amann et al. 1990)
HGC69a	Gram-positive bacteria with high DNA G+C content 23S rRNA, pos. 1901-1918	TATAGTTACCACCGCCGT 20	(Roller et al. 1994)
LGCa,b,c	Gram-positive bacteria with low DNA G+C content 16S rRNA, pos. 354 - 371	YSGAAGATTCCCTACTGC 35	(Meier et al. 1999)
CF319a	*Cytophaga-Flavobacterium* cluster of the CFB phylum 16S rRNA, pos. 319-336	TGGTCCGTGTCTCAGTAC 35	(Manz et al. 1996)
Pla5a	Planctomycetes 16S rRNA, pos. 45-62	GACTTGCATGCCTAATCC 30	(Neef et al. 1998)

Table C. 2. Oligonucleotide Probes used in Analyses on Concrete Deterioration.

Probe	Target	Sequence (5'-3') Formamide (%)	Reference
Ntspa712	Nitrospirae	CGCCTTCGCCACCGGCCTTCC 50	(Neef et al. 1998)
LF655	*Leptospirillum* groups I, II and III	CGCTTCCCTCTCCCAGCCT 35	(Bond and Banfield 2001)
ACD840	*Acidiphilium* species	CGACACTGAAGTGCTAAGC 10	(Bond and Banfield 2001)
G123T	Different *Thiothrix* species	CCTTCCGATCTCTATGCA 40	(Kangagawa et al. 2000)
21N	Eikelboom type 021N strain II-26	TCCCTCTCCCAAATTCTA 35	(Wagner et al. 1994)
Thio820	*Acidithiobacillus thiooxidans*, *A. ferrooxidans*	ACCAAACATCTAGTATTCATCG 30	(Peccia et al. 2000)
S-S-T.int-0442-a-A-18	*Thiomonas intermedia*	TCGATATTTCGCCCCCGC 10	(Okane et al. 2007)
S-S-T.plum-450-a-A-18	*Thiobacillus plumbophilus*	ATTAGCCTCAACTGTTTC 20	(Okane et al. 2007)
S-S-H.neap-635-a-A-19	*Halothiobacillus neapolitanus*	TAGAATCCCAGTATCCAAT 35	(Okane et al. 2007)

Epifluorescence microscopy

Slides were mounted with Citifluor AF1 solution (Citifluor Ltd., London, UK) and examined with a Nikon Eclipse 80*i* microscope, fitted for epifluorescence microscopy with a mercury lamp (X-Cite^{TM} 120; Nikon) and filter cubes UV-2E/C (Nikon; EX340-380, DM400, BA4435-485, for DAPI detection) and CY3 HYQ (Nikon; EX535/50, DM565, BA610/75, for Cy3 detection), respectively. Bacteria were counted at 1000 x magnification. Forty fields, selected at random, covering an area of 0.01 mm^2 each were examined from a sample distributed over eight circular areas of 53 mm^2 each. DAPI and Cy3 counts were obtained from the same image (Zarda et al. 1997). Pictures were taken from these images using a cooled CCD camera (CoolSNAP *ES*^{2}; Photometrics, Tucson AZ), and Nikon's NIS Elements imaging software (Version 3).

Statistical analyses

Log-transformed data of bacterial counts were assessed by a one-way-analysis of variance and afterwards by multiple pairwise comparisons with Tukeys HSD test (SYSTAT). The significance level was set at $\alpha = 0.05$.

Methodological considerations and adaptations

Two experimental challenges were encountered initially that impacted accurate detection and enumeration of microbial cells in almost all samples. The first challenge was a strong background signal which was found in all samples but one and was caused by non-specific binding of the fluorescent probes. As a result, many non-specific signals comparable in size and intensity to those found on bacteria were obtained. This non-specific binding was quenching signals on bacteria making them hardly visible, and at the same time resulted in a potentially large overestimation of target organisms if considered real signals. Control staining using DAPI (a DNA-intercalating dye that should detect all organisms) did not reveal staining and thus indicated non-specific binding. Non-specific binding was related to the presence of small minerals that were of similar size as the microbes. These minerals could be removed by HCl treatments (e.g. 1 M HCl in water for 5 minutes, or 0.1 M HCl for 30 minutes), and thus quite likely represent carbonates. This assumption is supported by pH measurements that were always above neutral (i.e. pH 7) within a depth of a millimeter measured directly at the site. Unfortunately, HCl treatment also resulted in a decline in cell numbers as determined after DAPI staining by about 30%. A strong reduction in non-specific binding of fluorescent probes to these minerals could finally be achieved by adding a pre-hybridization step with hybridization buffer that included blocking reagent to the *in situ* hybridization protocol (Hahn et al. 1997; Hahn et al.1993a; Hahn et al. 1993b).

The second challenge was the low number of cells detected by *in situ* hybridization even with probes targeting the Domain Bacteria (i.e., probe EUB338 which should detect all bacteria), while staining with DAPI revealed the presence of large numbers. This phenomenon is generally caused by low permeability of the cells present, generally due to morphological adaptations of microbial cells to adverse environmental conditions that render them inactive (e.g., spores with thick spore coats). Compared to labeled probes, DAPI is a much smaller molecule that is able to penetrate into cells even in the presence of thick cell walls or additional coats. Pretreatments with

lysozyme, an enzyme that catalyses the hydrolysis of 1,4-beta-linkages between N-acetylmuramic acid and N-acetyl-D-glucosamine residues in peptidoglycan which makes up the cell walls in bacteria, is a proven way to enhance cell permeability and consequently provide access for probes to rRNA target sequences in the cell (Hahn 1993b, Chatzinotas et al. 1998). A treatment with 0.1% lysozyme solution for 30 minutes was found sufficient to provide access of probes to target molecules in bacterial cells and allow reliable quantification.

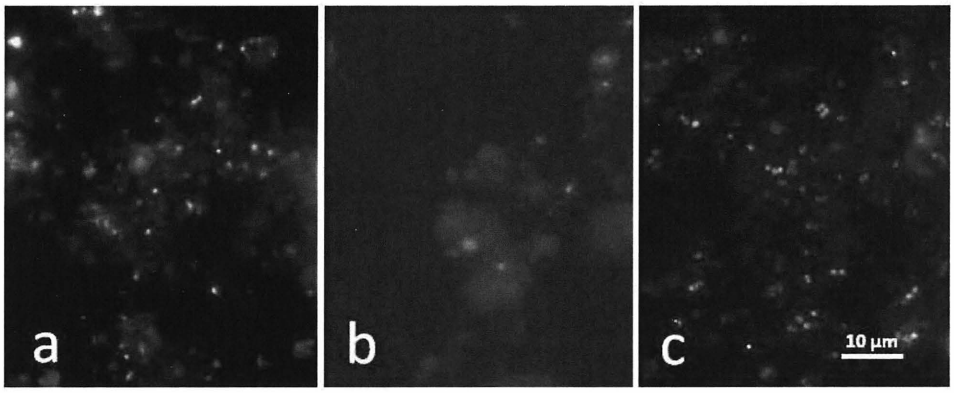

Figure C. 1. *In Situ* Hybridization with Cy3-labeled Probe EUB338 on Surface Concrete Samples (Bridge 3). (a) Standard Hybridization Protocol, (b) Additional Blocking Before and During Hybridization, (c) Lysozyme Pre-treatment and Subsequent Blocking Before and During Hybridization.

An additional methodological challenge was the detection of cell-like structures that could not be removed (Figure C. 2). These structures showed up occasionally, and did not represent any living cells as demonstrated by the absence of any DAPI signals (Figure C. 2). Since the size of these structures was unusually large, and DAPI staining was lacking, they were not considered in any quantitative evaluations of microbial community structure. The lack of DAPI staining in the same positions without Cy3-labeled probes (a and c) indicated the lack of DNA and thus some non-specific signals (i.e. signals not generated after binding of the probe to its target in a microbial cell)

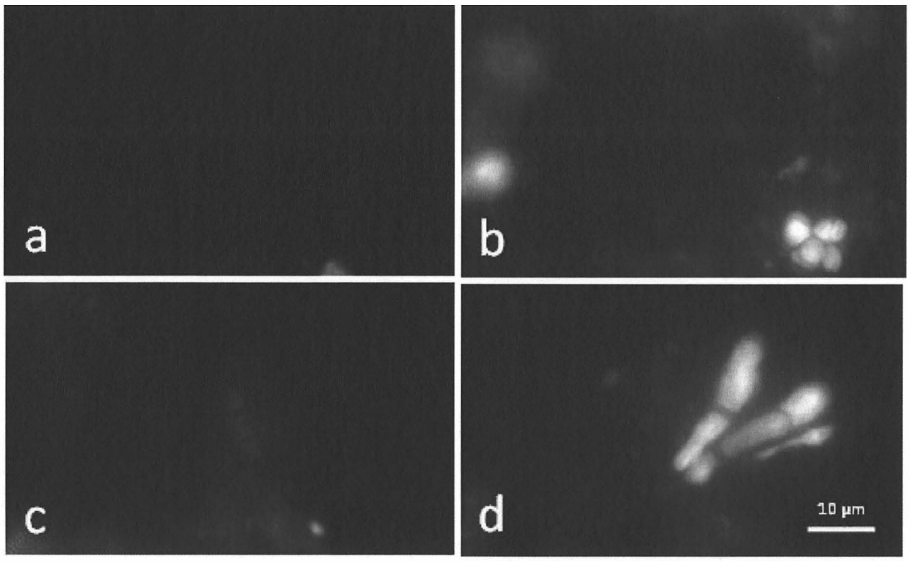

Figure C. 2. Detection of Cell-like Structures After *In Situ* Hybridization Without (a and c) and With Cy3-labeled Probes (b and d).

Examples of *In Situ* Hybridization Results

In situ hybridization provides information on the abundance and diversity of the microbial community in a top-down approach using a set of probes that target microbial populations with increasing specificity. Analyses were started with the analysis of DAPI stained cells that should represent all organisms. Since the amount of sample analyzed could not be quantified with respect to accurate weight or volume, only percentages are presented. Information of basic community structure for surface concrete and water samples from all twelve visited bridges are summarized in Table C. 3 to Table C. 15.

Results showed that large differences were obtained with respect to cell sizes and composition of the community. Samples from deteriored concrete close to the water level from Bridge 3 consisted of much larger cells than those from the same location, but more distant from the water level (and thus dry) and less deteriorated (Figure C. 3). As shown in Figure C. 3, samples from both sites clearly show the presence of different communities of bacteria as indicated by differences in size and morphology both after DAPI-staining (left panel) and hybridization with Cy3-labeled probe EUB338 (right panel).

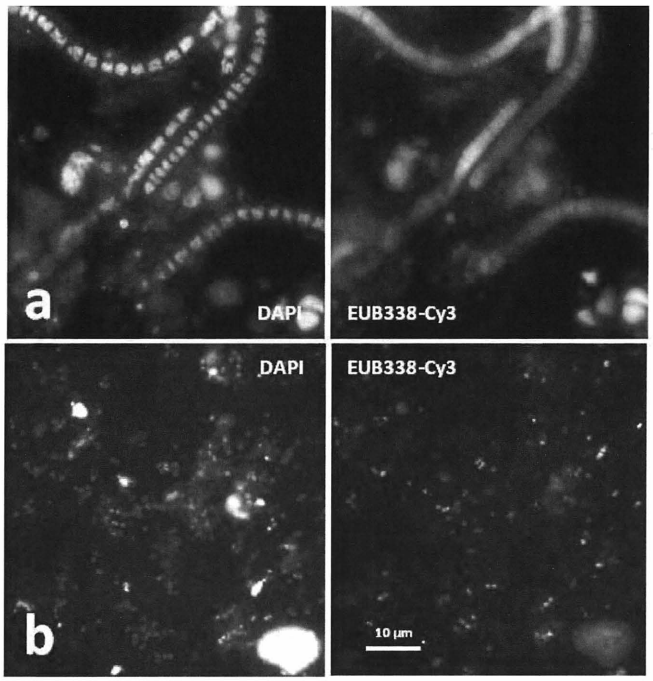

Figure C. 3. *In Situ* Detection of Bacteria in Biofilm Samples Collected from Bridge 3 Visibly Deteriorated (b) Non-Deteriorated Concrete Surface Samples.

Samples required pretreatment with lysozyme to increase the permeability of cells (and thus enabling hybridization and detection of cells), and blocking before and during hybridization to reduce non-specific binding of probes to minerals (i.e. carbonates) abundant in all samples. Cells in the deteriorated concrete (specimen height 6 inches) mainly consisted of Bacteria (more than 90%) and a few Eukarya (about 10%), while Archaea were not detected in significant numbers (Table C. 5). In non- deteriorated concrete, both Eukarya and Archaea were not detected in significant numbers. These results are mirroring our expectations on the prevalence of Bacteria, but not to the Archaea or Eukarya in deteriorated and non- deteriorated concrete samples.

More detailed analyses of members of the Domain Bacteria resulted in the detection of few phylogenetic groups only. In samples from deteriorated concrete, only members of the α-subdivision of Proteobacteria were detected with the respective probe (making up 13 % of the cells identified as belonging to the Domain Bacteria). None of the remaining probes resulted in the detection of significant numbers of cells (Table C. 5), which means that 87% of the bacterial cells remained unidentified. Morphological characteristics, however, such as size, autofluorescence, chain formation, etc, suggest that the majority of the remaining cells are

autotrophic cells, and thus very likely cyanobacteria. In contrast to samples from deteriorated concrete, in non-deteriorated concrete (specimen height 48 inches) all bacterial cells could be identified. All cells represented members of the α-subdivision of Proteobacteria. Again, none of the remaining probes identified other groups in significant numbers. The largest diversity of bacteria was obtained in non- deteriorated samples, with 4%, 10%, 13%, and 20% representing members of the α-, β-, γ- and δ-subdivision of Proteobacteria, respectively (Table C. **5**). The latter group represents many sulfate-reducing bacteria.

Similar results as retrieved for bridge 3 were obtained for the remaining eleven sites although individual sites differed from each other with respect to basic composition of microbial community structure, and detectability of microbes. Detectability of organisms was very high with essentially all organisms detectable by *in situ* hybridization. Detectability is determined as the percentage of organisms detected by specific probes (e.g. all Bacteria and all Eukarya) compared to those detected by the DNA-intercalating dye DAPI that stains all organisms. In all cases, Eukarya were detected only occasionally, and generally in percentages less than 1 % of the entire community (i.e. the DAPI-stained cells). Bacteria were detected in variable percentages of the DAPI stained cells, while Archaea were not detected at all. Similar to our previous studies, the addition of blocking reagent and pre-hybridization was necessary to reduce non-specific binding of the probes to carbonate particles and to achieve specific detection. Detectability of bacteria was not affected by sampling site at each column, i.e. height or distance from the water level which indicates an adequate permeability of cells for probes at all sites and in all samples. More detailed analyses of members of the Domain Bacteria resulted in the detection of few phylogenetic groups only. None of the respective probes resulted in the detection of significant numbers of cells, which means that most of the bacterial cells remained unidentified. Morphological characteristics, however, such as size, autofluorescence, chain formation, etc, suggest that the majority of the remaining cells are autotrophic cells, and thus very likely cyanobacteria.

These results are not supporting our hypothesis that members of the β- and γ-subdivision of Proteobacteria should be dominant in corroded concrete samples, comparable to results obtained for sewage plants where members of the β- and γ-subdivision of Proteobacteria have been shown to play a major role in the corrosion of concrete (Okabe et al. 2007). It was therefore not surprising that several phyla within the β- and γ-subdivision of Proteobacteria that have been

linked to concrete corrosion in sewage treatment plants with major populations (i.e., up to 80% of all bacteria) represented by *Acidithiobacillus thiooxidans*, *A. ferrooxidans* and other *Acidithiobacillus* species (probes Thio820, and ACD840), and to a lesser extent by members of *Leptospirillum* groups I, II and III, *Thiomonas intermedia, Thiobacillus plumbophilus* or *Halothiobacillus neapolitanus* (Okabe et al. 2007) were not detected . Since most of these are sulfur (or ferrous iron) oxidizing bacteria (usually autotrophic bacteria that use sulfide or sulfur as electron donor and oxygen as electron acceptor), oxidation of sulfide or sulfur would result in the generation of sulfate and protons, and thus in a reduction in pH, which, however, was also not detected.

DETAILED TEST RESULTS

Table C. 3. Basic Community Structure for Surface Concrete and Water Samples from Bridge 1.

		1-C1-1	1-C1-2	1-C1-3	1-Water
Height (in.)		6	30	66	
All organisms	DAPI (x 10^8 per sample)	14.8 (2.5)	12.8 (4.5)	23.4 (4.4)	47.3 (16.2)
Domain-level analyses (in percent of DAPI counts)	Eukarya	59 (1.9)	71 (4.5)	88 (3.1)	0
	Archaea	0	0	0	0
	Bacteria	41 (5.3)	29 (5.5)	12 (1.5)	100 (16.2)
Within domain Bacteria	α-subdivision of Proteobacteria	0	0	0	0
	β-subdivision of Proteobacteria	0	0	0	0
	γ-subdivision of Proteobacteria	0	0	0	0
	δ-subdivision of Proteobacteria	0	0	0	0
	Gram-positive bacteria with high DNA G+C content	0	0	0	0
	Gram-positive bacteria with low DNA G+C content	0	0	0	0
	Cytophaga-Flavobacterium cluster of the CFB phylum	0	0	0	0
Bacteria shown to inhabit deteriorating concrete in sewer systems	Leptospirillum groups I, II and III	0	0	0	0
	Acidithiobacillus thiooxidans, A. ferrooxidans	0	0	0	0
	Thiomonas intermedia	0	0	0	0
	Halothiobacillus neapolitanus	0	0	0	0

Notes:
[1] Due to the lack of reliable sample weights and volumes, no absolute numbers are presented
[2] All enumerations representing less than 1% of the detectable microbes (i.e., an occasional signal) were assumed to be insignificant for statistical comparison and were counted as "0"
[3]Estimated number of cells for the DAPI probe
[4]Standard deviations (+/-) for numerical values of all other probes excluding DAPI

Table C. 4. Basic Community Structure for Surface Concrete and Water Samples from Bridge 2.

		2-C1-1	2-C1-3
Height (in.)		6	36
All organisms	DAPI (x 10^8 per sample)	1.1 (6.4)	2.0 (17.1)
Domain-level analyses (in percent of DAPI counts)	Eukarya	0	25 (7.2)
	Archaea	0	0
	Bacteria	100 (13.5)	75 (15.6)
Within domain Bacteria	α-subdivision of Proteobacteria	22 (3.7)	30 (6.8)
	β-subdivision of Proteobacteria	14 (1.8)	0
	γ-subdivision of Proteobacteria	13 (2.4)	0
	δ-subdivision of Proteobacteria	0	0
	Gram-positive bacteria with high DNA G+C content	18 (2.9)	0
	Gram-positive bacteria with low DNA G+C content	0	0
	Cytophaga-Flavobacterium cluster of the CFB phylum	0	0
Bacteria shown to inhabit deteriorating concrete in sewer systems	Leptospirillum groups I, II and III	0	0
	Acidithiobacillus thiooxidans, A. ferrooxidans	0	0
	Thiomonas intermedia	0	0
	Halothiobacillus neapolitanus	0	0

Table C. 5. Basic Community Structure for Surface Concrete and Water Samples from Bridge 3.

		3-C131	3-C131
Height (in.)		6	48
All organisms	DAPI (x 10^8 per sample)	1.1 (14.7)	1.3 (35.2)
Domain-level analyses (in percent of DAPI counts)	Eukarya	43 (9.8)	0
	Archaea	0	0
	Bacteria	57 (13.8)	100 (11.4)
Within domain Bacteria	α-subdivision of Proteobacteria	26 (5.3)	4 (4.5)
	β-subdivision of Proteobacteria	0	10 (8.4)
	γ-subdivision of Proteobacteria	0	13 (15.7)
	δ-subdivision of Proteobacteria	0	8 (5.7)
	Gram-positive bacteria with high DNA G+C content	0	0
	Gram-positive bacteria with low DNA G+C content	0	0
	Cytophaga-Flavobacterium cluster of the CFB phylum	0	0
Bacteria shown to inhabit deteriorating concrete in sewer systems	Leptospirillum groups I, II and III	0	0
	Acidithiobacillus thiooxidans, A. ferrooxidans	0	0
	Thiomonas intermedia	0	0
	Halothiobacillus neapolitanus	0	0

Table C. 6. Basic Community Structure for Surface Concrete Samples from Bridge 4.

		4-C3
Height (in.)		6
All organisms	DAPI (x 10^8 per sample)	1.3 (25.4)
Domain-level analyses (in percent of DAPI counts)	Eukarya	19 (4.9)
	Archaea	0
	Bacteria	81 (19.1)
Within domain Bacteria	α-subdivision of Proteobacteria	0
	β-subdivision of Proteobacteria	0
	γ-subdivision of Proteobacteria	0
	δ-subdivision of Proteobacteria	0
	Gram-positive bacteria with high DNA G+C content	0
	Gram-positive bacteria with low DNA G+C content	0
	Cytophaga-Flavobacterium cluster of the CFB phylum	0
Bacteria shown to inhabit deteriorating concrete in sewer systems	Leptospirillum groups I, II and III	0
	Acidithiobacillus thiooxidans, A. ferrooxidans	0
	Thiomonas intermedia	0
	Halothiobacillus neapolitanus	0

Table C. 7. Basic Community Structure for Surface Concrete Samples from Bridge 5.

		5-C1	5-C1	5-C1	5-C2	5-C2	5-C2
Height (in.)		74	64	12	85	75	10
All organisms	DAPI (x 10^8 per sample)	4.3 (1.2)	4.2 (1.3)	3.7 (1.3)	4.1 (0.9)	4.5 (0.9)	4.6 (1.1)
Domain-level analyses (in percent of DAPI counts)	Eukarya	0	0	0	0	0	0
	Archaea	0	0	0	0	0	0
	Bacteria	82.8 (11.8)	91.2 (12.1)	86.2 (8.0)	78.3 (14.8)	77.5 (10.3)	77.0 (9.5)
Within domain Bacteria	α-subdivision of Proteobacteria	0	0	0	0	0	0
	β-subdivision of Proteobacteria	0	0	0	0	0	0
	γ-subdivision of Proteobacteria	5.8 (7.9)	5.2 (6.3)	6.4 (8.1)	7.6 (7.5)	0.8 (3.7)	6.5 (11.9)
	δ-subdivision of Proteobacteria	0	0	0	0	0	0
	Gram-positive bacteria with high DNA G+C content	0	0	0	0	0	0
	Gram-positive bacteria with low DNA G+C content	0	0	0	0	0	0
	Cytophaga-Flavobacterium cluster of the CFB phylum	0	0	0	0	0	0
Bacteria shown to inhabit deteriorating concrete in sewer systems	Leptospirillum groups I, II and III	7.1 (8.8)	4.6 (5.5)	3.1 (3.3)	5.5 (8.7)	1.6 (3.5)	5.7 (8.7)
	Acidithiobacillus thiooxidans, A. ferrooxidans	0	0	0	0	0	0
	Thiomonas intermedia	0	0	0	0	0	0
	Halothiobacillus neapolitanus	0	0	0	0	0	0

Table C. 8. Basic Community Structure for Surface Concrete Samples from Bridge 6.

		6-C1	6-C1	6-C1	6-C3	6-C3	6-C3
Height (in.)		108	96	6	106	96	6
All organisms	DAPI (x 10^8 per sample)	5.2 (1.2)	4.2 (0.8)	4.1 (1.1)	1.5 (0.6)	3.2 (1.4)	3.3 (0.9)
Domain-level analyses (in percent of DAPI counts)	Eukarya	0	0	0	0	0	0
	Archaea	0	0	0	0	0	0
	Bacteria	74.0 (13.5)	54.2 (15.5)	53.0 (14.8)	37.0 (10.4)	52.0 (18.6)	35.2 (14.8)
Within domain Bacteria	α-subdivision of Proteobacteria	0	0	0	0	0	0
	β-subdivision of Proteobacteria	0	0	0	0	0	0
	γ-subdivision of Proteobacteria	7.3 (8.5)	4.3 (4.9)	3.8 (4.2)	1.5 (4.2)	8.6 (8.2)	5.1 (5.6)
	δ-subdivision of Proteobacteria	0	0	0	0	0	0
	Gram-positive bacteria with high DNA G+C content	0	0	0	0	0	0
	Gram-positive bacteria with low DNA G+C content	0	0	0	0	0	0
	Cytophaga-Flavobacterium cluster of the CFB phylum	0	0	0	0	0	0
Bacteria shown to inhabit deteriorating concrete in sewer systems	Leptospirillum groups I, II and III	5.6 (6.9)	0	3.3 (5.6)	4.5 (10.3)	0	3.0 (4.0)
	Acidithiobacillus thiooxidans, A. ferrooxidans	0	0	0	0	0	0
	Thiomonas intermedia	0	0	0	0	0	0
	Halothiobacillus neapolitanus	0	0	0	0	0	0

Table C. 9. Basic Community Structure for Surface Concrete Samples from Bridge 7.

		7-C3	7-C3	7-C1	7-C1
Height (in.)		90	6	90	6
All organisms	DAPI (x 10^8 per sample)	2.4 (1.4)	2.1 (0.9)	1.7 (0.5)	3.1 (1.2)
Domain-level analyses (in percent of DAPI counts)	Eukarya	0	0	0	0
	Archaea	0	0	0	0
	Bacteria	51.9 (22.0)	51.8 (15.5)	53.3 (16.5)	51.2 (15.7)
Within domain Bacteria	α-subdivision of Proteobacteria	0	0	0	0
	β-subdivision of Proteobacteria	0	0	0	0
	γ-subdivision of Proteobacteria	7.3 (7.7)	4.8 (4.4)	1.5 (3.6)	4.8 (7.3)
	δ-subdivision of Proteobacteria	0	0	0	0
	Gram-positive bacteria with high DNA G+C content	0	0	0	0
	Gram-positive bacteria with low DNA G+C content	0	0	0	0
	Cytophaga-Flavobacterium cluster of the CFB phylum	0	0	0	0
Bacteria shown to inhabit deteriorating concrete in sewer systems	Leptospirillum groups I, II and III	0	0	0	0
	Acidithiobacillus thiooxidans, A. ferrooxidans	0	0	0	0
	Thiomonas intermedia	0	0	0	0
	Halothiobacillus neapolitanus	0	0	0	0

Table C. 10. Basic Community Structure for Surface Concrete Samples from Bridge 8.

		8-C2	8-C2	8-C2	8-C2
Height (in.)		6	18	30	54
All organisms	DAPI (x 10^8 per sample)	1.4 (0.3)	1.2 (0.2)	1.1 (0.3)	1.5 (0.5)
Domain-level analyses (in percent of DAPI counts)	Eukarya	18.5 (14.8)	32.8 (19.1)	26.6 (17.4)	22.3 (14.6)
	Archaea	0	0	0	0
	Bacteria	20.3 (15.8)	21.5 (12.5)	20.7 (10.8)	22.3 (13.4)
Within domain Bacteria	α-subdivision of Proteobacteria	0	0	0	0
	β-subdivision of Proteobacteria	0	0	0	0
	γ-subdivision of Proteobacteria	15.7 (11.8)	19.9 (13.5)	18.1 (9.2)	21.0 (14.0)
	δ-subdivision of Proteobacteria	0	0	0	0
	Gram-positive bacteria with high DNA G+C content	0	0	0	0
	Gram-positive bacteria with low DNA G+C content	0	0	0	0
	Cytophaga-Flavobacterium cluster of the CFB phylum	0	0	0	0
Bacteria shown to inhabit deteriorating concrete in sewer systems	Leptospirillum groups I, II and III	0	0	0	0
	Acidithiobacillus thiooxidans, A. ferrooxidans	0	0	0	0
	Thiomonas intermedia	0	0	0	0
	Halothiobacillus neapolitanus	0	0	0	0

Table C. 11. Basic Community Structure for Surface Concrete Samples from Bridge 9.

		9-C4	9-C4	9-C4	9-C4
Height (in.)		6	18	30	54
All organisms	DAPI (x 10^8 per sample)	2.1 (0.4)	1.6 (0.4)	2.5 (0.5)	1.5 (0.5)
Domain-level analyses (in percent of DAPI counts)	Eukarya	14.7 (8.7)	30.9 (21.1)	21.8 (12.7)	20.8 (10.8)
	Archaea	0	0	0	0
	Bacteria	17.8 (6.8)	21.5 (11.7)	10.4 (5.6)	16.6 (11.2)
Within domain Bacteria	α-subdivision of Proteobacteria	0	0	0	0
	β-subdivision of Proteobacteria	0	0	0	0
	γ-subdivision of Proteobacteria	18.0 (11.4)	18.6 (16.3)	21.4 (18.5)	27.1 (14.3)
	δ-subdivision of Proteobacteria	0	0	0	0
	Gram-positive bacteria with high DNA G+C content	0	0	0	0
	Gram-positive bacteria with low DNA G+C content	0	0	0	0
	Cytophaga-Flavobacterium cluster of the CFB phylum	0	0	0	0
Bacteria shown to inhabit deteriorating concrete in sewer systems	Leptospirillum groups I, II and III	0	0	0	0
	Acidithiobacillus thiooxidans, A. ferrooxidans	0	0	0	0
	Thiomonas intermedia	0	0	0	0
	Halothiobacillus neapolitanus	0	0	0	0

Table C. 12 Basic Community Structure for Surface Concrete Samples from Bridge 10.

		10-C2	10-C2	10-C2
Height (in.)		6	42	90
All organisms	DAPI (x 10^8 per sample)	2.1 (0.4)	1.6 (0.4)	2.5 (0.5)
Domain-level analyses (in percent of DAPI counts)	Eukarya	15.9 (7.0)	19.1 (8.0)	20.6 (9.1)
	Archaea	0	0	0
	Bacteria	19.3 (7.8)	23.4 (8.1)	13.3 (5.3)
Within domain Bacteria	α-subdivision of Proteobacteria	0	0	0
	β-subdivision of Proteobacteria	0	0	0
	γ-subdivision of Proteobacteria	21.2 (9.3)	19.9 (12.1)	19.1 (7.8)
	δ-subdivision of Proteobacteria	0	0	0
	Gram-positive bacteria with high DNA G+C content	0	0	0
	Gram-positive bacteria with low DNA G+C content	0	0	0
	Cytophaga-Flavobacterium cluster of the CFB phylum	0	0	0
Bacteria shown to inhabit deteriorating concrete in sewer systems	Leptospirillum groups I, II and III	0	0	0
	Acidithiobacillus thiooxidans, A. ferrooxidans	0	0	0
	Thiomonas intermedia	0	0	0
	Halothiobacillus neapolitanus	0	0	0

Table C. 13. Basic Community Structure for Surface Concrete Samples from Bridge 11.

		11-C1	11-C1	11-C1
Height (in.)		6	30	66
All organisms	DAPI (x 10^8 per sample)	1.6 (0.5)	1.8 (0.5)	2.3 (0.6)
Domain-level analyses (in percent of DAPI counts)	Eukarya	21.7 (10.1)	23.5 (1.0)	23.2 (1.0)
	Archaea	0	0	0
	Bacteria	19.5 (8.5)	20.5 (13.4)	15.5 (0.9)
Within domain Bacteria	α-subdivision of Proteobacteria	0	0	0
	β-subdivision of Proteobacteria	0	0	0
	γ-subdivision of Proteobacteria	17.6 (11.6)	21.6 (12.1)	17.4 (10.8)
	δ-subdivision of Proteobacteria	0	0	0
	Gram-positive bacteria with high DNA G+C content	0	0	0
	Gram-positive bacteria with low DNA G+C content	0	0	0
	Cytophaga-Flavobacterium cluster of the CFB phylum	0	0	0
Bacteria shown to inhabit deteriorating concrete in sewer systems	Leptospirillum groups I, II and III	0	0	0
	Acidithiobacillus thiooxidans, A. ferrooxidans	0	0	0
	Thiomonas intermedia	0	0	0
	Halothiobacillus neapolitanus	0	0	0

Table C. 14. Basic Community Structure for Surface Concrete Samples from Bridge 12.

		12-C1	12-C1	12-C1
Height (in.)		6	30	54
All organisms	DAPI (x 10^8 per sample)	1.9 (0.5)	1.5 (0.3)	1.3 (0.2)
Domain-level analyses (in percent of DAPI counts)	Eukarya	20.8 (11.3)	19.5 (8.0)	28.5 (11.9)
	Archaea	0	0	0
	Bacteria	13.7 (0.9)	22.8 (11.6)	23.6 (10.0)
Within domain Bacteria	α-subdivision of Proteobacteria	0	0	0
	β-subdivision of Proteobacteria	0	0	0
	γ-subdivision of Proteobacteria	20.5 (10.7)	17.8 (8.7)	17.8 (9.4)
	δ-subdivision of Proteobacteria	0	0	0
	Gram-positive bacteria with high DNA G+C content	0	0	0
	Gram-positive bacteria with low DNA G+C content	0	0	0
	Cytophaga-Flavobacterium cluster of the CFB phylum	0	0	0
Bacteria shown to inhabit deteriorating concrete in sewer systems	Leptospirillum groups I, II and III	0	0	0
	Acidithiobacillus thiooxidans, A. ferrooxidans	0	0	0
	Thiomonas intermedia	0	0	0
	Halothiobacillus neapolitanus	0	0	0

Table C. 15. Basic Community Structure for Surface Concrete Samples from Bridge 1 Revisit.

		1R-C1	1R-C1	1R-C1
Height (in.)		6	18	42
All organisms	DAPI (x 10^8 per sample)	1.6 (0.5)	2.4 (0.7)	1.9 (0.5)
Domain-level analyses (in percent of DAPI counts)	Eukarya	34.9 (21.1)	27.8 (15.2)	21.4 (16.4)
	Archaea	0	0	0
	Bacteria	20.9 (18.2)	10.5 (9.3)	11.0 (8.5)
Within domain Bacteria	α-subdivision of Proteobacteria	0	0	0
	β-subdivision of Proteobacteria	0	0	0
	γ-subdivision of Proteobacteria	33.5 (32.1)	19.3 (18.8)	24.0 (18.6)
	δ-subdivision of Proteobacteria	0	0	0
	Gram-positive bacteria with high DNA G+C content	0	0	0
	Gram-positive bacteria with low DNA G+C content	0	0	0
	Cytophaga-Flavobacterium cluster of the CFB phylum	0	0	0
Bacteria shown to inhabit deteriorating concrete in sewer systems	Leptospirillum groups I, II and III	0	0	0
	Acidithiobacillus thiooxidans, A. ferrooxidans	0	0	0
	Thiomonas intermedia	0	0	0
	Halothiobacillus neapolitanus	0	0	0

APPENDIX D:

DETAILED CHEMICAL ANALYSIS PROCEDURES AND RESULTS

TEST PROCEDURES

Determination of pH

The pH of the water samples, mud and concrete scrapings was determined using a pH meter. For the water the pH was measured directly. For the mud and concrete scrapings, approximately 0.5 grams of either dried mud or crushed concrete was weighed and placed in solution with 10 mL of DI water. Samples were vortexed vigorously and sonicated. The samples were extracted at room temperature for approximately 72 hours and pH measurements were taken after calibrating the pH meter at 4, 7, and 10 pH.

The pH of various core samples was measured using phenolphthalein indicator. Upon application of a phenolphthalein solution to the surface of concrete, areas with low or no corrosion turn pink because of a relatively high alkalinity, while other areas remain colorless indicating deterioration and a reduced pH value (lower than 8), likely due to either chemical or microbial attack. For each site, the degree of penetration was also measured. The degree of penetration for each sample was measured around the perimeter of the core, at one centimeter intervals, measuring from the surface towards the interior, using a ruler. From these measurements an average, range, and standard deviation were calculated for each core sample. Approximate organic material coverage was visually observed from the top surface and the approximate height of the organic material was measured from the top surface using a ruler. Outlier data were discarded using the Dixon Q-test.

Sulfate and Chloride Determination

Mud samples were left to air dry over the course of several days and then ground into a fine powder before extracting with water. Concrete scrapings were ground into a fine powder using a mortar and pestle, then weighed and extracted with either water or 5 N HCl at a ratio of 2:1 water: scrapings. The samples were vortexed vigorously for several minutes then left for a minimum of three days in the extracting medium. The samples where then centrifuged 1,500 X G for 15 minutes, the supernatant filtered through 2μm filter paper and then placed in a 50 mL polypropylene conical vial. During the extraction procedure it was noted that the samples containing HCl had turned a yellow color while the samples containing water remained colorless. After extraction, samples were analyzed using a Lachet ion chromatograph. Standards and samples were run using the Lachet QuickChem 8500, rapid anion analytical column. The eluent flow rate was 1.4 mL/min, and the aqueous eluent concentration, 9.0 mM $NaHCO_3$, and 0.5 mM

Na_2CO_3. The analysis protocol was EPA method 300.0 Water samples were used as is though filtered prior to chromatographic analysis. The analysis protocol utilized EPA method 300.0. The standard curve for sulfate ranged from 2.5 mg/L to 250 mg/L; 1.5 mg/L to 150 mg/L for chloride.

As all samples were diluted in order to have adequate amounts for ion chromatography, following steps were applied to calculate sulfate and chloride contents. As an example, for sample 1-C-1-6, 0.2522 gram of sample was extracted into 0.500 mL of DI water, then diluted with water to 10.0 mL. The reported concentration obtained for this sample from ion chromatography was 1.01 mg/L for sulfate. The percent sulfate for sample 1-C-1-6 was then calculated in the following manner:

$$(1.01 \text{ mg/L})\ (1\text{L}/1000 \text{ mL})\ (1\text{g}/1000 \text{ mg}) = 1.01\text{X}10^{-6} \text{ g/mL}$$

$$10 \text{ mL}\ (1.01\text{X}10^{-6} \text{ g/mL}) = 1.01\text{X}10^{-5} \text{ g}$$

$$(1.01\text{X}10^{-5} \text{ g}/0.2522 \text{ g})(100\%) = .004\%$$

The % sulfate and % chloride for all samples were calculated in the same manner.

RESULTS

Phenolphthalein Tests

The pH was determined using phenolphthalein indicator for core halves obtained from the Bridge 1, 2, 3 and 4. The core halves that had organic growth tested colorless on the surface. The inside of the core halves tested pink to dark pink with a change within 1mm to 30mm within the top surface of the core. Generally, the aggregate within the core halves remained colorless and if the aggregate impinged on the surface that portion of the surface remained colorless indicating a lack of permeability of the phenolphthalein into the aggregate. For the concrete core samples, the pH at or near the surface was less than a pH of 8 as determined from a lack of color in the phenolphthalein, but within a few millimeters of the surface the concrete becomes very basic as indicated by the pink color of the phenolphthalein indicator. The interior appears to be unaffected by exposure to the elements except in some cases where aggregate is near the surface and provides a conduit for diffusion of water into the interior and a subsequent lowering of the pH.

Table D. 1 depicts the results from the pH determination of 15 core samples obtained from the SH82@ Alligator Bayou site using phenolphthalein as an indicator. The results show

the average depth of penetration of corrosion, range, standard deviation. In addition the table shows whether or not organic material was present (Y(yes) or N (no)), percent organic coverage of the surface and height of organic material on the surface for a number of core halves. The results show that when organic material is located on the outer surface, the depth of penetration of the colorless region ranges from 2.41 to 11.66 mm indicating that the concrete near the surface is more acidic with a pH less than 8. Invariably, the inside of all the core samples tested pink indicating that the inside has a basic pH as expected for concrete. The Q test was used to determine outliers in the determination of the depth of penetration from points on the surface. Generally, values which were too high reflected penetration depths that originated with points on the surface that included aggregate. The interfacial region between aggregate and concrete is surmised to provide a flow path for the diffusion of acidic species originating either from the water or from microbes on the surface.

Table D. 1. pH Deterioration from Phenolphthalein Tests.

		Height (in.)	Average, mm	Range, mm	Standard Deviation	RSD	Organic Material on top surface	% coverage of organic material	Thickness of organic material, mm
1	1-C1-1a	6	4.15	1 to 10	3.29	79.22	Y	80	1
1	1-C1-1b	6	0.75	0 to 3	0.866	115.5	Y	25	1
1	1-C1-2a	22	1.6	1 to 5	1.35	84.4	Y	75	1
1	1-C1-2b	22	1	1	0	0	Y	80	1
1	1-C2-1	20	2.556	1 to 5	1.51	59.07	Y	40	1
1	1-C2-2a	27	1.67	1 to 4	0.9848	58.966	Y	10	1
1	1-C2-2b	27	1.3	1 to 2	0.4827	37.13	Y	90	1
1	1-C2-3a	34	1.5	1 to 3	0.84	55.78	N	--	--
1	1-C2-3b	34	1.4	1 to 2	0.5477	39.12	N	--	--
1	1-C3-3	21	1.64	0 to 4	1.6895	103.02	N	--	--
1	1-C4-1a	26	3.38	1 to 5	4.407	130.4	Y	40	1
1	1-C4-1a	26	1	0 to 3	0.9428	94.28	Y	70	1
1	1-C4-3a	10	4.167	1 to 12	3.62	86.96	Y	30	1
1	1-C4-3b	10	0.75	0 to 3	0.866	115.47	Y	60	1

Table D. 1. pH Deterioration from Phenolphthalein Tests. (continuous)

		Height (in.)	Average, mm	Range, mm	Standard Deviation	RSD	Organic Material on top surface	% coverage of organic material	Thickness of organic material, mm
2	2-W1-1a	0	24	10 to 38	8.16	33.99	Y	10	<1
2	2-W1-1b	0	0.38	0 to 3	0.9693	255.08	Y	10	1
2	2-C1-1a	6	5	3 to 8	1.5	30	Y	<10	<1
2	2-C1-1b	6	3.75	0 to 6	2.34	62.41	Y	<10	<1
2	2-C1-2a	22	3.25	1 to 8	3.24	99.7	Y	80	<1
2	2-C1-2b	22	0.75	0 to 3	1.03	138.07	Y	50	1
2	2-C2-1	56	16.167	12 to 20	2.4058	14.88	N	--	--
3	3-C131-1a	6	0.5	0 to 5	1.44	288	Y	60	1
3	3-C131-1b	6	0.25	0 to 2	0.621	248.6	N	--	--
3	3-C131-2	24	21.92	10 to 36	8.73	39.83	Y	10	--
3	3-C131-3	6	3.7	0 to 10	4.64	125.5	Y	90	<1
3	3-C131-4a	24	6.45	0 to 12	4.1319	64.06	Y	50	<1
3	3-C131-4b	4	1.85	0 to 5	2.444	132.1	Y	50	<1
3	3-C131-5	48	11.64	0 to 25	9.61	82.61	N	--	--
3	3-C131-6	48	8.18	0 to 40	14.71	179.8	N	--	--
4	4-C3-5a	8	5.375	3 to 7	1.3	24.23	Y	30	3
4	4-C3-5b	8	5.44	3 to 7	1.23	23.16	Y	20	1
4	4-C6-1a	45	2.83	2 to 4	0.7528	26.6	Y	90	1
4	4-C6-1b	45	3.77	1 to 7	1.64	34.5	Y	90	1
4	4-C3-6a	28	5	4 to 6	0.577	11.54	Y	65	1
4	4-C3-6b	28	4.71	2 to 8	1.98	41.95	Y	90	1
4	4-C6-2a	85	5.78	5 to 9	1.39	24.12	Y	60	2
4	4-C6-2b	85	2.6	0 to 8	3.02	116.4	Y	60	2
4	4-C3-8a	40	3.09	1 to 5	1.25	40.56	N	-	-
4	4-C3-8b	40	3.33	1 to 7	2.12	63.7	Y	25	2
4	4-C3-4a	4	7.33	1 to 11	3.78	51.53	Y	45	1
4	4-C3-4b	4	3.89	0 to 7	3.18	81.74	Y	40	2
4	4-C6-1c	45	8.55	3 to 20	4.74	55.44	Y	35	3
4	4-C6-1d	45	2.5	0 to 5	2.67	106.9	Y	50	1

Detailed Chemical Analysis Results

The following tables (Table D. 2 to Table D. 14) represent pH, percent sulfate and percent chloride values for water (W), mud (M) and surface concrete (C) scrapings. For each sample, the designation: number-letter-number-number refers to the location-type of sample-

concrete column-inches above ground respectively. For example (1-C-1-22) means the sample was acquired at Tarkington Bayou from the first concrete column 22 inches above the water line.

Table D. 2 presents the results for pH and percent sulfate analysis for mud, water and concrete scrapings obtained from Bridge 1. As shown in Table D. 2, the pH of the water was slightly acidic while the pH of the concrete was essentially neutral. The amounts of sulfate and chloride were generally low. The microbial samples from Bridge 1 concentrated the amount of sulfate. The sulfate concentration was 5 ppm in the brackish water, while 40 to 460 ppm in the microbes situated on the concrete.

Table D. 2. Chemical Analysis Results from Bridge 1.

Sample	Height (in.)	pH	Weight (g)	SO_4^{-2} (mg/L)	Amt SO_4	SO_4^{-2} (ppm)	Cl^- (mg/L)	Amt Cl^-	%Cl^- (ppm)
1-W1		5.4	--	5.23	--		--	8.96	
1-W2		5.55	--	5.68	--		--	6.5	
1-W3		5.25	--	5.22	--		--	7.47	
1-C1-6	6	--	0.2522	1.01	4.00E-05	40.0	3.37	1.34E-04	133.6
1-C1-22	22	--	0.2531	7.02	4.62E-04	462.0	1.44	9.48E-05	94.8
1-C2-20	20	6.95	1.0169	2.93	5.76E-05	58.0	3.91	7.69E-05	77.0
1-C3-21	21	7.84	1.017	3.86	6.32E-05	63.0	5.12	8.39E-05	84.0

Note that extraction with 5N HCl always led to a vigorous reaction with concrete and low values for sulfate and so those results were deemed an inaccurate assessment of the amount of sulfate and have not been reported. As an example, approximately 65% more sulfate was extracted from the mud using water than with 5N HCl.

Table D. 3 presents the results for pH and percent sulfate analysis for mud, water and concrete scrapings obtained from Bridge 2. For the mud at Bridge 2, the pH and sulfate analysis of the water in contact with the concrete columns, yielded a pH that was relatively neutral but with a high quantity of sulfate. Results also show that the pH of the water and the mud were slightly acidic with the third water sample having approximately 5 times less sulfate and twice as much chloride as the other two water samples. The mud sample pH was slightly acidic with a high level of sulfate. When taking into consideration the sample height of the concrete shaving samples and the amount of sulfate, there was less sulfate present at 12 inches and at the water line (samples 2-C2-12 and 2-F-0) when compared to 36 inches above the water (samples 2-C1-36 and 2-C3-36). The concrete shavings from Bridge 2 after extraction with water also yielded a

higher concentration of sulfate than in the adjacent water. The concentration of sulfide in the water was 3 x 10^{-7}M while the concentration of sulfate in the water varied from about 11-56 ppm. The concentration of sulfate in the concrete shavings varied from 39 to 208 ppm.

Table D. 3. Chemical Analysis Results from Bridge 2.

Sample	Height (in.)	pH	Weight (g)	SO_4^{-2} (mg/L)	Amt SO_4	SO_4^{-2} (ppm)	Cl^- (mg/L)	Amt Cl^-	%Cl^- (ppm)
2-W1		6.05	--	53.5	--		48.9	--	
2-W2		6.1	--	55.6	--		43.1	--	
2-W3		6.35	--	11.2	--		88	--	
2-M1		6.77	5.0168	64.9	1.29E-04	129.0	16.1	3.21E-05	32.0
2-C1-36	6	7.72	5.0037	55.4	1.11E-04	111.0	27.4	5.48E-05	55.0
2-C2-12	12	8.95	5.0191	19.6	3.91E-05	39.0	88.9	1.77E-04	177.0
2-C3-36	36	7.69	5.0052	104	2.08E-04	208.0	109	2.18E-04	218.0
2-F-0	0	7.7	5.025	55.1	1.10E-04	110.0	84.8	1.69E-04	169.0

Table D. 4 presents the results for pH and percent sulfate analysis for mud, water and concrete scrapings obtained from Bridge 3. For the water at Bridge 3, the pH is slightly basic with a low quantity of sulfate. The result was expected as the bridge is exposed to a large size of open water body (Lake Tawakoni). For the concrete column scrapings (samples 3-C131-24 and 3-C131-6), when comparing the amount of sulfate found at 24 inches with that found at 6 inches above the water line, nine times as much sulfate was present at the lower sampling site suggesting either a chemical or microbial source was responsible for the elevated presence of sulfate. The lower sampling site also had eight times as much chloride present as the sample obtained higher up.

Table D. 4. Chemical Analysis Results from Bridge 3.

Sample	Height (in.)	pH	Weight (g)	SO_4^{-2} (mg/L)	Amt SO_4	SO_4^{-2} (ppm)	Cl^- (mg/L)	Amt Cl^-	%Cl^- (ppm)
3-W1		7.35	--	11.8	--		7.52	--	
3-W2		7.4	--	11.4	--		7.32	--	
3-C131-6	6	7.45	5.0051	1110	2.20E-03	2200.0	126.2	2.52E-04	252.0
3-C131-24	24	8.43	5.0042	106	2.12E-04	212.0	15.3	3.06E-05	30.6

Table D. 5 presents the data for percent sulfate for both water and mud samples obtained from the Bridge 4. The pH, sulfate and chloride analyses of the water in contact with the

concrete columns yielded a pH that was slightly basic but with high quantities of sulfate and chloride. For one of the mud samples located near span 1 but underwater (sample 5-M-1) the percent sulfate was approximately three times as much as that for a mud sample which was collected on the bank (sample 4-M2). It is interesting to note that the mud collected underwater has much more sulfate than the water samples and the mud sample obtained from the bank. The results suggest that microbes in the underwater mud concentrated the amount of sulfate.

Table D. 5 also presents data for percent sulfate and chloride for a number of scrapings. In comparing the deteriorated concrete to the concrete coated with a biofilm, the deteriorated d concrete had approximately four times as much sulfate present. For the chloride analyses, the two deteriorated samples 4-C6-6 and 4-C5-3 had four times as much as the non-deteriorated sample 4-S0-C5-34 and approximately eight times as much as the sample with the biofilm 4-C3-6. Also, the non-corroded sample had the lowest pH and the highest amount of sulfates. This result was unexpected since the non-corroded sample had more limited contact with the water in the bayou. One explanation might be that the non-corroded sample (scraping 4-S0-C5-34) may actually have been degraded through the action of SO_2 in the air (acid rain).

Table D. 5. Chemical Analysis Results from Bridge 4.

Sample	Height (in.)	pH	Weight (g)	SO_4^{-2} (mg/L)	Amt SO_4	SO_4^{-2} (ppm)	Cl^- (mg/L)	Amt Cl^-	%Cl^- (ppm)
4-W1		7.5	--	148	--		189	--	
4-W2		7.4	--	148	--		192	--	
4-M1		7.95	5	261	5.22E-04	522.0	43.1	8.62E-05	86.2
4-M2		7.65	4.9999	75.6	1.51E-04	151.0	48.1	9.62E-05	96.2
4-C3-6	6	8.55	4.9937	75.5	1.51E-04	151.0	28.5	5.71E-05	57.0
4-C5-3	3	8.2	4.9909	390	7.81E-04	781.0	290	5.81E-04	581.0
4-C6-6	6	8.1	5.0046	314	6.27E10-4	627.0	220	4.40E-04	440.0
4-S0-C5-34	34	7.4	5.0017	1136	2.30E-03	2271.0	70.8	1.41E-04	2271.0

Table D. 6 presents the data for percent sulfate for both water and mud samples obtained from the Bridge 5. As shown in Table D. 6, the pH of the mud and water was acidic. The pH of the concrete samples was basic. The two mud samples had the lowest levels of sulfates and chlorides. For the concrete samples taken from the first column at 12 inches above the water line (5-C1-12) , the sample had about the same amount of sulfate as the sample taken at 72 inches (5-C1-72), however the lower elevation had nine times more chloride than the sample acquired at

the higher elevation. For column 2, the sample taken at 24 inches (5-C2-24) had twice as much sulfate as the sample taken at 65 inches (5-C2-65); the chloride amount for both of these samples was low and approximately the same.

Table D. 6. Chemical Analysis Results from Bridge 5.

Sample	Height (in.)	pH	Weight (g)	SO_4^{-2} (mg/L)	Amt SO_4	SO_4^{-2} (ppm)	Cl^- (mg/L)	Amt Cl^-	%Cl^- (ppm)
5-W1		5.9	--	20.7	--		19.2	--	
5-W2		5.55	--	18.6	--		17.4	--	
5-M1		6.2	5.0046	10.4	2.08E-05	21.0	0.361	7.21E-07	0.7
5-M2		4.6	4.9966	8.17	1.64E-05	20.0	2.49	4.98E-06	5.0
5-C1-12	12	7.6	5.0091	58.4	1.17E-04	120.0	9.47	1.89E-05	20.0
5-C1-72	72	7.75	5.004	63.8	1.20E-04	127.0	1.04	2.02E-06	2.0
5-C2-24	24	8.15	5.0095	211	4.21E-04	420.0	18.4	3.67E-05	37.0
5-C2-65	65	7.95	5.0023	119	2.38E-04	240.0	17.2	3.44E-05	30.0

Table D. 7 presents the data for percent sulfate for both water and mud samples obtained from the Bridge 6. In Table D. 7, the pH of the water and mud was slightly acidic and the concrete ranged was basic. When comparing the water, mud, and concrete samples the levels of sulfate and chloride were low with the exception of sample 6-C3-12; this sample had approximately four times more sulfate and five times more chloride than the other samples.

Table D. 7. Chemical Analysis Results from Bridge 6.

Sample	Height (in.)	pH	Weight (g)	SO_4^{-2} (mg/L)	Amt SO_4	SO_4^{-2} (ppm)	Cl^- (mg/L)	Amt Cl^-	%Cl^- (ppm)
6-W2		6.15	--	18.8	--		18.4	--	
6-M1		5.85	4.9955	8.21	1.64E-05	16.0	ND	--	
6-M2		6.25	5.0079	15.2	3.04E-05	30.0	5.84	1.17E-05	12.0
6-C1-6	6	7.5	5.0038	24.2	4.84E-05	50.0	11.8	2.36E-05	20.0
6-C1-96	96	7.75	5.0245	31.3	6.23E-05	60.0	ND	--	
6-C3-12	12	8	5.0252	90.8	1.81E-04	181.0	56.3	1.12E-04	112.0
6-C3-96	96	7.75	5.011	43.1	8.60E-05	86.0	7.26	1.45E-05	14.0

Table D. 8 presents the data for percent sulfate for both water and mud samples obtained from the Bridge 7. In Table D. 8, the water and mud samples tested acidic and the concrete samples taken at 90 inches above the water line had pH values well above 10 while the other concrete samples were slightly basic. Mud sample 7-M1 had approximately 2.5 times more

sulfate than mud sample 7-M2. The sulfate levels for the concrete when comparing samples on column 1, the sample taken at 6" (7-C1-6) had four times as much sulfate as the sample taken at 90" (7-C1-90) and ten times as much chloride as the higher sample. The opposite occurs for column 3, with the higher sample (7-C3-90) having three times more sulfate than the lower sample (7-C3-6).

Table D. 8. Chemical Analysis Results from Bridge 7.

Sample	Height (in.)	pH	Weight (g)	SO_4^{-2} (mg/L)	Amt SO_4	SO_4^{-2} (ppm)	Cl^- (mg/L)	Amt Cl^-	%Cl^- (ppm)
7-W1		6.15	--	19.3	--		15.7	--	
7-W2		6.1	--	18.9	--		15.3	--	
7-M1		5.35	4.9961	73.4	1.47E-04	147.0	ND	--	
7-M2		5.7	5	32.2	6.44E-05	60.0	12.4	2.48E-05	24.8
7-C1-6	6	7.85	5.0186	219	4.36E-04	440.0	84.4	1.68E-04	170.0
7-C1-90	90	10	5.0039	52.6	1.05E-04	105.0	8.97	1.79E-05	18.0
7-C3-6	6	7.95	5.0137	36.2	7.22E-05	72.0	12.6	2.51E-05	25.0
7-C3-90	90	10	5.0086	99.2	1.98E-04	200.0	11.5	2.30E-05	23.0

Results for pH and percent sulfate analysis for mud, water and concrete scrapings obtained from Bridge 8 are summarized in Table D. 9. As shown in Table D. 9, the pH of the mud and water was acidic. The pH of the concrete samples was between low acidic and basic. With the lower elevation, sulfate contents were five to ten times higher than the sample acquired at the higher elevation. An increase of chloride content with the decrease of elevation of sample location was also observed.

Table D. 9. Chemical Analysis Results from Bridge 8.

Sample	Height (in.)	pH	Weight (g)	SO_4^{-2} (mg/L)	Amt SO_4	SO_4^{-2} (ppm)	Cl^- (mg/L)	Amt Cl^-	%Cl^- (ppm)
8-W1-S		5.58	--	55.3	--		38.1	--	
8-W2-N		5.68	--	54.9	--		38	--	
8-M1-S		5.75	4.9731	71.5	1.44E-04	144.0	8.4	1.69E-05	16.9
8-M2-N		4.88	5.0013	65.3	1.31E-04	131.0	6.88	1.38E-05	13.7
8-C2-6	6	7.11	5.0055	690	1.40E-03	1378.0	290	5.79E-04	579.0
8-C2-18	18	7.57	5.0086	274	5.47E-04	547.0	56.8	1.13E-04	113.0
8-C2-30	30	7.08	5.0009	165	3.30E-04	330.0	69.9	1.40E-04	140.0
8-C2-54	54	6.76	5.0043	221	4.42E-04	442.0	68.4	1.37E-04	137.0
8-C4-6	6	6.97	5.0004	695	1.39E-03	1390.0	195	3.90E-04	390.0
8-C4-18	18	7.16	5.0000	150	3.00E-04	300.0	46.1	9.22E-05	92.2
8-C4-30	30	7.39	5.0016	55.7	1.11E-04	110.0	121	2.42E-04	240.0
8-C4-54	54	6.95	5.0012	82.1	1.64E-04	164.0	75.8	1.52E-04	152.0

Results for pH and percent sulfate analysis for mud, water and concrete scrapings obtained from Bridge 9 are summarized in Table D. 10. Note that as Bridge 9 and Bridge 8 are essentially under same water body, very similar observation was made. As shown in Table D. 10, the pH of the mud and water was acidic. Except a specimen taken in high elevation in column 3 (9-C3-54), the pH of the concrete samples was between low acidic and basic. With the lower elevation, sulfate contents were five to ten times higher than the sample acquired at the higher elevation. An increase of chloride content with the decrease of elevation of sample location was also observed.

Table D. 10. Chemical Analysis Results from Bridge 9.

Sample	Height (in.)	pH	Weight (g)	SO_4^{-2} (mg/L)	Amt SO_4	SO_4^{-2} (ppm)	Cl^- (mg/L)	Amt Cl^-	%Cl^- (ppm)
9-W1-N		5.55	--	27.8	--		35.3	--	
9-W2-S		6.09	--	24.2	--		37.8	--	
9-M1-N		3.95	5.0012	291	5.82E-04	581.0	21.6	4.32E-05	43.0
9-M2-S		5.93	4.9994	196	3.92E-04	392.0	15.8	3.16E-05	32.0
9-C3-6	6	7.67	5.0026	598	1.20E-03	1200.0	233	4.66E-04	466.0
9-C3-18	18	7.73	4.9996	194	3.88E-04	390.0	116	2.32E-04	230.0
9-C3-30	30	7.61	5.0025	98.2	1.96E-04	196.0	108	2.16E-04	216.0
9-C3-54	54	11.8	5.007	1.96	3.91E-06	3.9	78.7	1.57E-04	160.0
9-C4-6	6	7.91	4.9998	487	9.74E-04	974.0	188	3.76E-04	380.0
9-C4-18	18	7.53	5.0057	393	7.85E-04	790.0	38.2	7.63E-05	76.0
9-C4-30	30	7.30	5.0029	199	3.98E-04	400.0	76.5	1.53E-04	153.0
9-C4-54	54	8.10	5.0016	109	2.18E-04	218.0	1.06	2.12E-06	2.1

Results for pH and percent sulfate analysis for mud, water and concrete scrapings obtained from Bridge 10 are summarized in Table D. 11. As shown in Table D. 11, the pH of the mud and water was low acidic or basic. Except a specimen taken in high elevation in column 2 (10-C2-90), the pH of the concrete samples was between low acidic and basic. With the lower elevation, sulfate contents were higher than the sample acquired at the higher elevation. No clear trend of chloride content with the change of elevation of sample location was observed.

Table D. 11. Chemical Analysis Results from Bridge 10.

Sample	Height (in.)	pH	Weight (g)	SO_4^{-2} (mg/L)	Amt SO_4	SO_4^{-2} (ppm)	Cl^- (mg/L)	Amt Cl^-	%Cl^- (ppm)
10-W1		6.78	--	17.2	--	--	5.73	--	--
10-W2		7.19	--	16.4	--	--	5.71	--	--
10-M-1		7.1	5.0063	97.6	1.95E-04	195.0	2.92	5.43E-06	5.4
10-M-2		7.14	5.0261	151	3.00E-04	300.4	6.4	1.27E-05	12.7
10-C2-6	6	5.63	3.0088	120	1.60E-04	160.0	3.84	5.10E-06	5.1
10-C2-42	42	5.61	3.007	0.74	9.84E-07	1.0	10.4	1.38E-05	13.8
10-C2-90	90	10	2.0076	0.167	3.33E-07	0.3	4.83	9.62E-06	9.6

Results for pH and percent sulfate analysis for mud, water and concrete scrapings obtained from Bridge 11 are summarized in Table D. 12. As shown in Table D. 12, the pH of the water was low acidic. No data of the pH of mud was available as specimen was not available at the time of visit. The pH of the concrete samples was acidic. With the lower elevation, both sulfate and chloride contents were higher than the sample acquired at the higher elevation.

Table D. 12. Chemical Analysis Results from Bridge 11.

Sample	Height (in.)	pH	Weight (g)	SO_4^{-2} (mg/L)	Amt SO_4	SO_4^{-2} (ppm)	Cl^- (mg/L)	Amt Cl^-	%Cl^- (ppm)
11-W-1		6.62	--	9.7	--	--	9.06	--	--
11-W-2		6.58	--	9.44	--	--	8.35	--	--
11-C-6	6	6.99	5.0023	93.8	1.88E-04	187.5	9.66	1.93E-05	19.3
11-C-1-30	30	6.07	5.0025	80.5	1.61E-04	160.9	14.8	2.96E-05	29.6
11-C-1-66	60	5.9	3.0019	25.8	3.44E-05	34.4	3.59	4.78E-06	4.8

Results for pH and percent sulfate analysis for mud, water and concrete scrapings obtained from Bridge 12 are summarized in Table D. 13. As shown in Table D. 13, the pH of the water was low acidic. No data of the pH of mud was available as specimen was not available at

the time of visit. Except sample at high elevation in column 1 (12-C1-54), the pH of the concrete samples was acidic. With the lower elevation, both sulfate and chloride contents were higher than the sample acquired at the higher elevation.

Table D. 13. Chemical Analysis Results from Bridge 12.

Sample	Height (in.)	pH	Weight (g)	SO_4^{-2} (mg/L)	Amt SO_4	SO_4^{-2} (ppm)	Cl^- (mg/L)	Amt Cl^-	%Cl^- (ppm)
12-W-1		6.8	--	9.64	--	--	8.09	--	--
12-W-2		6.77	--	9.89	--	--	8.01	--	--
12-C1-6	6	5.83	3.9925	13.4	1.34E-05	13.4	2.52	2.52E-06	2.5
12-C1-30	30	5.96	2.9837	5.31	8.90E-06	8.9	3.16	5.30E-06	5.3
12-C1-54	54	7.5	5.0084	130	2.60E-04	260.0	116	2.32E-04	231.6

Results for pH and percent sulfate analysis for mud, water and concrete scrapings obtained from Bridge 1 revisit are summarized in Table D. 14. As shown in Table D. 14, the pH of the water was low acidic and the pH of the mud was low basic. Note that the pH of both water and mud sample was higher than first visit, which is likely due to the change of seasonal change. The pH of the concrete samples was either low acidic or basic. While sulfate content was found to be relative high, no clear trend of chloride content with the change of elevation of sample location was observed.

Table D. 14. Chemical Analysis Results from Bridge 1R.

Sample	Height (in.)	pH	Weight (g)	SO_4^{-2} (mg/L)	Amt SO_4	SO_4^{-2} (ppm)	Cl^- (mg/L)	Amt Cl^-	%Cl^- (ppm)
1R-W1		6.12	--	2.7	--	--	45.1	--	--
1R-W-US		6.35	--	2.8	--	--	48.8	--	--
1R-M		7.16	5.0021	53.5	1.07E-04	107.0	27.3	5.46E-05	54.6
1R-C-W1-6	6	7.17	5.0019	189	3.78E-04	378.0	103	2.06E-04	206.0
1R-C-W1-18	18	7.8	5.007	18.4	3.67E-05	36.7	1.06	2.12E-06	2.1
1R-C-W1-42	42	7.8	5.005	25.7	5.13E-05	51.3	1.06	2.12E-06	2.1
1R-C1-6	6	6.9	5.0079	118	2.36E-04	236.0	128	2.55E-04	255.0
1R-C1-18	18	7.22	5.0044	227	4.54E-04	454.0	22.5	4.50E-05	45.0
1R-C1-42	42	7.94	4.9972	165	3.30E-04	330.0	9.61	1.92E-05	19.2

In summary, for all of the samples the pH of the water and the mud track each other while the pH of the concrete shavings is higher and slightly basic ranging mostly from about 7.4 to 8.4 which is lower than what is found in the interior of the concrete. For Bridges 3,4,5,6 and 7

(Lake Tawakoni, Alligator Bayou, Patroon Bayou, Carrice Creek and Palo Gaucho Bayou), the concrete shavings had more sulfate than could be found either in the water or in the mud. The only exception was a concrete shaving sample that was taken below the water line at Bridge 4 (Alligator Bayou). Bridges 1 and 2 (Tarkington Bayou and Navasota River) did not follow the trend of higher sulfate in the concrete shavings than in the water. The water at these two sites was fairly acidic and may be a factor. For Bridges 2 and 3 (Navasota River and Lake Tawakoni), the chloride concentration in the concrete was higher than in the water. With respect to elevation along a concrete column, no clear trend emerged with respect to the concentration of sulfate or chloride.

APPENDIX E:

DETAILED MINERALOGY AND PETROGRAPHIC ANALYSES PROCEDURES AND RESULTS

Table E. 1. Results from Semi-Quantitative XRD Analysis.

Bridge	Specimen ID	Carbonates									Clay Minerals				
		Quartz	K-feldspar	Plagioclase	Calcite	Dolomite	Portlanclite	Gypsum	brushite	illite + mica	I/S mixed-layer	smectite	attapulgite	kaolinite	chlorite
1	C1-1-1	25	3	2	40		15	5							
1	C1-1-3	55	3	2	10		15	5							
1	C1-2-1	50	3	2	25	2	8								
1	C1-2-3	50	5	5	10		18	2							
1	C3-3-1	87	1		12										
1	C3-3-3	80			5		10								
1	C4-3-1	60	5	5	10		13	2							
1	C4-3-1	45	2	3	25		15	5							
4	C8-1	85	5		5		5								
4	C8-3	65	5	3	2		15								
4	C4-1	85	3	2	10										
4	C4-3	70	2	5	3	5	10								
4	C5-1	75	5	5	5	5									
4	C5-3	80	3	2	3	2	5								
4	C6-1	85	7	3	5										
4	C6-3	70	2	2	10	1	10								
5	5-B	44	1		30	9			6			10			
6	6-C	70	1		10				5	4		10			
7	7-B	20			62	3			5			10			
8	8-A	52	3		35				3			7			
9	9-A	50	7	5	20	3			5	3		7			

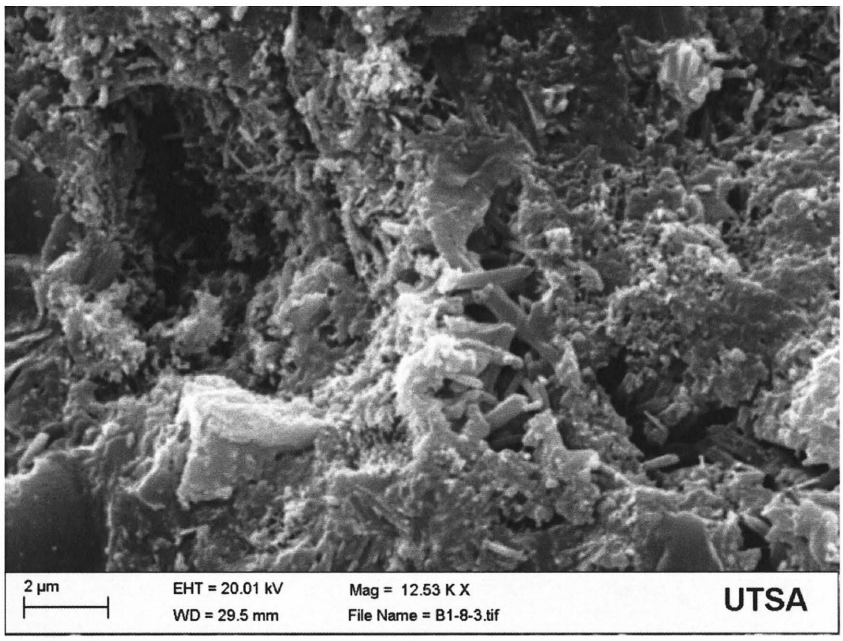

(a)

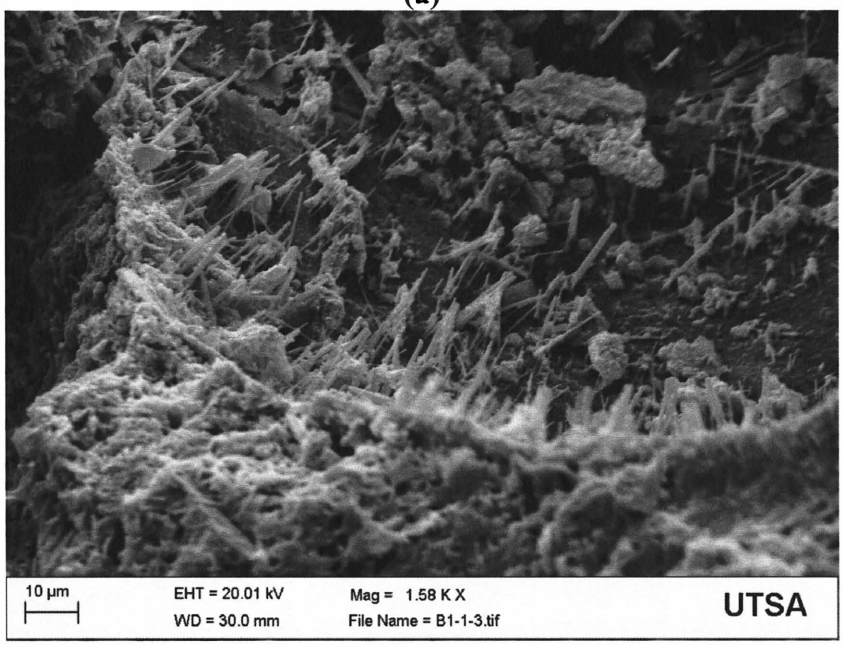

(b)

Figure E. 1. Examples of SEM images of the cores from Bridge 1. (a). Short laths of portlandite, (b). Bundles of ettringite fibers and laths up to 20 microns in length.

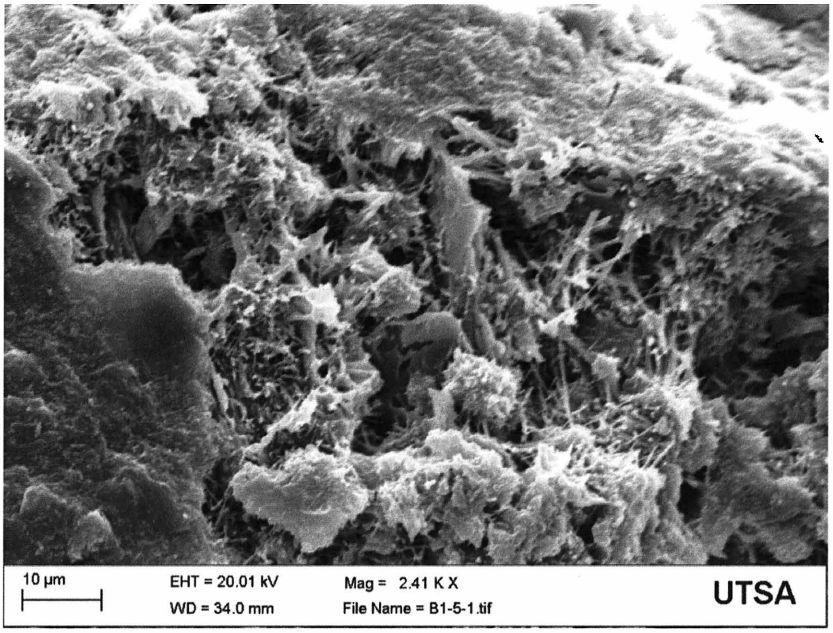

(c)

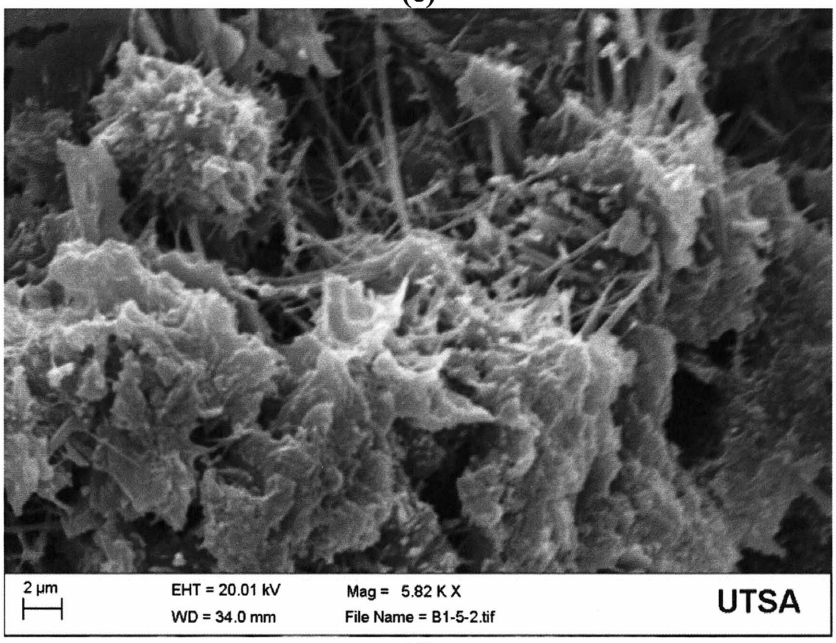

(d)

Figure E. 1. Examples of SEM images of the cores from Bridge 1. (continuous) (c). Fibrous precipitates of ettringite, (d). Closer view precipitates of ettringite.

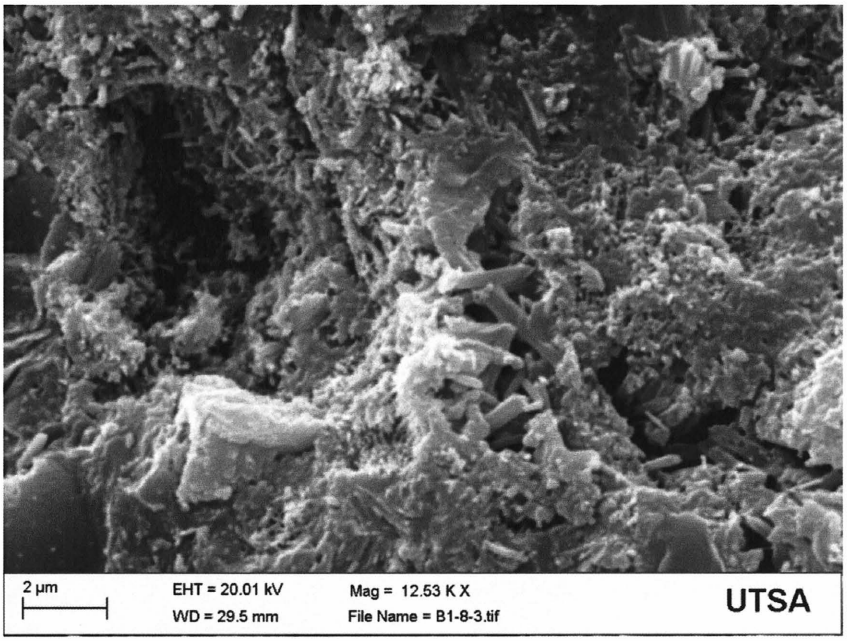

(a)

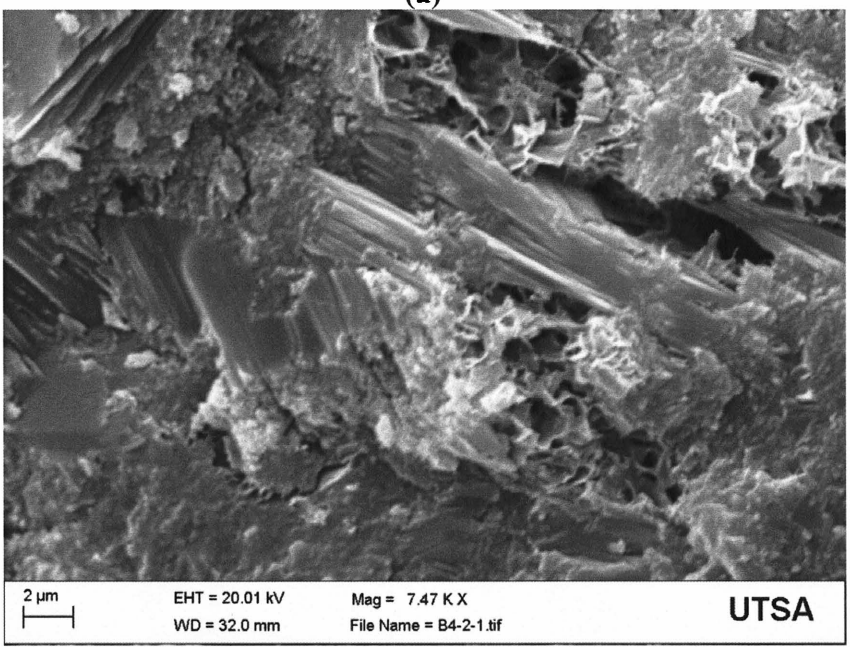

(b)

Figure E. 2. Examples of SEM images of the cores from Bridge 4. (a). Typical portlandite crystals, (b). A cluster of prismatic portlandites.

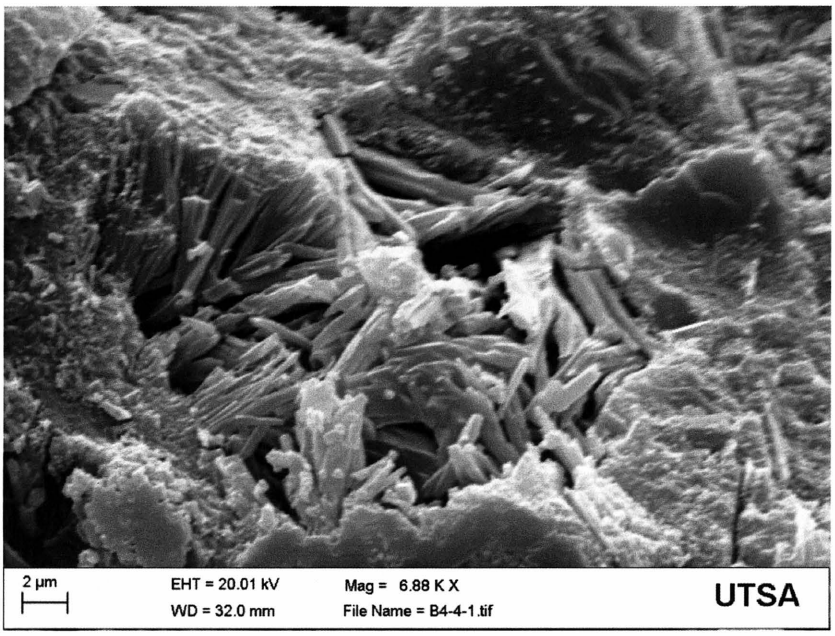

(c)

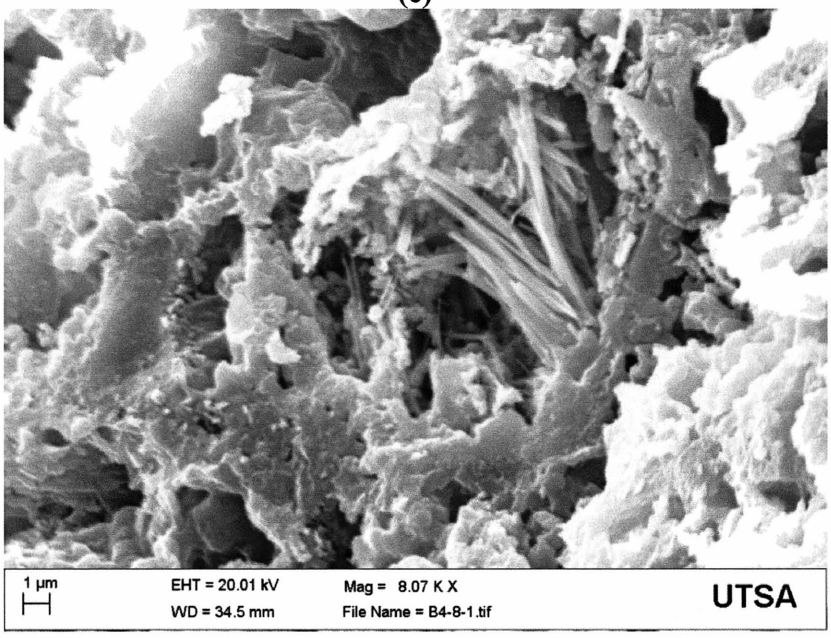

(d)

Figure E. 2. Examples of SEM images of the cores from Bridge 4. (continuous). (c). Typical stacks of ettringite laths, (d). A bundle of portlandite and ettringite laths.

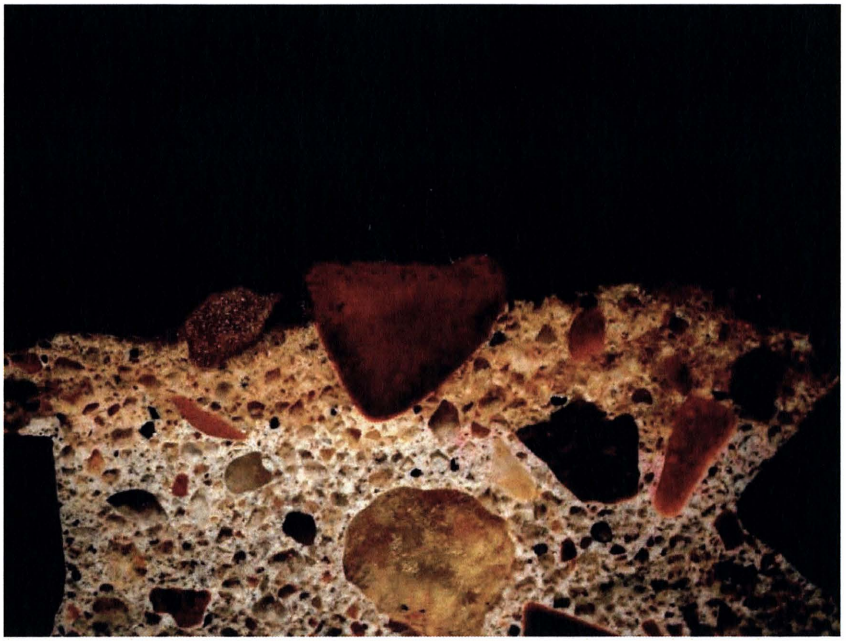

(a)

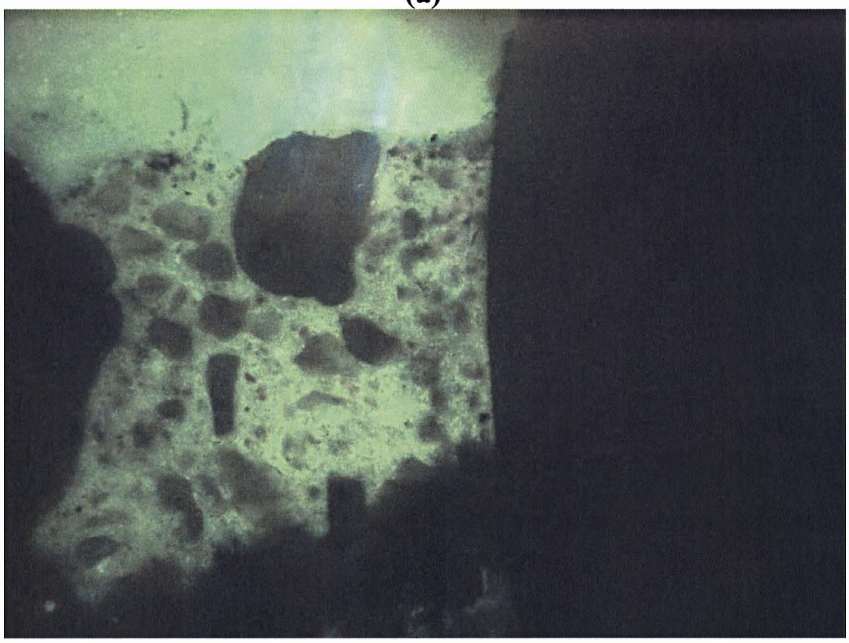

(b)

Figure E. 3. Examples of petrographic image from Bridge 1. (a). Polarized light image, (b). Fluorescent light image.

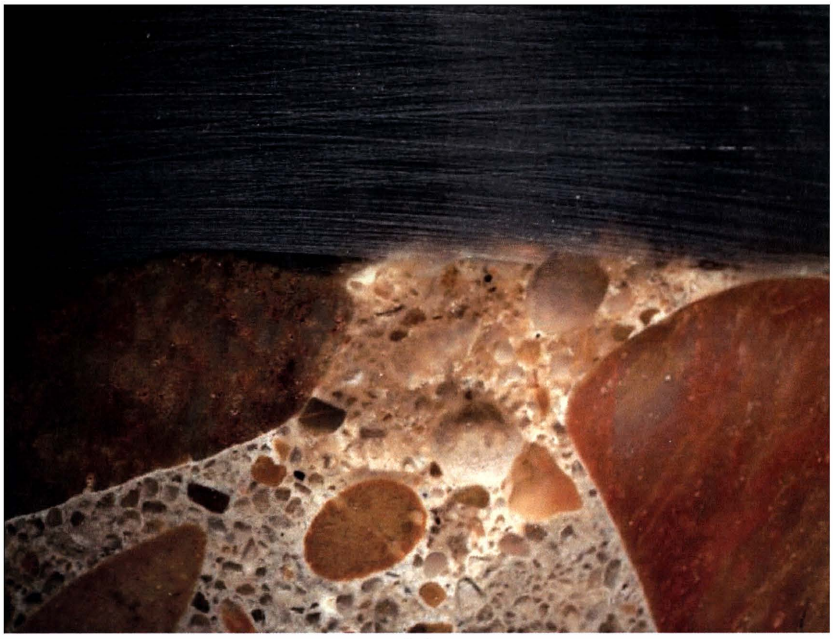

(a)

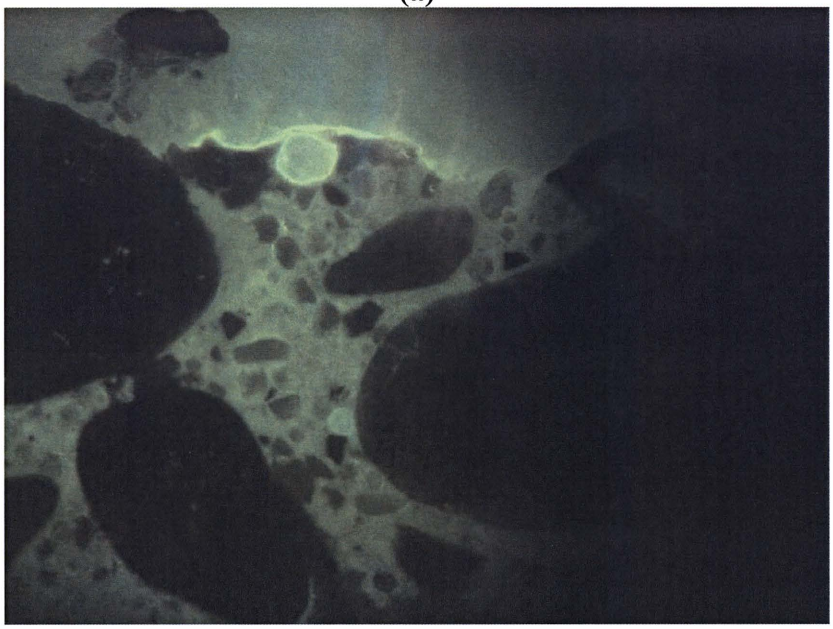

(b)

Figure E. 4. Examples of petrographic image from Bridge 2. (a). Polarized light image, (b). Fluorescent light image.

(a)

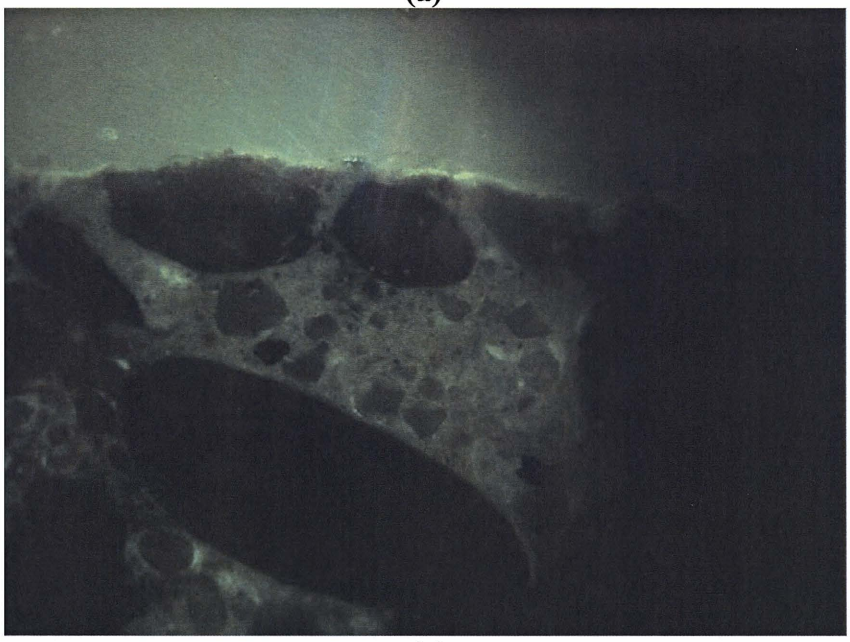

(b)

Figure E. 5. Examples of petrographic image from Bridge 3. (a). Polarized light image, (b). Fluorescent light image.

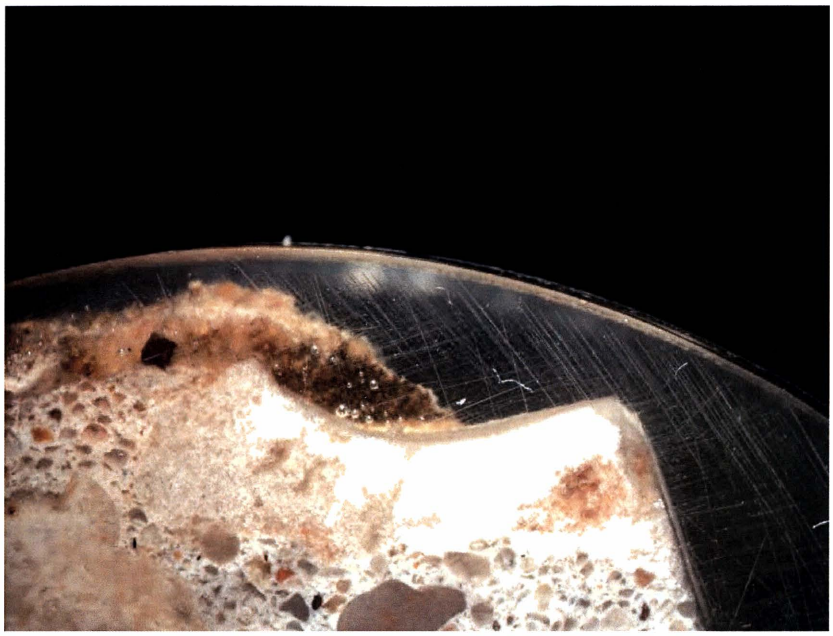

(a)

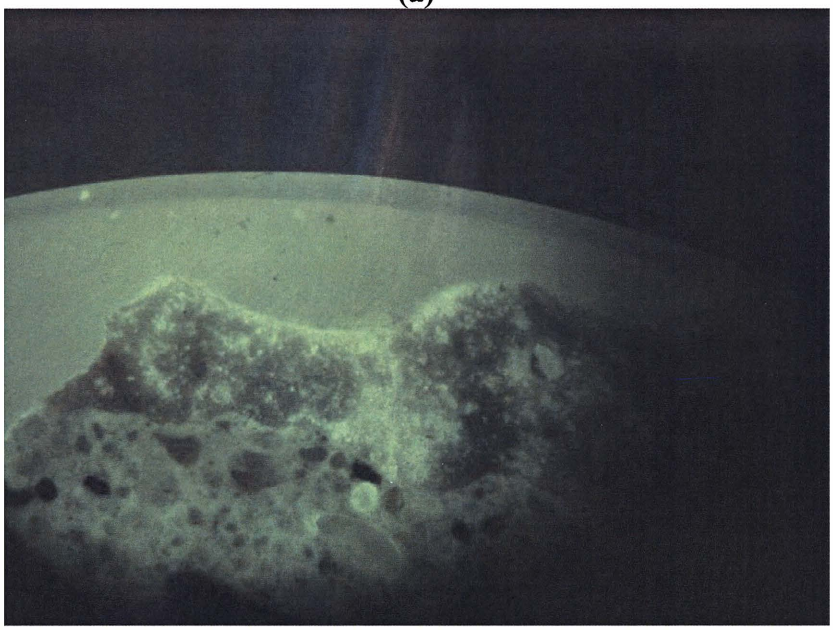

(b)

Figure E. 6. Examples of petrographic image from Bridge 9. (a). Polarized light image, (b). Fluorescent light image.

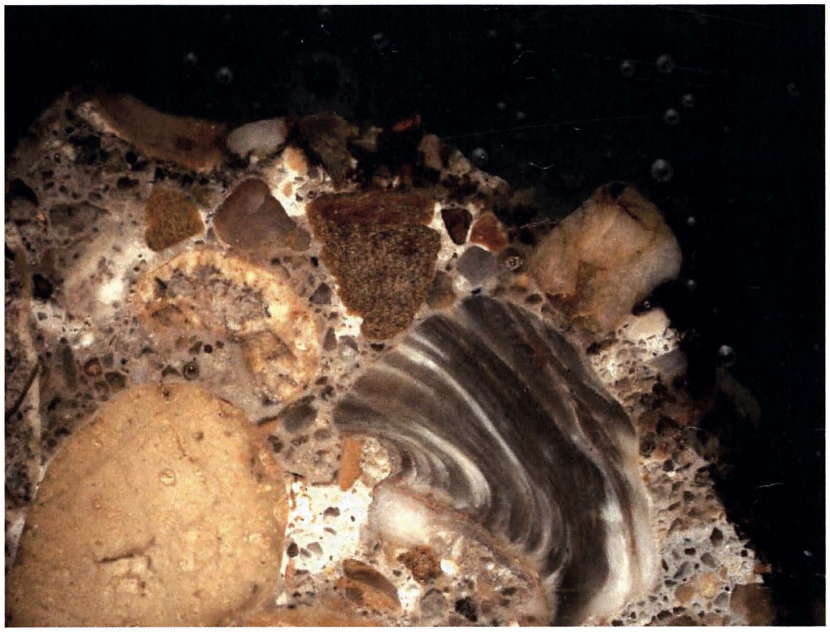

(a)

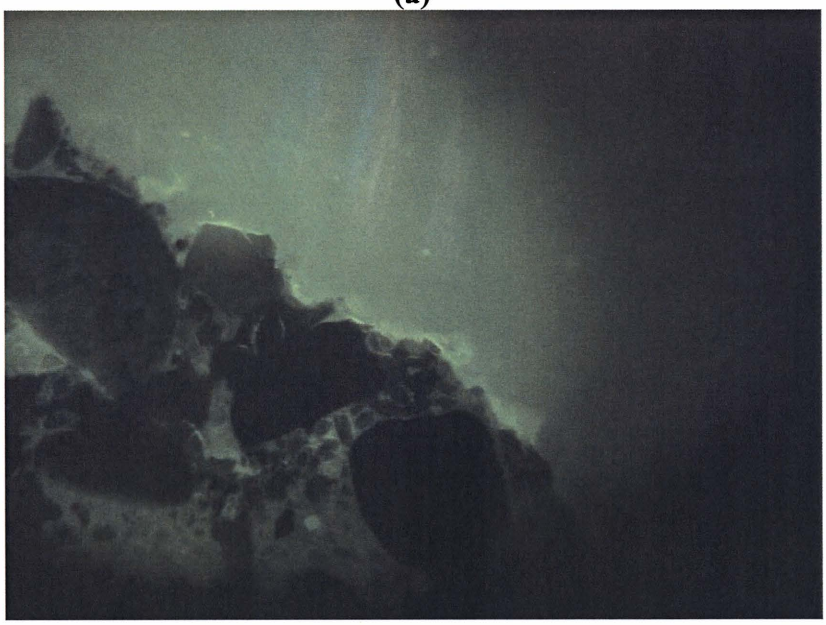

(b)

Figure E. 7. Examples of petrographic image from Bridge 10. (a). Polarized light image, (b). Fluorescent light image.

APPENDIX F:

DETAILED MICROBIAL ATTACK SIMULATION PROCEDURES AND RESULTS

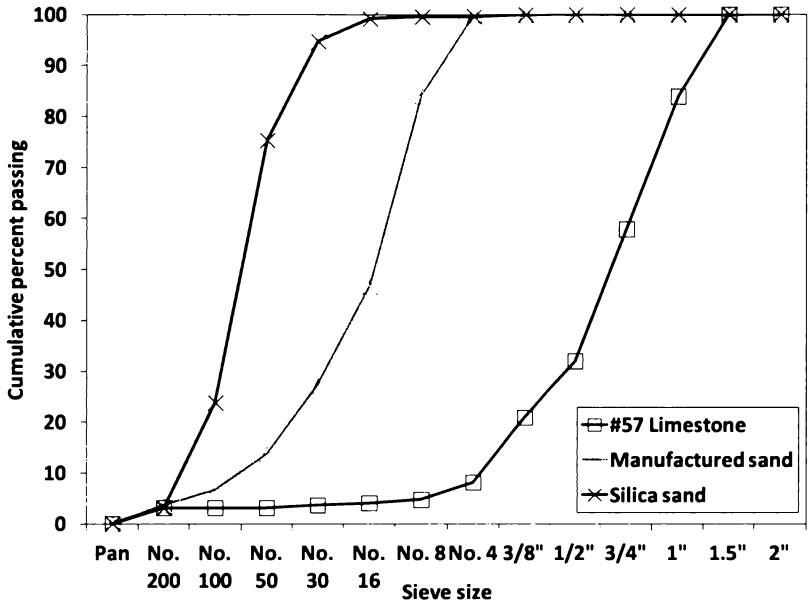

Figure F. 1.Gradations of Fine and Coarse Aggregate.

Table F. 1. Physical properties and fineness modulus of fine and coarse aggregate.

	Limestone Coarse Aggregate	Manufactured Sand	Silica Sand
Specific Gravity (OD)	2.38	2.48	2.65
Specific Gravity (SSD)	2.47	2.56	2.66
Absorption, %	3.80%	2.98%	0.60%
Fineness Modulus	6.94	3.22	1.08

Table F. 2. Designs of Concrete Mixtures.

Mix ID	Cement	SCMs	Chemical	SCMs (%)	w/b
C-I	Type I	NA	NA	0	0.48
C-I-CPTS	Type I	NA	CPT-2000	0	0.48
C-V	Type V	NA	NA	0	0.49
C-I-CFA	Type I	Class C fly ash	NA	20	0.49
C-I-FFA	Type I	Class F fly ash	NA	20	0.49
C-I-SF	Type I	Silica fume	NA	7	0.48
C-I-RPP	Type I	NA	RheoPel Plus	0	0.48

Table F. 3. Concrete Mix Proportion.

Mix ID	Cement (pcy)	SCMs (pcy)	CA (pcy)	FA1 (pcy)	FA2 (pcy)	Water (pcy)	Chemical Admixtures (fl oz/cwt)		
							AE90	HRWR	RheoPel Plus
C-I	574	0	1727	936	164	275	1.3	0	0
C-I-CPTS	574	0	1727	936	164	275	1.3	0	0
C-V	573	0	1721	936	164	278	1.8	0	0
C-I-CFA	448	112	1728	939	165	272	1.3	0	0
C-I-FFA	432	108	1743	946	166	262	2.0	0	0
C-I-SF	519	39	1731	943	164	270	1.2	6.0	0
C-I-RPP	574	0	1727	936	164	275	1.3	0	3.5

Table F. 4. Physical Properties of Concrete Mixtures.

Mix ID	Unite Weight (pcf)	Slump (in)	Air (%)	$f'_{c,56}$ (psi)
C-I	136.0	4.5	6.75	4047
C-I-CPTS	136.0	4.5	6.75	4047
C-V	138.5	3.5	4	4481
C-I-CFA	135.6	7	8.75	4328
C-I-FFA	136.6	7.5	8	4043
C-I-SF	134.1	5.75	9.5	4058
C-I-RPP	134.6	6.5	9.75	3223

Table F. 5. Designs of Mortar Mixtures.

Mix ID	Cement	SCMs	AE 90	SCMs (%)	w/b	s/b
M-I	Type I	NA	2.30fl oz/cwt	0	0.45	2.50
M-I-CPTS	Type I	NA	2.30fl oz/cwt	0	0.45	2.50
M-V	Type V	NA	2.30fl oz/cwt	0	0.45	2.50
M-I-CFA	Type I	Class C Fly Ash	2.30fl oz/cwt	30	0.45	2.50
M-I-FFA	Type I	Class F Fly Ash	2.30fl oz/cwt	30	0.45	2.50
M-I-SF	Type I	Silica fume	2.30fl oz/cwt	10	0.45	2.50

Table F. 6. Physical Properties of Mortar Mixtures.

Mix ID	Unit Weight (pcf)	$f'_{c,90}$ (psi)
M-I	131.9	4657
M-I-CPTS	131.9	4657
M-V	136.2	6832
M-I-CFA	127.4	4971
M-I-FFA	129.7	5661
M-I-SF	129.8	5451

Table F. 7. pH Values of 1% Sulfuric Solutions for Mortar Specimens Storage.

Mix ID	Initial	91 days	111 days	126 days	154 days
M-I	1.29	1.18	0.81	1.33	1.01
M-I-CPTS	1.29	1.22	0.83	1.29	1.02
M-V	1.29	1.14	0.21	1.88	1.05
M-I-CFA	1.29	1.35	2.25	3.30	1.16
M-I-FFA	1.29	1.20	1.49	3.15	1.08
M-I-SF	1.29	1.10	0.40	1.45	1.03

Table F. 8. pH Values of 3% Sulfuric Solutions for Mortar Specimens Storage.

Mix ID	Initial	7 days	25 days	50 days
M-I	0.72	0.43	0.94	1.82
M-I-CPTS	0.72	0.40	1.09	2.04
M-V	0.72	2.02	1.15	2.07
M-I-CFA	0.72	1.96	1.65	3.29
M-I-FFA	0.72	0.32	1.29	3.12
M-I-SF	0.72	0.57	1.16	2.27

Table F. 9. pH Values of 3% Sulfuric Solutions for Concrete Specimens Storage.

Mix ID	Initial	7d	25d	50d
C-I	0.72	0.29	1.02	1.04
C-I-CPTS	0.72	0.72	1.01	1.01
C-V	0.72	0.62	1.01	0.99
C-I-CFA	0.72	0.25	1.19	1.87
C-I-FFA	0.72	0.31	1.03	1.26
C-I-SF	0.72	0.60	1.06	1.16
C-I-RPP	0.72	0.38	1.08	1.14

Table F. 10. pH Values of Water at Site Exposure Locations.

Location	Sample ID	Sample Date	pH
Site A	1-W-1	11/5/2009	5.40
Site A	1-W-2	11/5/2009	5.55
Site A	1-W-3	11/5/2009	5.25
Site A	B1R-W1	4/15/2011	6.12
Site B	B10-W1-S	7/20/2011	5.58
Site B	B10-W2-N	7/20/2011	5.68

Table F. 11. pH Values of 1% Sulfuric Solutions for Concrete Specimens Storage.

Mix ID	0d	35d	42d	48d	55d	63d	69d	77d	91d	111 d	126 d	154 d
C-I	1.29	2.61	2.13	2.28	2.67	2.42	1.46	1.39	1.14	0.09	1.45	0.95
C-I-CPTS	1.29	2.36	2.08	2.24	2.58	3.26	1.19	0.57	1.17	0.36	2.22	0.97
C-V	1.29	2.11	2.27	2.45	2.93	3.83	0.40	0.15	1.23	1.20	1.90	1.08
C-I-CFA	1.29	2.00	1.72	1.72	2.01	0.81	1.62	1.02	1.28	0.63	2.89	1.08
C-I-FFA	1.29	2.04	2.09	2.21	2.54	2.24	1.74	1.21	1.18	0.06	1.43	1.05
C-I-SF	1.29	2.07	2.10	2.32	2.71	3.22	1.30	0.79	1.21	0.23	1.80	1.06
C-I-RPP	1.29	1.87	2.15	2.17	2.20	1.01	1.62	1.52	1.26	N/A	1.40	1.00

Figure F. 2. Storage of Concrete Specimen in Laboratory Simulation.

Figure F. 3. Storage of Mortar Specimen in Laboratory Simulation.

Table F. 12. Preliminary Study of Deterioration of Dummy Mortar Specimens Exposed to Different Concentrations of Sulfuric Solutions.

	1% Sulfuric Solution	3% Sulfuric Solution	5% Sulfuric Solution	10% Sulfuric Solution
Day 1		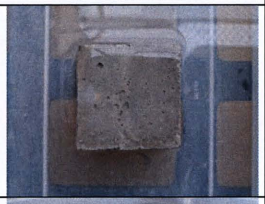	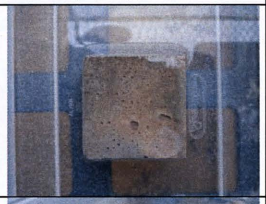	
Day 2				
Day 6				
Day 13				
Day 33			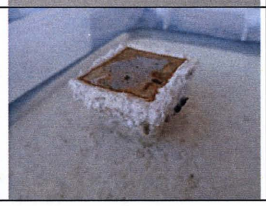	

Figure F. 4. Reaction Products on the Surface of Specimen (C-I) after 83 days' Exposure in 3% Sulfuric Solution.

Table F. 13. Visual Inspection of Concrete Specimen after Different Ages of Direct Field Exposure (Scenario I).

	40 days	96 days	174 days
C-I			
C-I-CPTS			
C-V			
C-I-CFA			
C-I-FFA			
C-I-SF			
C-I-RPP			

Table F. 14. Visual Inspection of Concrete Specimen after Different Ages of 1% Sulfuric Solution Exposure (Scenario II).

	20 days	48 days	148 days
C-I		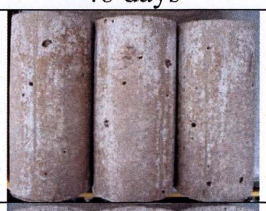	
C-I-CPTS			
C-V			
C-I-CFA			
C-I-FFA			
C-I-SF			
C-I-RPP			

Table F. 15. Visual Inspection of Concrete Specimen after Different Ages of Field Exposure Following 57 Days of 1% Sulfuric Solution Exposure (Scenario III).

	40 days	96 days	174 days
C-I			
C-I-CPTS			
C-V			
C-I-CFA			
C-I-FFA			
C-I-SF			
C-I-RPP			

Table F. 16. Visual Inspection of Concrete Specimen after Different Ages of 3% Sulfuric Solution Exposure (Scenario IV).

	1 day	42 day	112 day
C-I	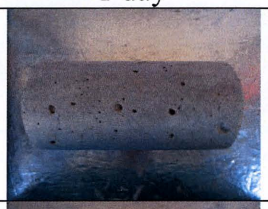	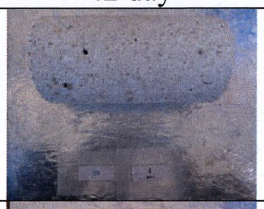	
C-I-CPTS	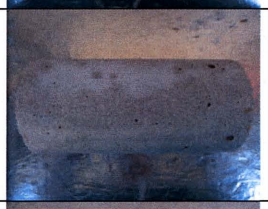		
C-V	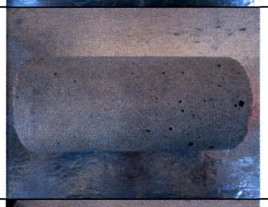		
C-I-CFA	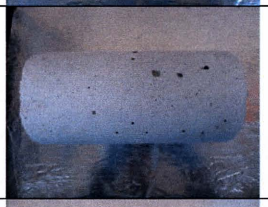		
C-I-FFA			
C-I-SF	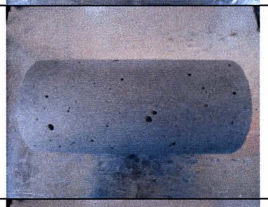		
C-I-RPP			

Table F. 17. Visual Inspection of Concrete Specimen after Different Ages of Field Exposure Following 15 Days of 3% Sulfuric Solution Exposure (Scenario V).

	34 days	112 days
C-I		
C-I-CPTS		
C-V		
C-I-CFA		
C-I-FFA		
C-I-SF		
C-I-RPP		

Table F. 18. Visual Inspection of Mortar Specimen after Different Ages of Direct Field Exposure (Scenario I).

	40 days	96 days	174 days
M-I			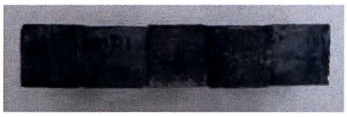
M-I-CPTS	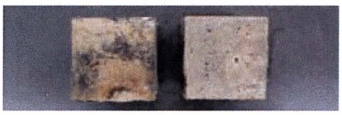		
M-V			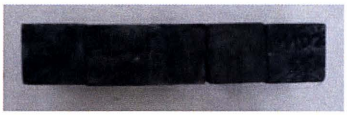
M-I-CFA	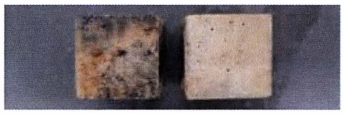	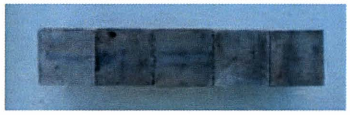	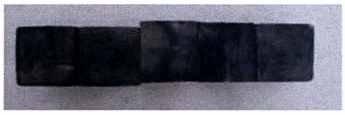
M-I-FFA	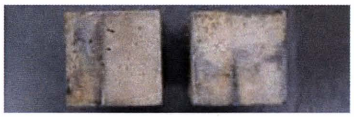		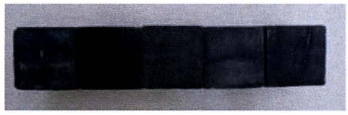
M-I-SF	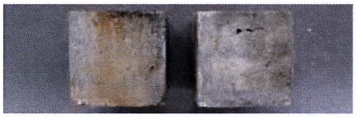		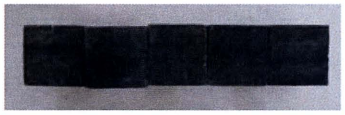

Table F. 19. Visual Inspection of Mortar Specimen after Different Ages of 1% Sulfuric Solution Exposure (Scenario II).

	7 days	48 days	148 days
M-I			
CPTS			
M-V			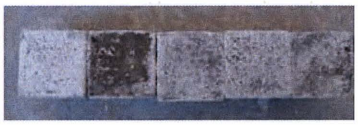
CFA			
M-I-FFA		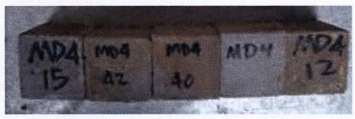	
M-I-SF			

Table F. 20. Visual Inspection of Mortar Specimen after Different Ages of Field Exposure Following 57 days of 1% Sulfuric Solution Exposure (Scenario III).

	40 days	96 days	174 days
M-I	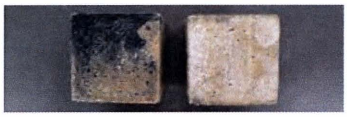		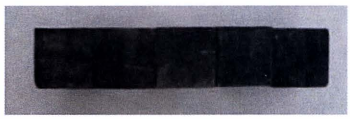
M-I-CPTS			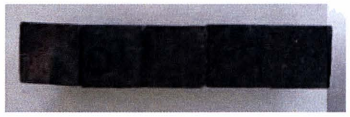
M-V			
M-I-CFA	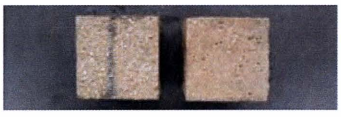		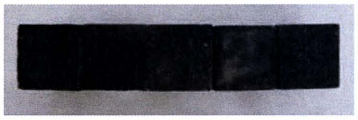
M-I-FFA	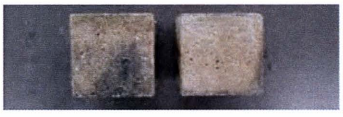		
M-I-SF			

Table F. 21. Visual Inspection of Mortar Specimen after Different Ages of 3% Sulfuric Solution Exposure (Scenario IV).

	7 days	36 days	112 days
M-I			
M-I-CPTS			
M-V			
M-I-CFA			
M-I-FFA			
M-I-SF			

Table F. 22. Visual Inspection of Mortar Specimen after Different Ages of Field Exposure Following 15 Days of 3% Sulfuric Solution Exposure (Scenario V).

	34 days	112 days
M-I	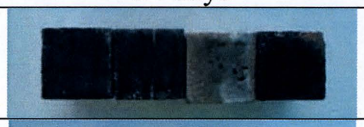	
M-I-CPTS		
M-V		
M-I-CFA		
M-I-FFA	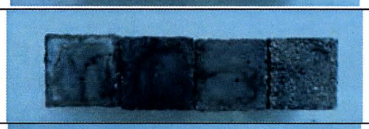	
M-I-SF		

Table F. 23. Phenolphthalein Color Change Test of Mortar Cube Specimens after Different Ages of Field Exposure (Scenario I).

	96 days
M-I	
M-I-CPTS	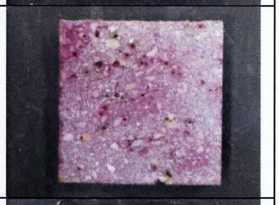
M-V	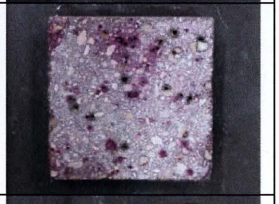
M-I-CFA	
M-I-FFA	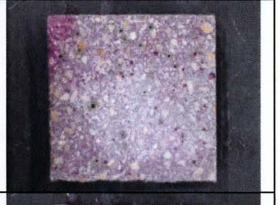
M-I-SF	

Table F. 24. Phenolphthalein Color Change Test of Mortar Cube Specimens after Different Ages of 1% Sulfuric Solution Exposure (Scenario II).

	28 days	91 days	221 days
M-I	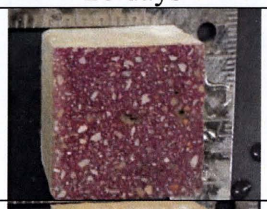		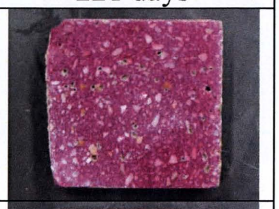
M-I-CPTS			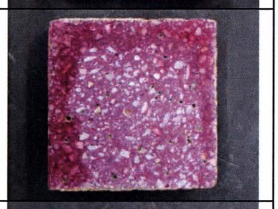
M-V			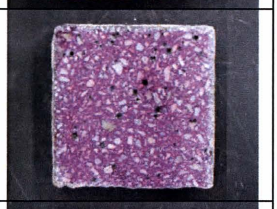
M-I-CFA			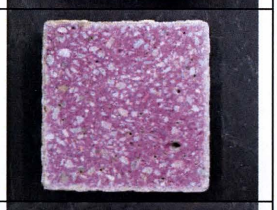
M-I-FFA			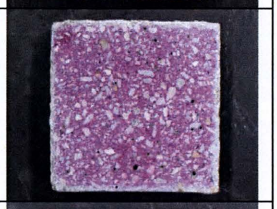
M-I-SF			

Table F. 25. Phenolphthalein Color Change Test of Mortar Cube Specimens After Different Ages of Field Exposure Following 57 Days 1% Sulfuric Solution Exposure (Scenario III).

	96 days
M-I	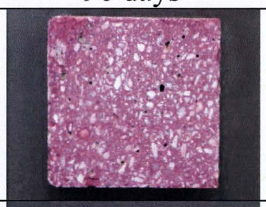
M-I-CPTS	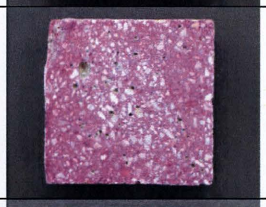
M-V	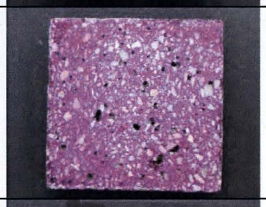
M-I-CFA	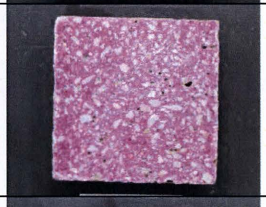
M-I-FFA	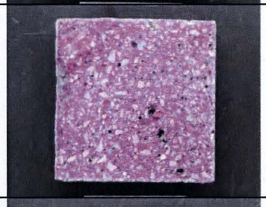
M-I-SF	

Table F. 26. Phenolphthalein Color Change Test of Mortar Cube Specimens After Different Ages of 3% Sulfuric Solution Exposure (Scenario IV).

	7 days	25 days	50 days
M-I			
M-I-CPTS			
M-V	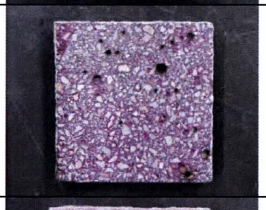		
M-I-CFA		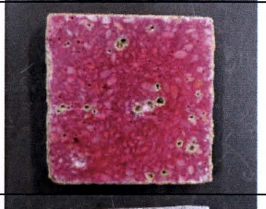	
M-I-FFA		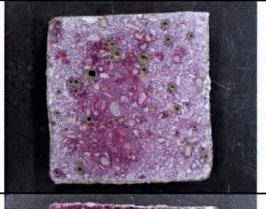	
M-I-SF			

Table F. 27. Phenolphthalein Color Change Test of Mortar Cube Specimens After Different Ages of Field Exposure Following 15 Days3% Sulfuric Solution Exposure (Scenario V).

	34 days
M-I	
M-I-CPTS	
M-V	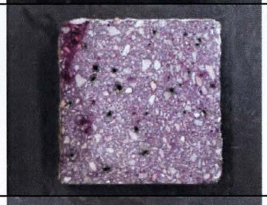
M-I-CFA	
M-I-FFA	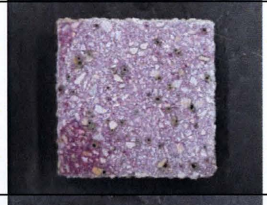
M-I-SF